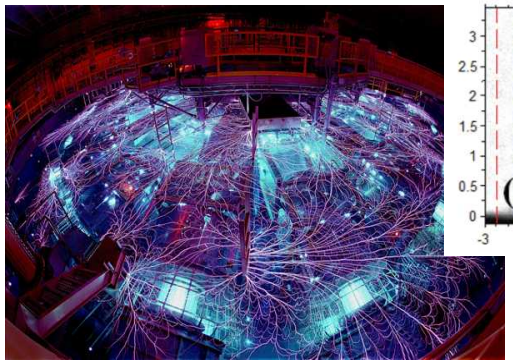

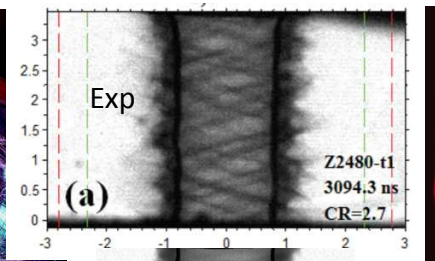

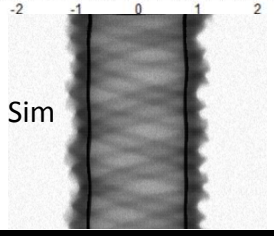

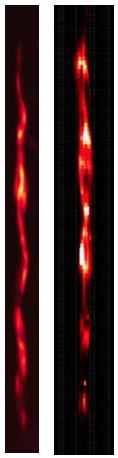

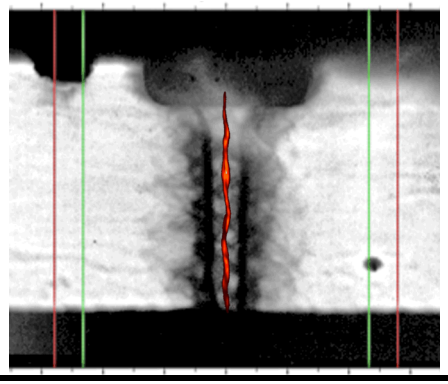

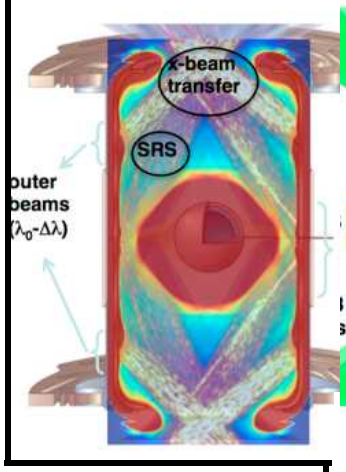

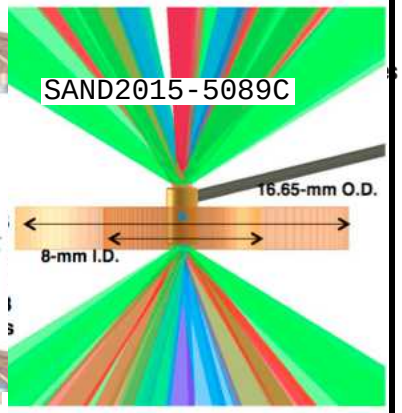

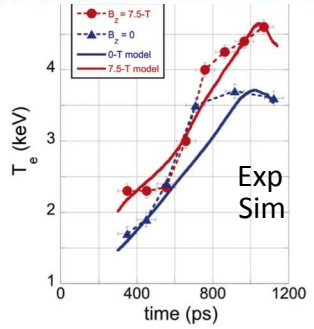

FIG. 3. Measured electron temperature versus time for B = 0 (blue triangles) and B = 7.5-T (red circles). Over-plotted as solid lines are the 2-D HYDRA model for B = 0 (blue) and B = 7.5-T (red).

Adventures in ICF with magnetic fields

Anomalous Absorption Conference
Wednesday, June 17th, 2015

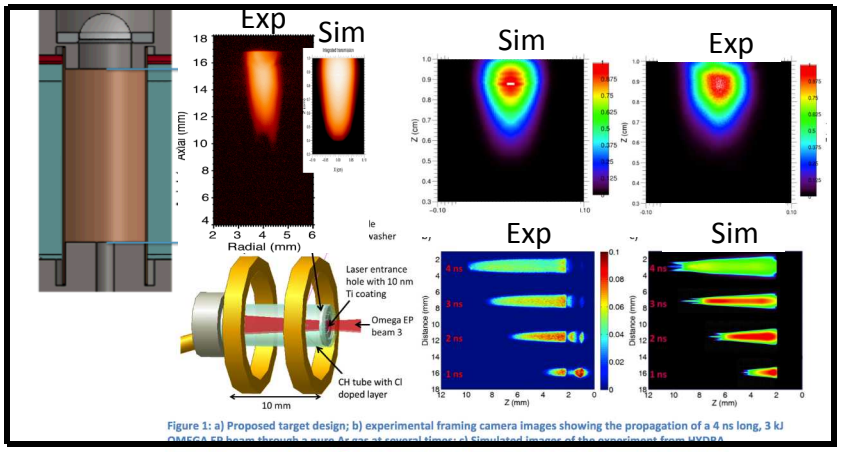

Figure 1: a) Proposed target design; b) experimental framing camera images showing the propagation of a 4 ns long, 3 kJ OMEGA EP beam through a pure Ar gas at several times c) Simulated images of the experiment from HYDRA

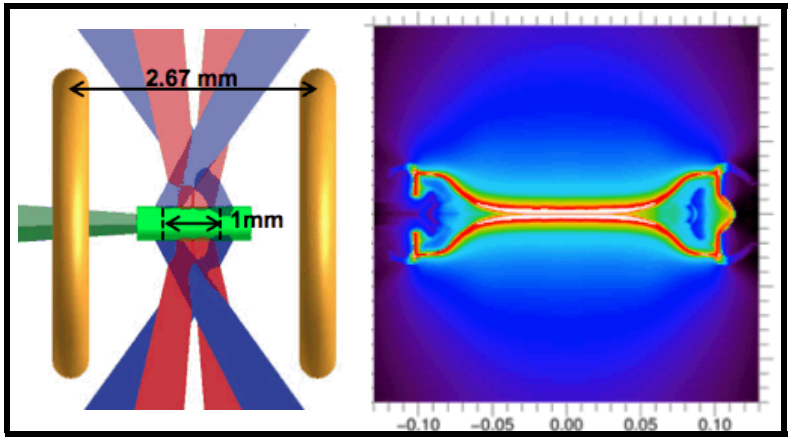

Many groups want to use magnetic fields to relax inertial fusion stagnation requirements

Sandia National Laboratories

SNL Phi Target

1982 Demonstration of enhanced fusion yield with magnetization (~1e6 DD yield)

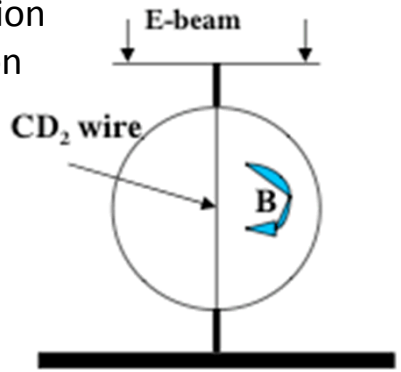

Max Planck/ITEP

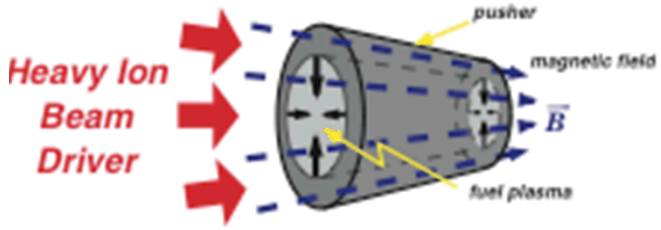

Basko, Kemp, Meyer-ter-Vehn, *Nucl. Fusion* **40**, 59 (2000)
Kemp, Basko, Meyer-ter-Vehn, *Nucl. Fusion* **43**, 16 (2003)

LLNL

(Perkins *et al.*, Phys Plasmas 2013)

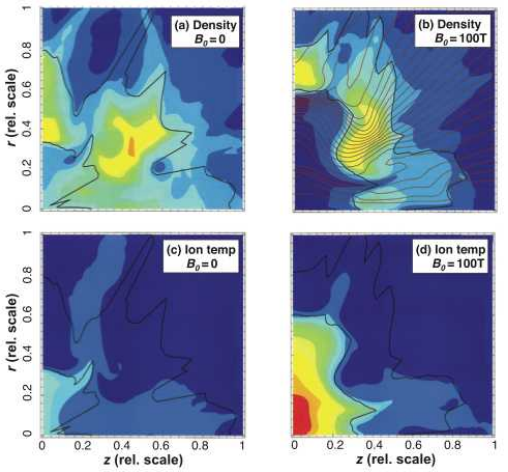

University of Rochester/LLE

2011 Demonstration of enhanced fusion yield with magnetization (~5e9 DD yield)

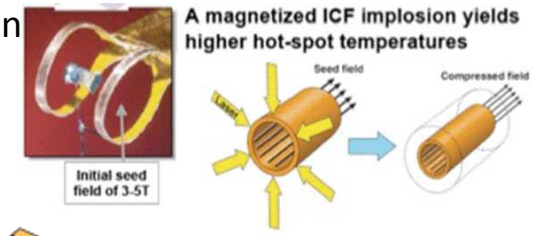

Gotchev *et al.*, *Rev. Sci. Instr.* **80**, 043504 (2009)

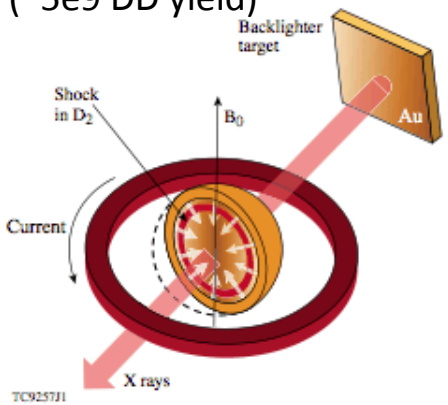

P.Y. Chang *et al.*, PRL (2011).

Los Alamos/Air Force Research Lab

Field Reversed Configuration FRC
Magnetic Target Fusion
Shiva Star
closed field lines
FRC

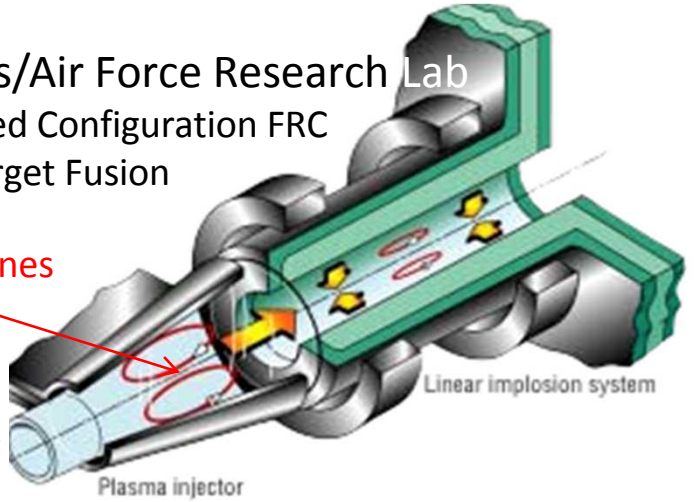

Taccetti, Intrator, Wurden *et al.*, *Rev. Sci, Instr.* **74**, 4314 (2003)
Degnan *et al.*, *IEEE Trans. Plas. Sci.* **36**, 80 (2008)

and many others…

We are building a national program

Contributors to this work (and their associated teams):

A. B. Sefkow[1], J. M. Koning[2], T. J. Awe[1], R. Betti[3], B. E. Blue[4], E. L. M. Campbell[3], G. A. Chandler[1], P.-Y. Chang[3], R. E. Clark[6], K. Cochrane[1], M. E. Cuneo[1], J. R. C. Davies[3], M. J. Edwards[2], G. Fiksel[3], M. Geissel[1], M. R. Gomez[1], K. D. Hahn[1], S. B. Hansen[1], E. C. Harding[1], A. J. Harvey-Thompson[1], M. H. Hess[1], C. Jennings[1], P. F. Knapp[1], D. C. Lamppa[1], J. Lash[1], B. G. Logan[2], M. M. Marinak[2], M. K. Matzen[1], R. D. McBride[1], D. S. Montgomery[5], J. D. Moody[2], C. Mostrom[6], T. Nagayama[1], K. J. Peterson[1], J. L. Porter[1], G. A. Rochau[1], D. V. Rose[6], D. Rovang[1], C. L. Ruiz[1], P. F. Schmit[1], M. B. Schneider[2], D. B. Sinars[1], S. A. Slutz[1], I.C. Smith[1], W. Stygar[1], C. Thoma[6], K. Tomlinson[4], R. A. Vesey[1], M. S. Wei[4], and D. R. Welch[6]

[1] Sandia National Laboratories, Albuquerque, NM
[2] Lawrence Livermore National Laboratory, Livermore, CA
[3] Laboratory for Laser Energetics, Rochester, NY
[4] General Atomics, San Diego, CA
[5] Los Alamos National Laboratory, Los Alamos, NM
[6] Voss Scientific, Albuquerque, NM

Outline

1. Magnetized Liner Inertial Fusion (MagLIF)
2. Comparisons of MagLIF-related experiments to simulations
3. OMEGA-EP laser-heating experiments
4. Magnetized hohlraum experiments at OMEGA
5. Mini-MagLIF at OMEGA

Outline

1. Magnetized Liner Inertial Fusion (MagLIF)
2. Comparisons of MagLIF-related experiments to simulations
3. OMEGA-EP laser-heating experiments
4. Magnetized hohlraum experiments at OMEGA
5. Mini-MagLIF at OMEGA

The accumulation and transmission of electromagnetic energy, called “pulsed power”, has been investigated for over a century

Sandia National Laboratories

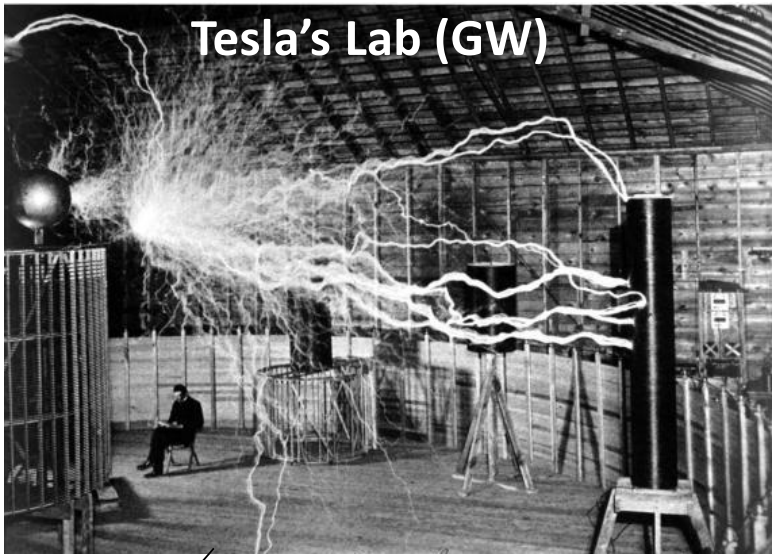

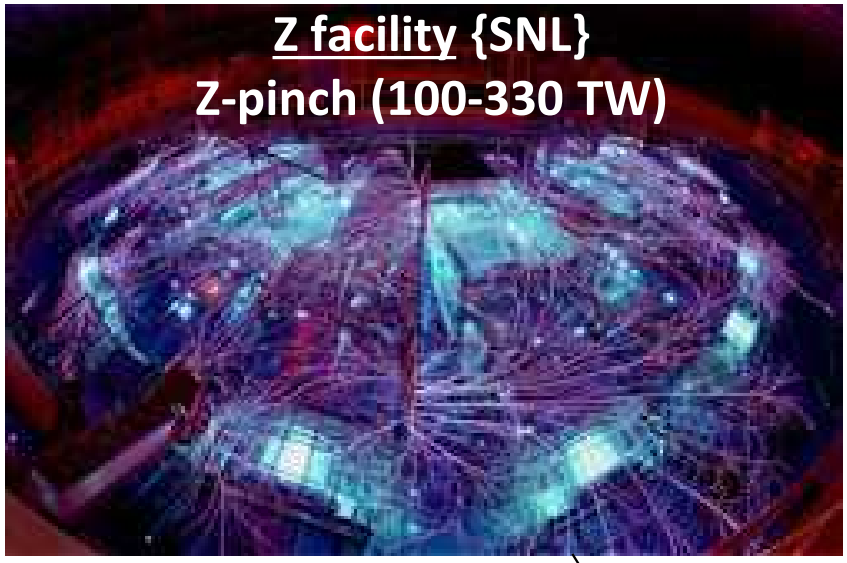

1900 1920 1940 1960 1980 2000

WWII

Hermes - II {SNL}
e-beam (TW)

PBFA - II {SNL}
Ion Beams (20 TW)

Radar (MW)
- Germany
- US
- Russia
- Great Britain

Angara - II {Russia}
Simulator (TW)

DARHT {LANL}
Radiography (10 GW)

“Z” is the world’s largest pulsed-power facility

Sandia National Laboratories

Tank~10,000 ft^2

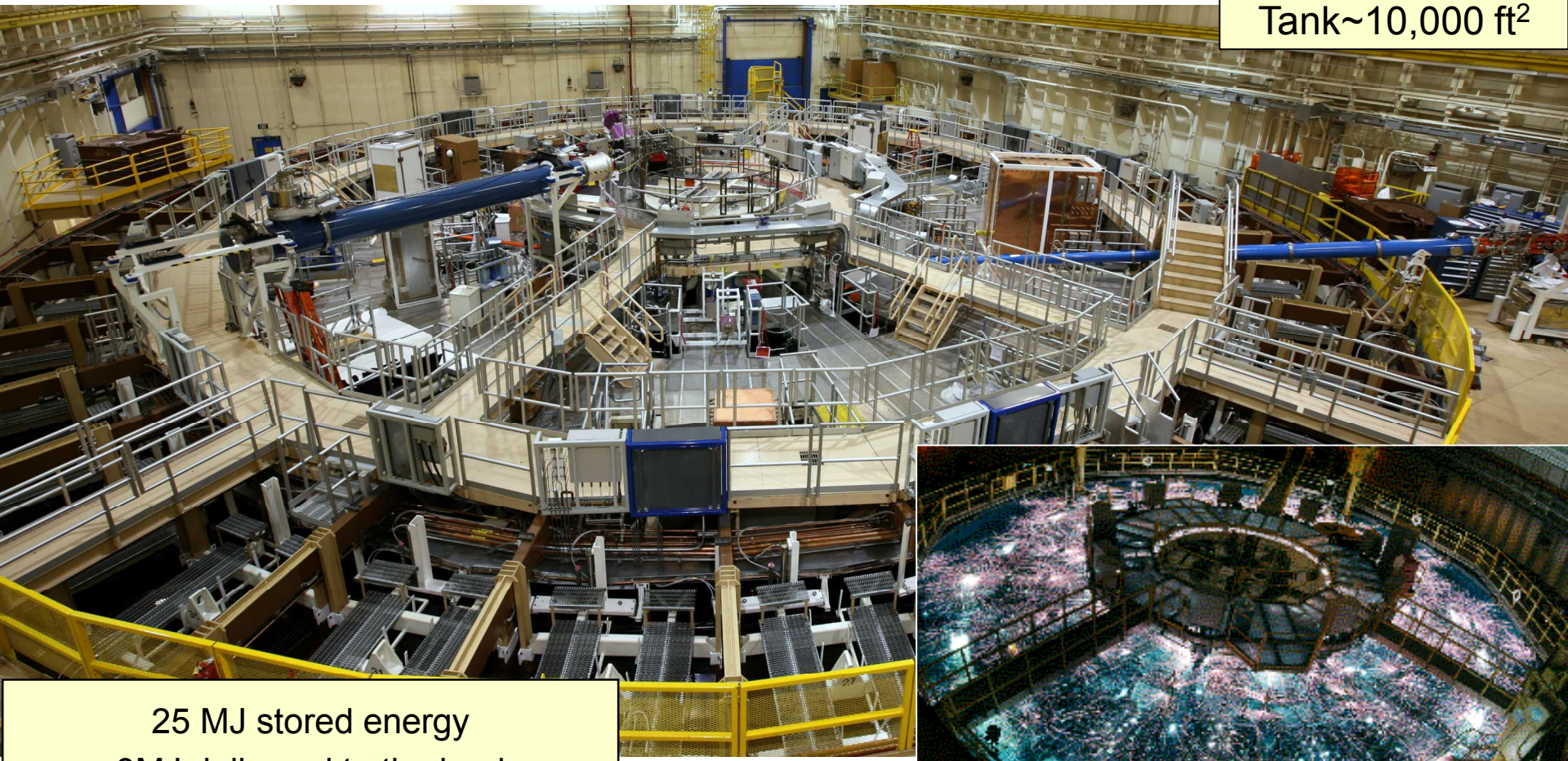

25 MJ stored energy

3MJ delivered to the load

27 MA peak current

5 – 50 Megagauss (1-100 Megabar)

100-600 ns pulse length

Cross section of the Z facility at Sandia National Laboratories

Sandia National Laboratories

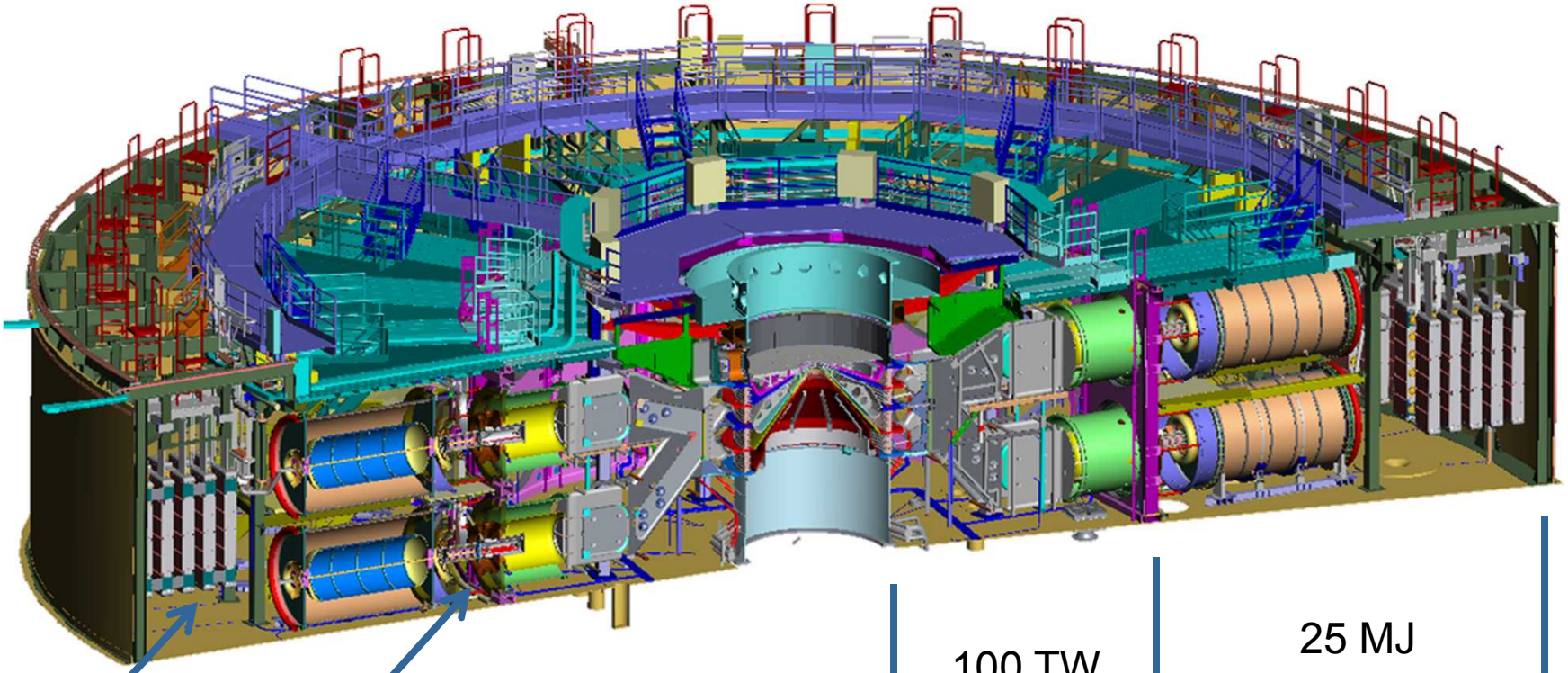

Marx Generator

Laser-triggered Gas Switch

27 MA Current

100 TW Electrical

25 MJ Electrical

Large currents create large B fields and pressures

A single wire carrying current produces a magnetic field that encircles it according to the right-hand rule

Two parallel wires carrying current along the same direction will attract each other (Biot-Savart Law, "JxB force")

Definition of an Ampere: If two very long parallel wires 1 m apart carry equal currents, the current in each is defined to be 1 A when the force/length is 2e-7 N/m

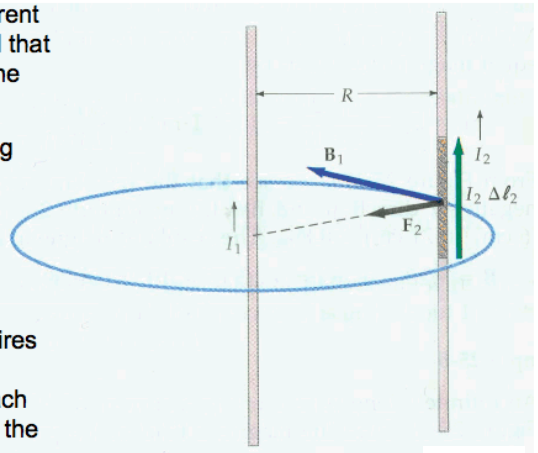

$$\nabla \times \mathbf{B} = \frac{4\pi \mathbf{J}}{c}$$

Ampere's law

$$\oint_C \mathbf{B} \bullet dl = \frac{4\pi}{c} \iint_S \mathbf{J} \bullet d\mathbf{S}$$

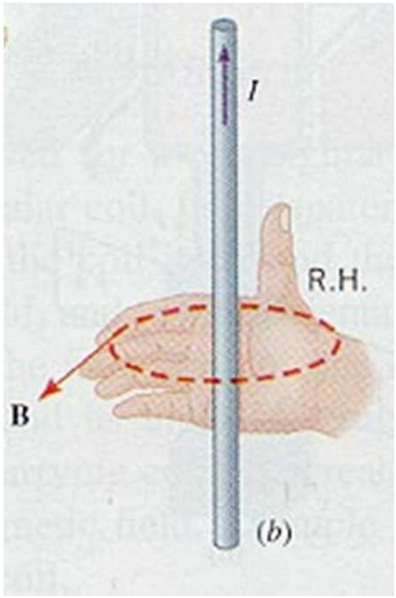

For an axial current I:

$$2\pi r B_\theta = \frac{4\pi}{c} I$$

$$B_\theta = \frac{2}{c}\frac{I}{r} \quad (cgs)$$

$$B_\theta(G) = \frac{I(A)}{5\, r(cm)} \longrightarrow \mathbf{P_{mag} \sim B^2 \sim I^2 r^{-2}}$$

100 A at 2 mm radius is 100 G

1.0×10^7 A (**10 MA**) at **4 mm** radius is 50 MG = **1 MBar** of pressure!

2.5×10^7 A (**25 MA**) at **1 mm** radius is 500 MG = **100 MBar** of pressure!! ←**Z Machine**

(~1000x more than high explosives)

We are working toward the evaluation of the Magnetized Liner Inertial Fusion concept

Sandia National Laboratories

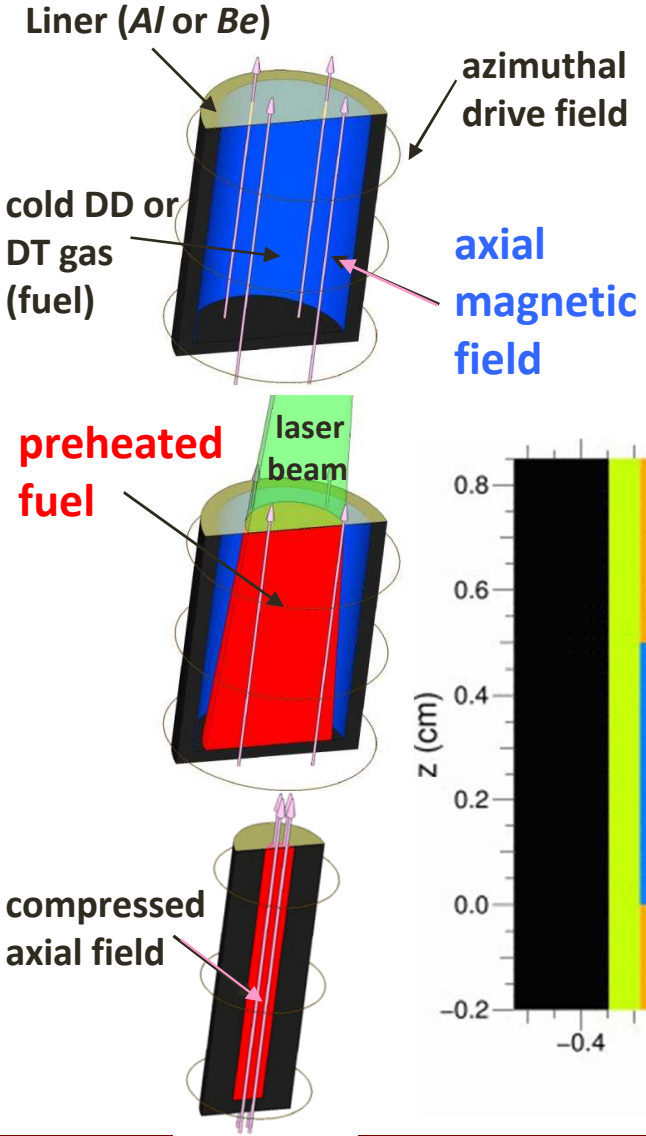

- The **initial B_z~10-40 T** flux is compressed to ~5-15 kT (~50-150 MG)
  - to reduce thermal electron conduction losses
  - to enable low ρR_{fuel} ignition ($B_z R_{fuel}$ and ρR_{liner} required instead)
- The fuel is **preheated** using the Z-Beamlet laser in order to reduce:
  - the convergence ratio (CR) needed to obtain T_{ion} > 4 keV
  - the implosion velocity needed to ≤ 100 km/s
  - the stagnation pressure needed to a few Gbar (not 100s Gbar)
- ***Thermonuclear yields have been measured on Z***

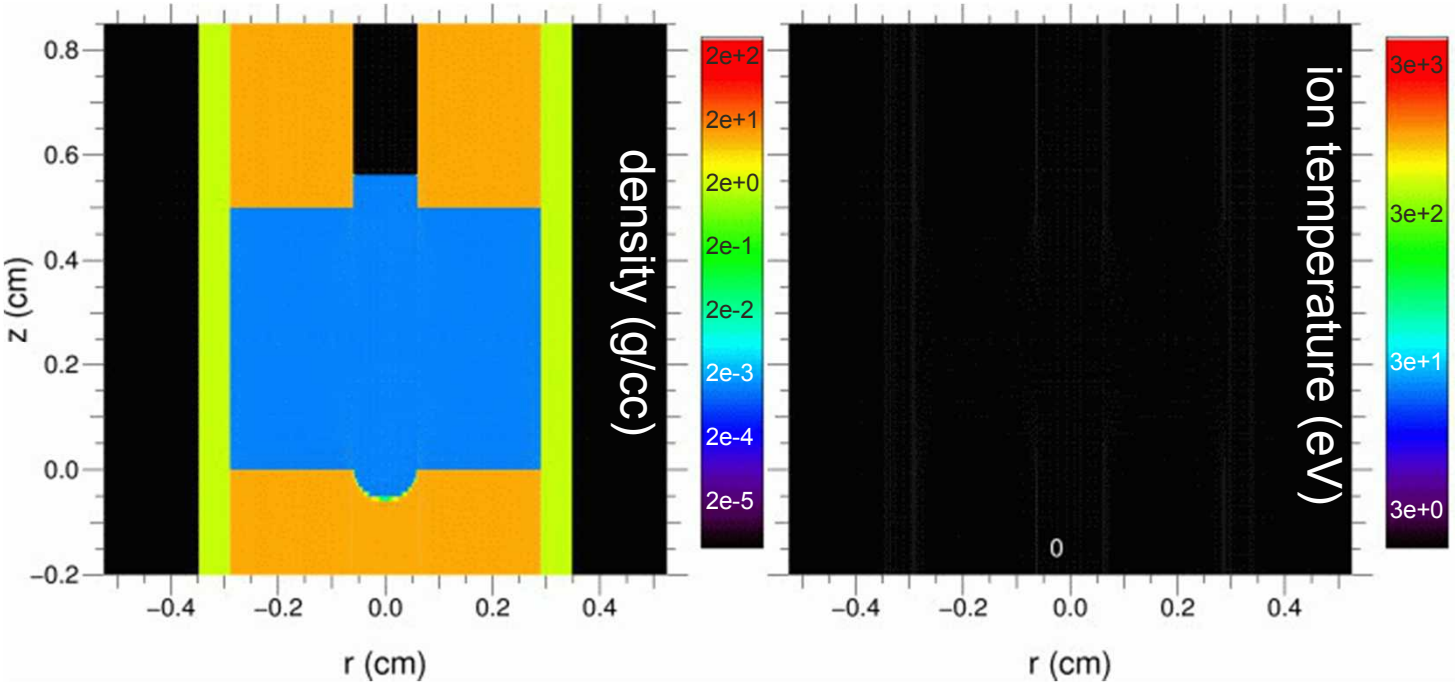

S. A. Slutz, et. al., Phys. Plasmas 17, 056303 (2010).

MagLIF uses the Z facility to compress a liner containing pre-magnetized and pre-heated D_2 gas

Sandia National Laboratories

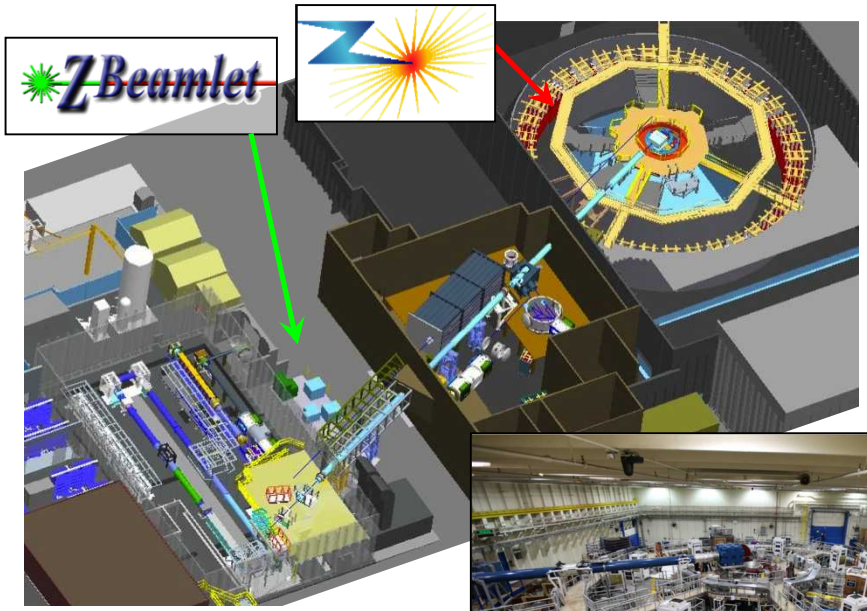

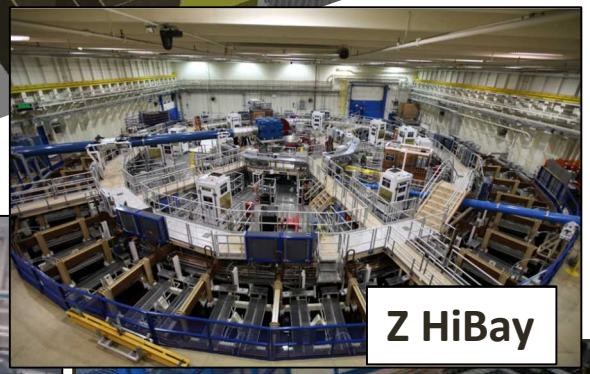

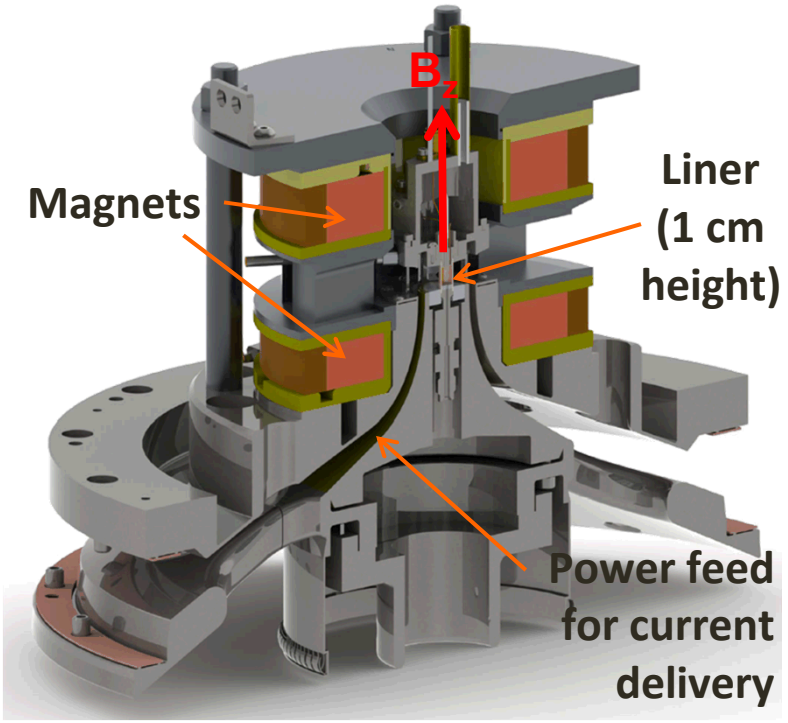

The necessary components were separately tested prior to integrated experiments

- Laser preheat
- Applied magnetic field
- Liner Stability
- Modified power flow

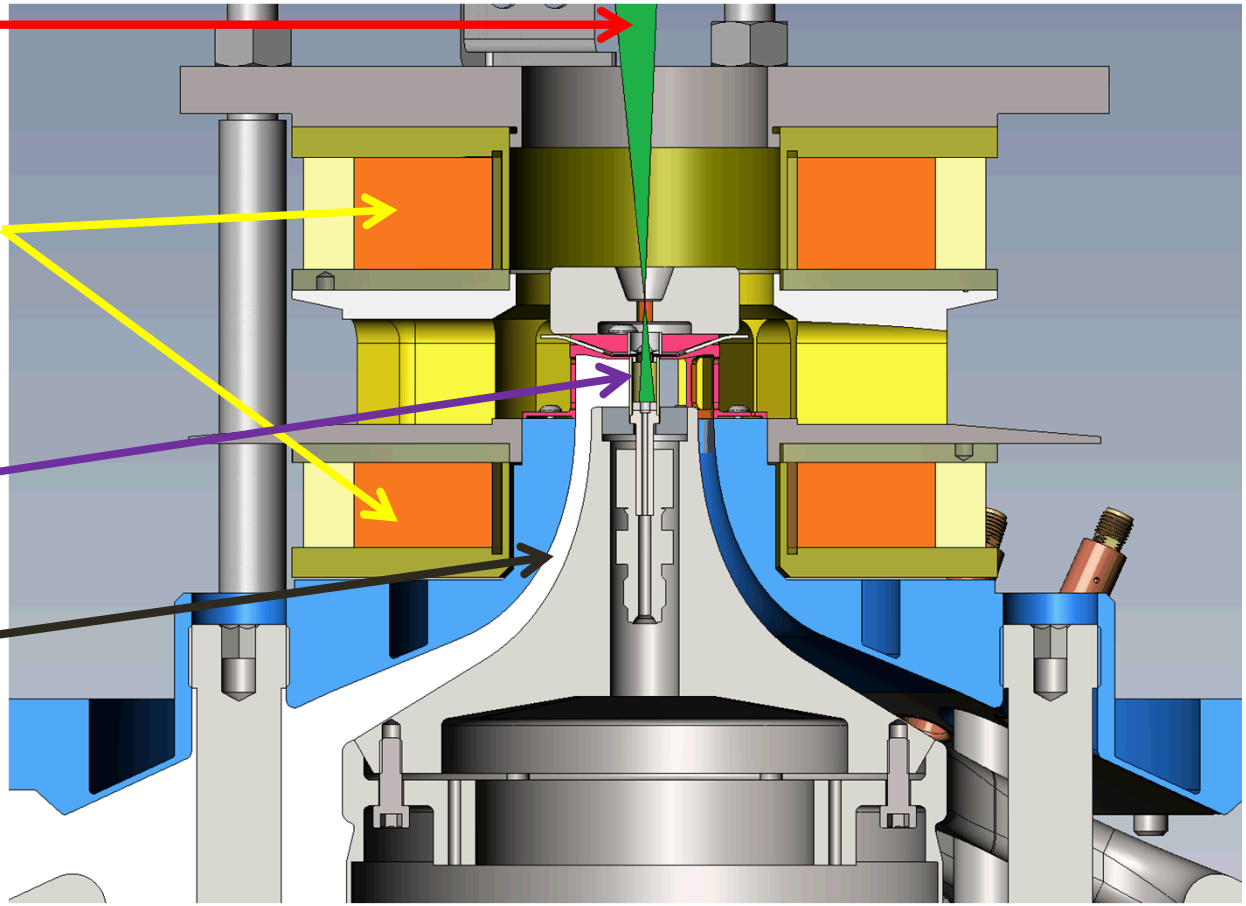

Radiographs of magnetized liners (no preheat) gave us a surprise and suggested enhanced stability

Sandia National Laboratories

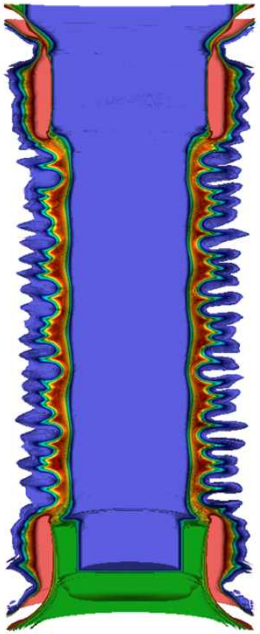

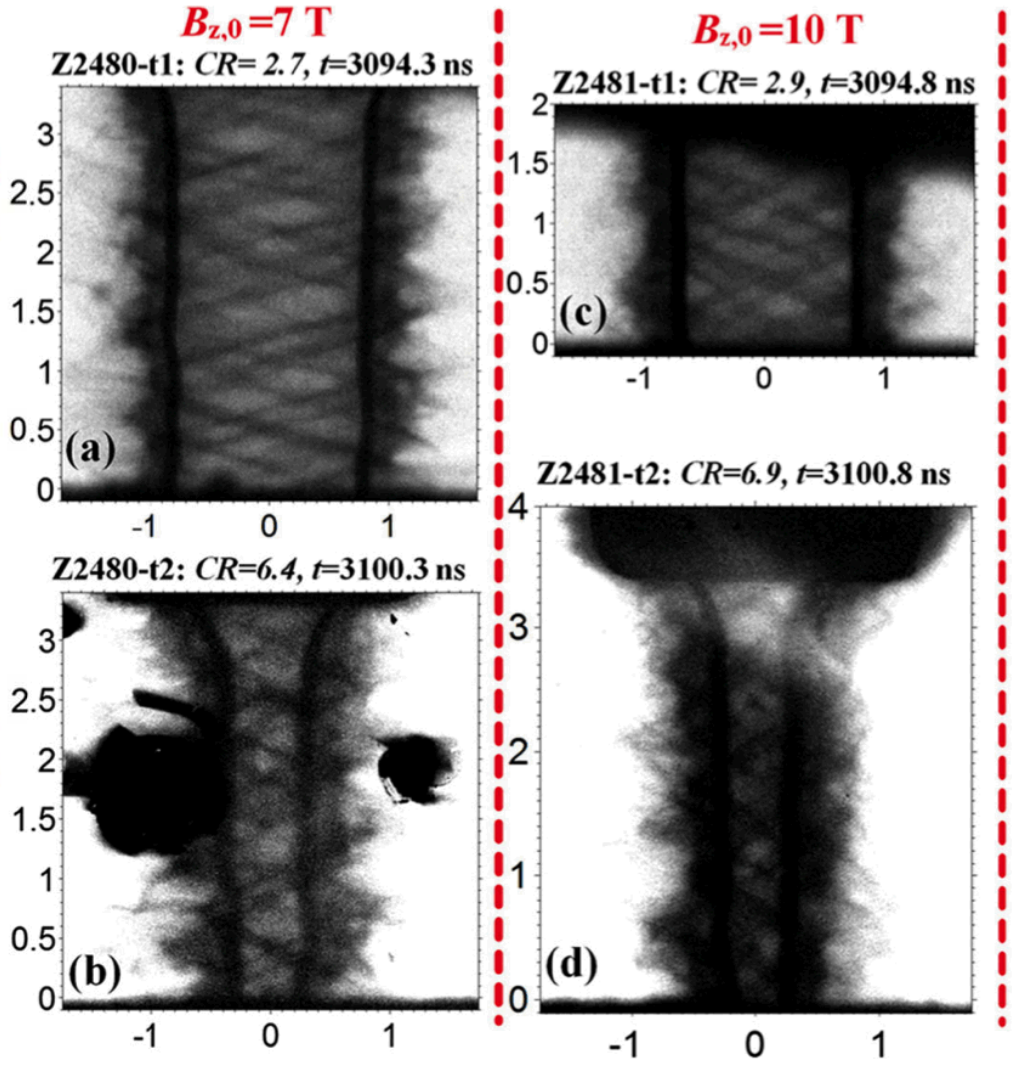

Liner-only flux compression experiments (with B_z, but without laser) measure $B_z(t)$ and $r_{inner}(t)$

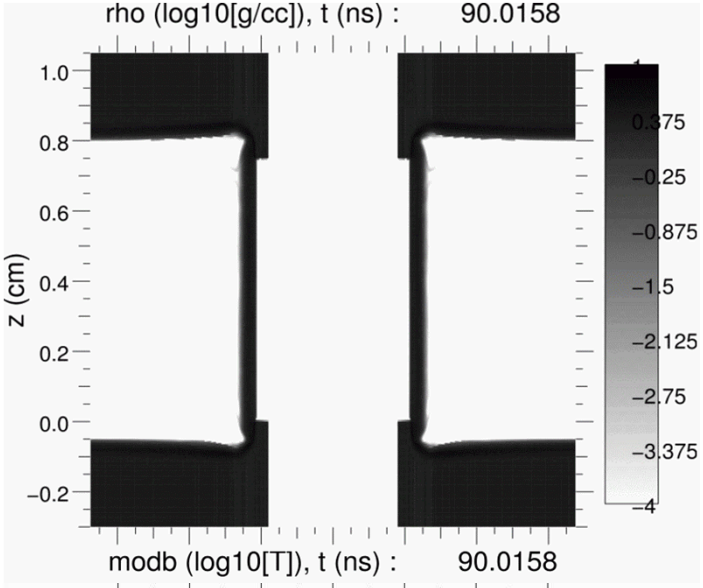

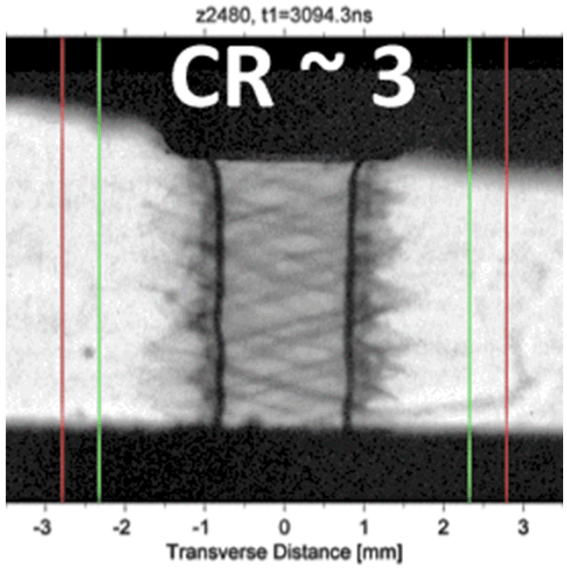

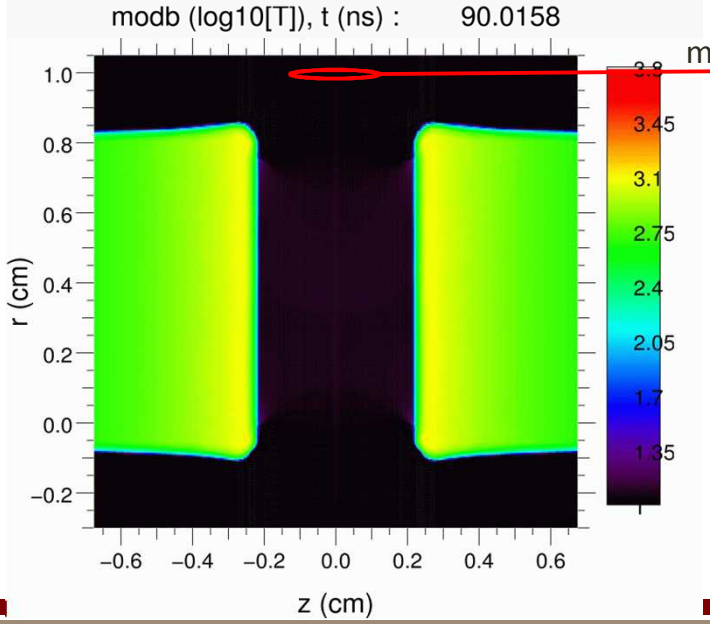

micro-Bdot probe

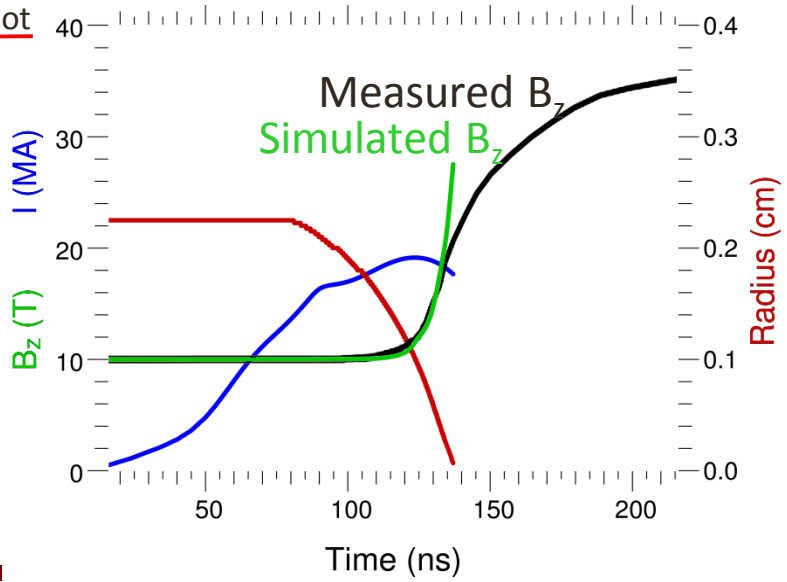

R. D. McBride, et. al., unpublished.

First integrated MagLIF experiments successfully demonstrated the concept

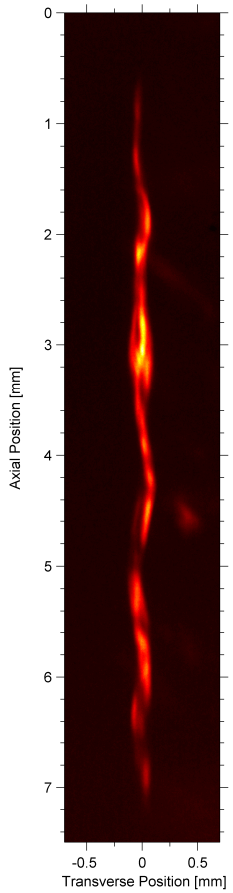

- Thermonuclear neutron generation up to 2e12
- Fusion-relevant stagnation temperatures
- Stable pinch with narrow emission column at stagnation
- Successful flux compression

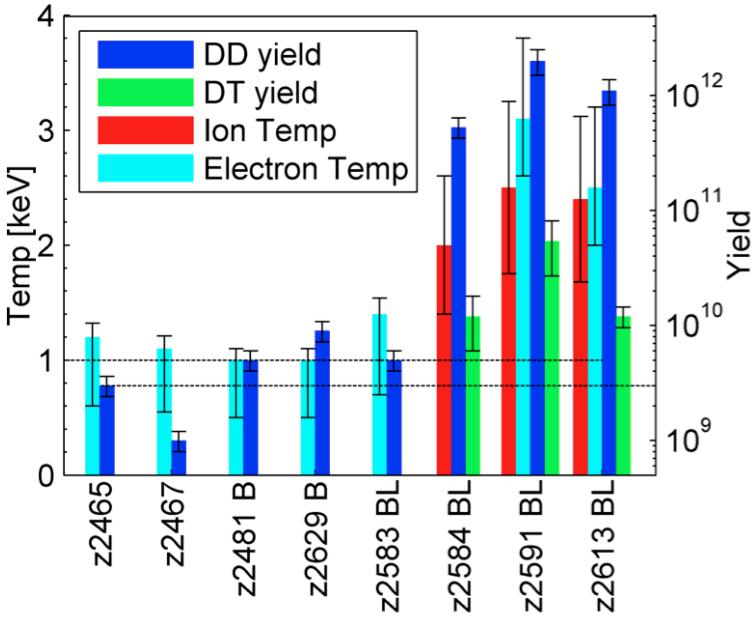

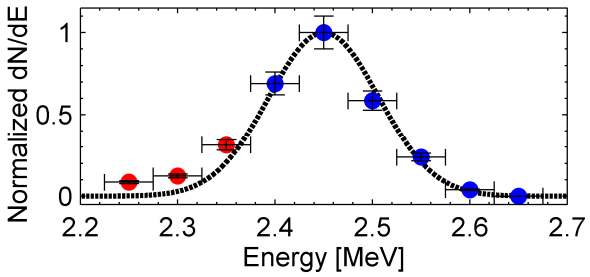

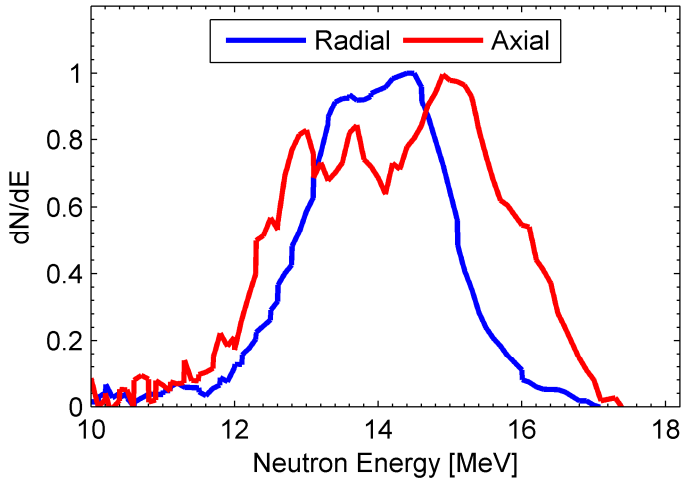

M. R. Gomez, et. al., Phys. Rev. Lett. (2014).

Outline

1. Magnetized Liner Inertial Fusion (MagLIF)
2. Comparisons of MagLIF-related experiments to simulations
3. OMEGA-EP laser-heating experiments
4. Magnetized hohlraum experiments at OMEGA
5. Mini-MagLIF at OMEGA

An integrated model seeks to realistically simulate experiments as they would occur on Z

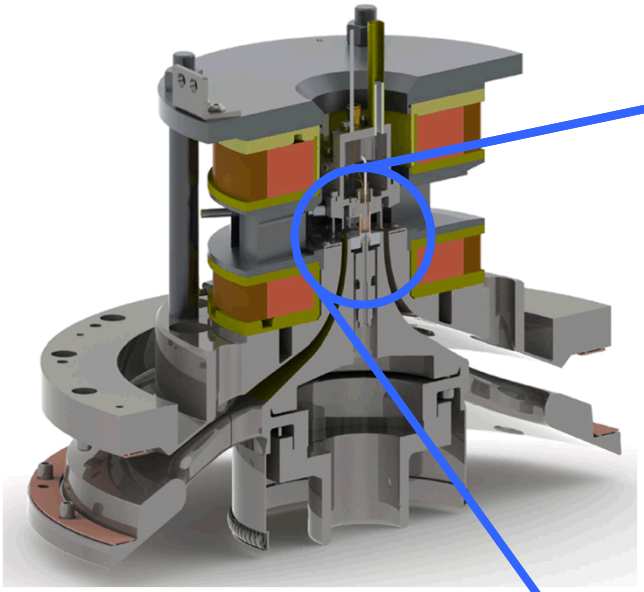

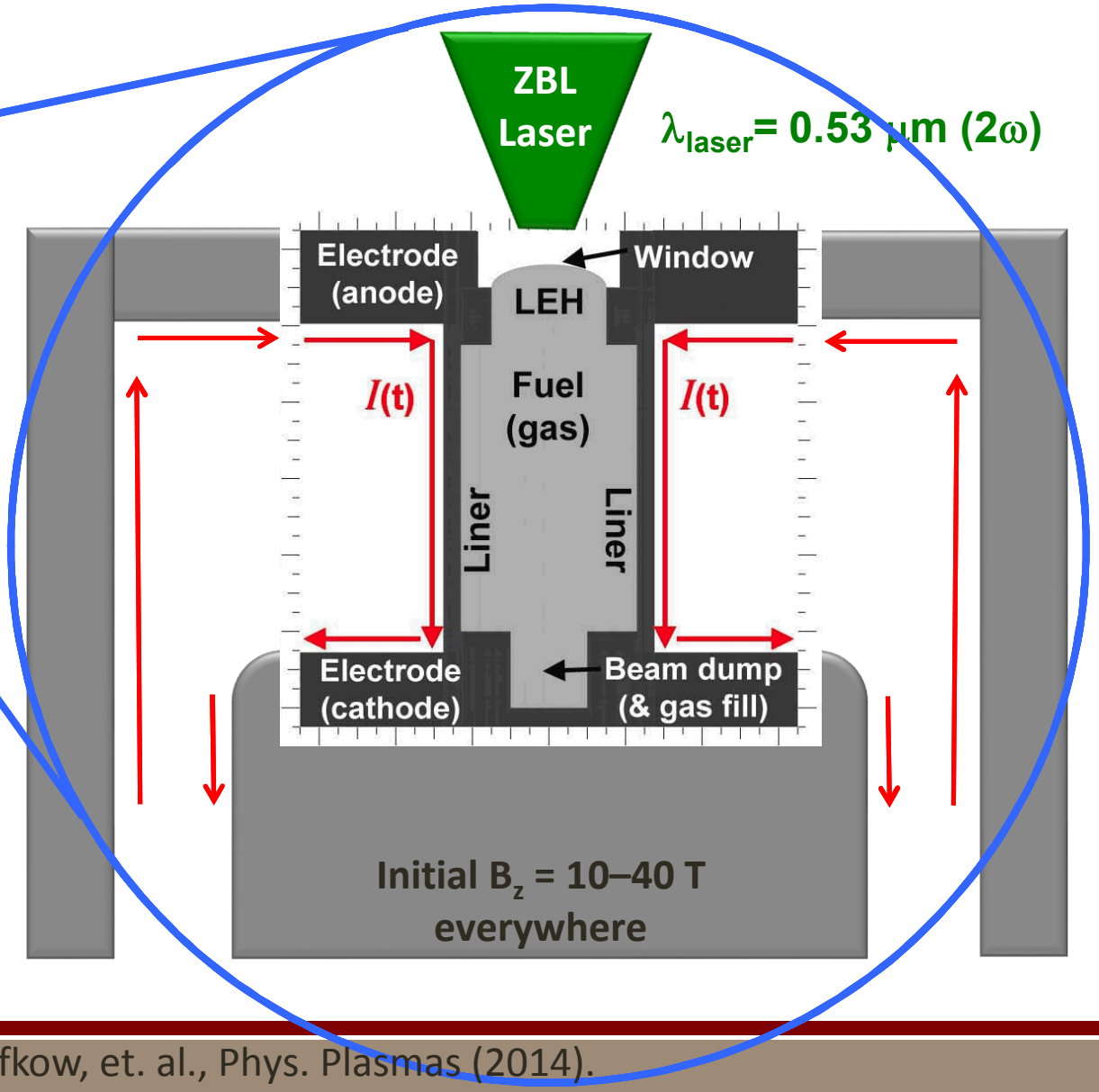

Self-consistently integrated into one simulation:

(1) Laser

(2) Laser entrance hole (LEH) and window

(3) Liner and circuit

(4) Electrode end caps

(5) Component interactions, timing, and optimization

A. B. Sefkow, et. al., Phys. Plasmas (2014).

An integrated model seeks to realistically simulate experiments as they would occur on Z

Sandia National Laboratories

And 3D is required for helical magneto-RT growth and 3D laser effects

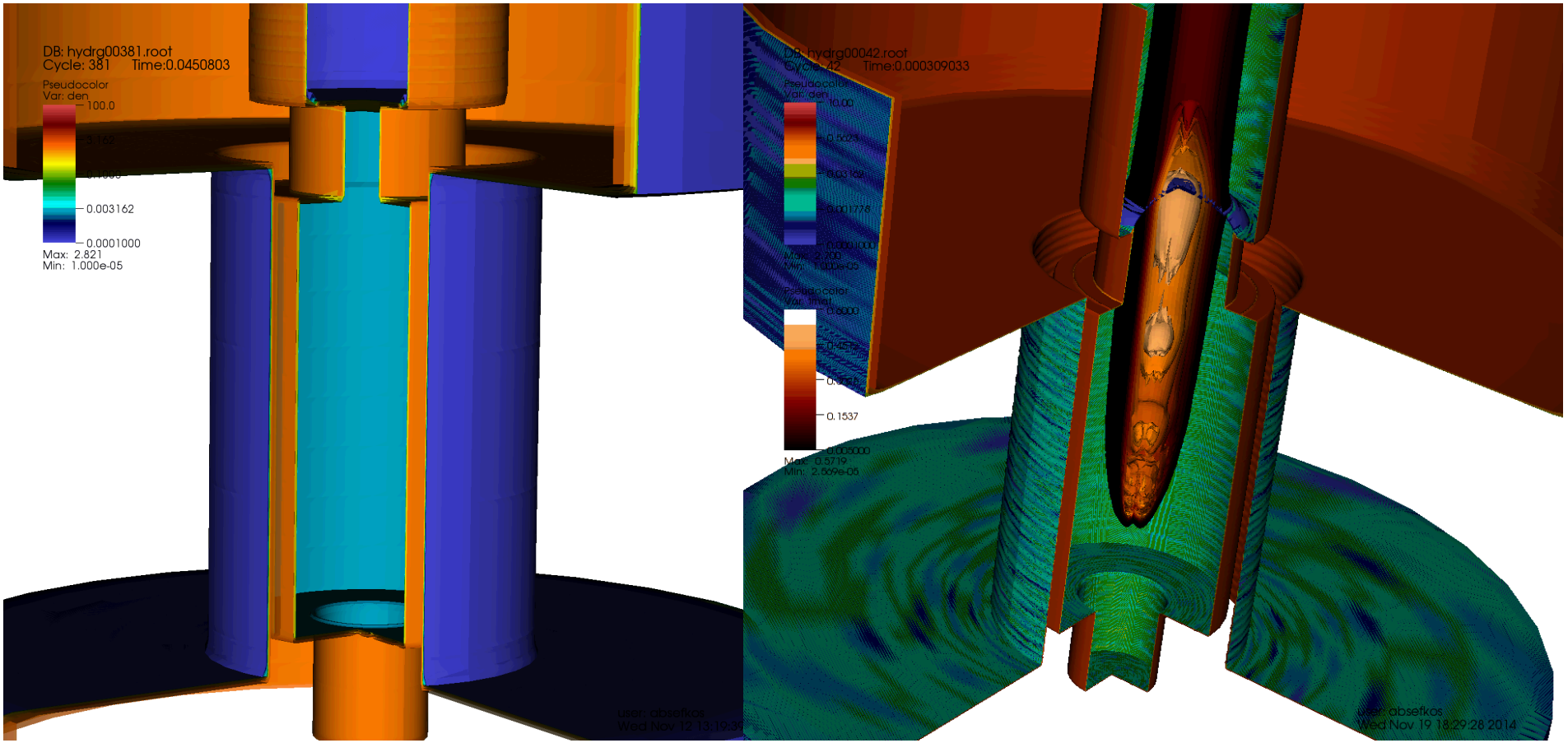

Laser-energy coupling reduction for near-term integrated experiments on Z

Sandia National Laboratories

If the energy absorbed by the gas is less than the optimal amount (due to low window transmission and/or LPI), temperature and yield reductions would be expected.

The effect is approximated with a series of integrated calculations wherein the main pulse energy is decreased from full to none.

The experimental yields may be consistent with low transmitted laser energies measured in related "focused" experiments

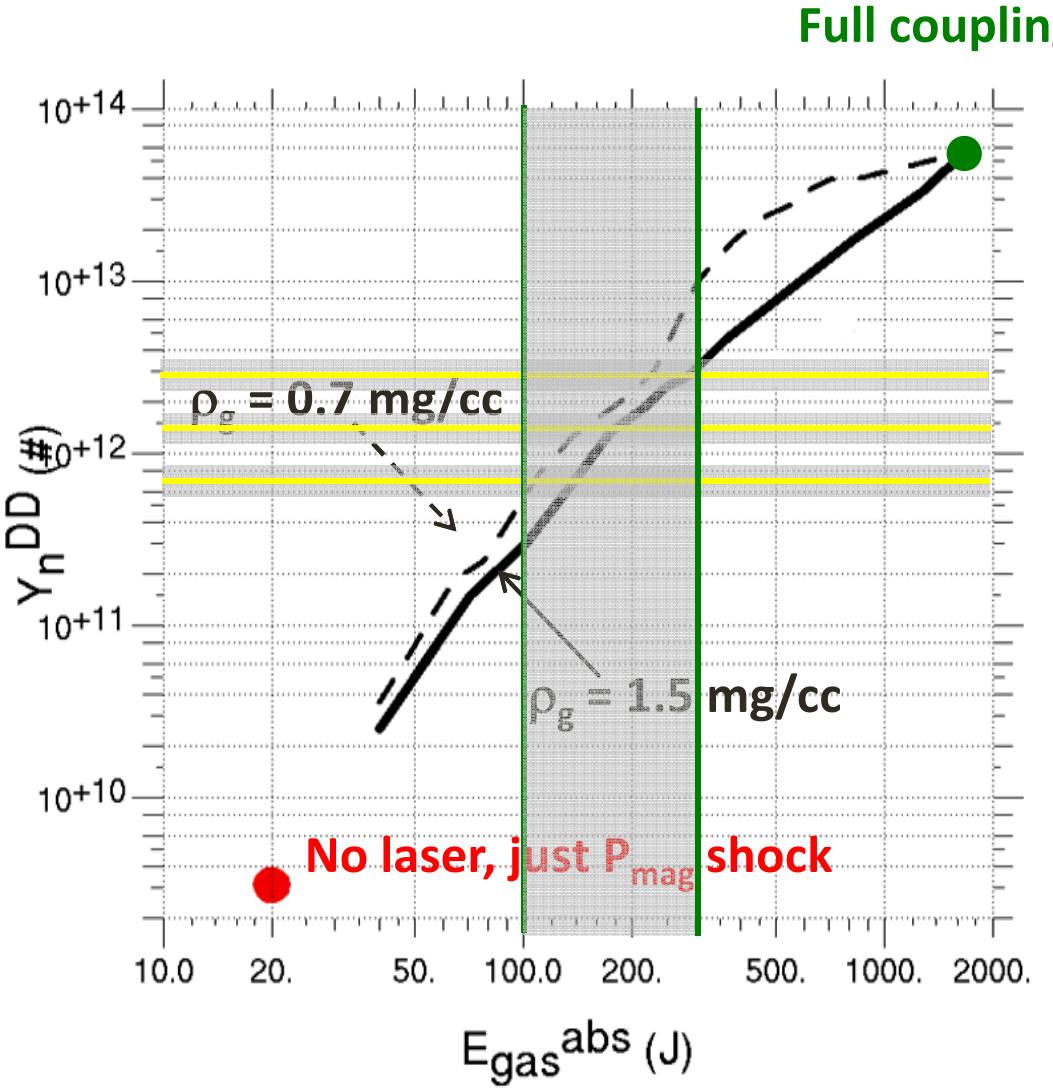

A. B. Sefkow, et. al., Phys. Plasmas (2014).

Estimate for 3.4 μm window transmission is FWHM~450±150 μm gaussian beam with ~200 J

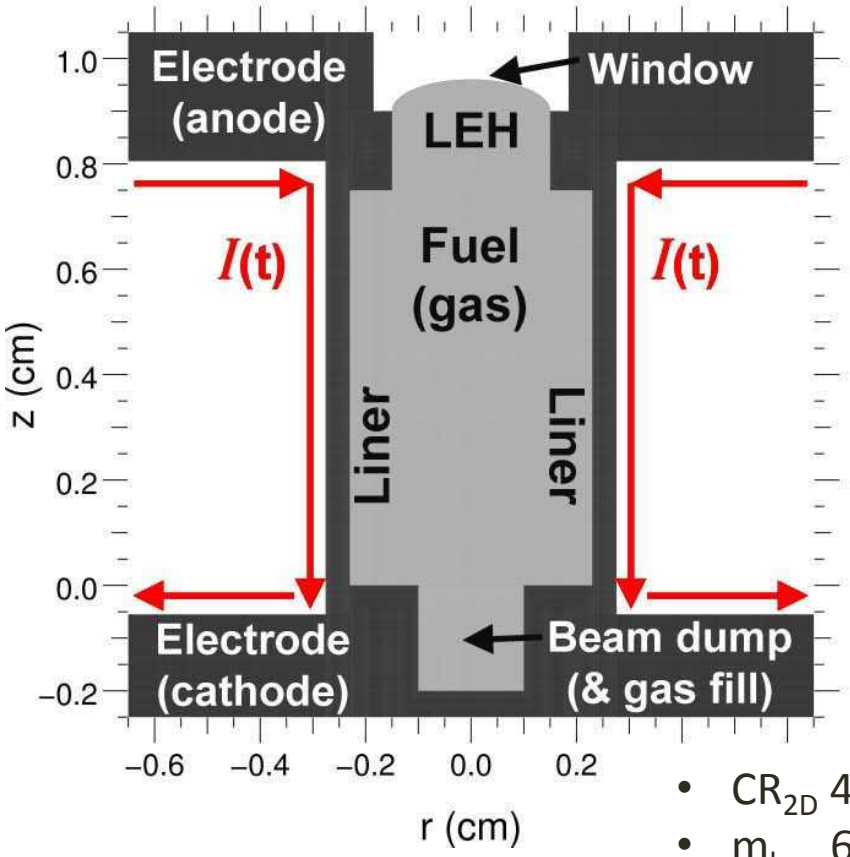

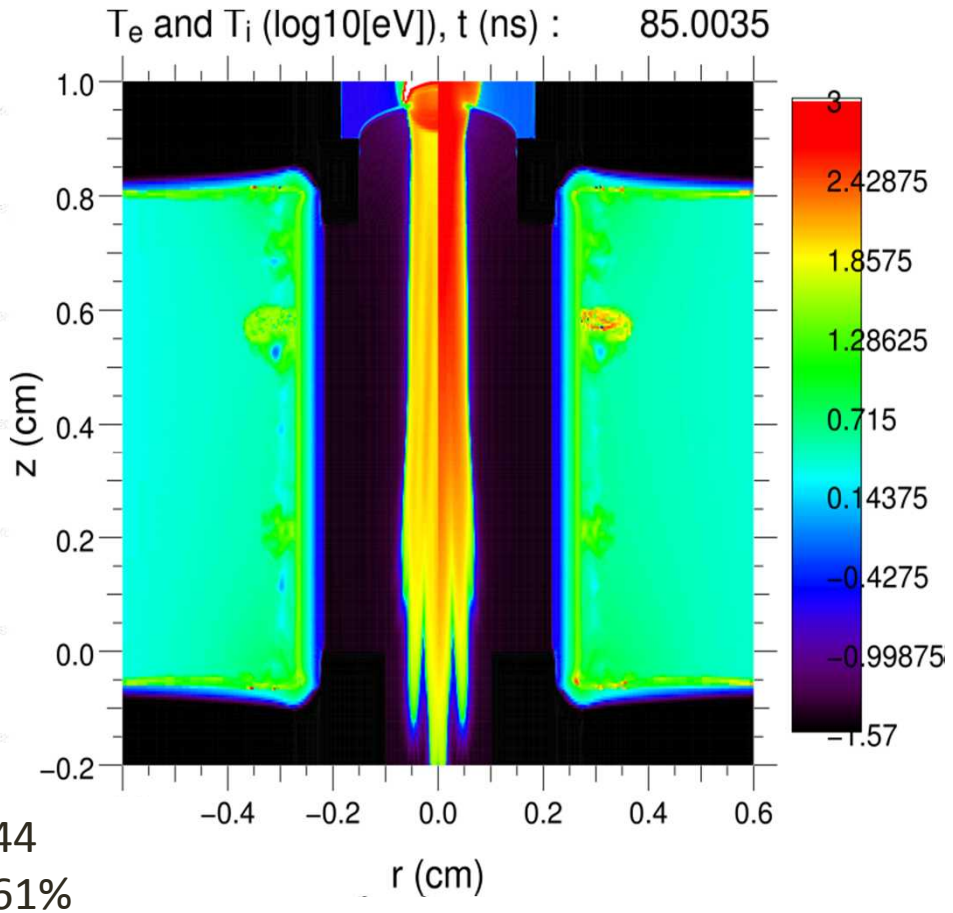

- CR_{2D} 44
- m_{loss} 61%
- Φ_{loss} 53%
- $\langle T_i \rangle^{DD}$ 3.0 keV
- $\langle T_{e/i} \rangle$ 2.7 keV

Current and implosion time agree within error

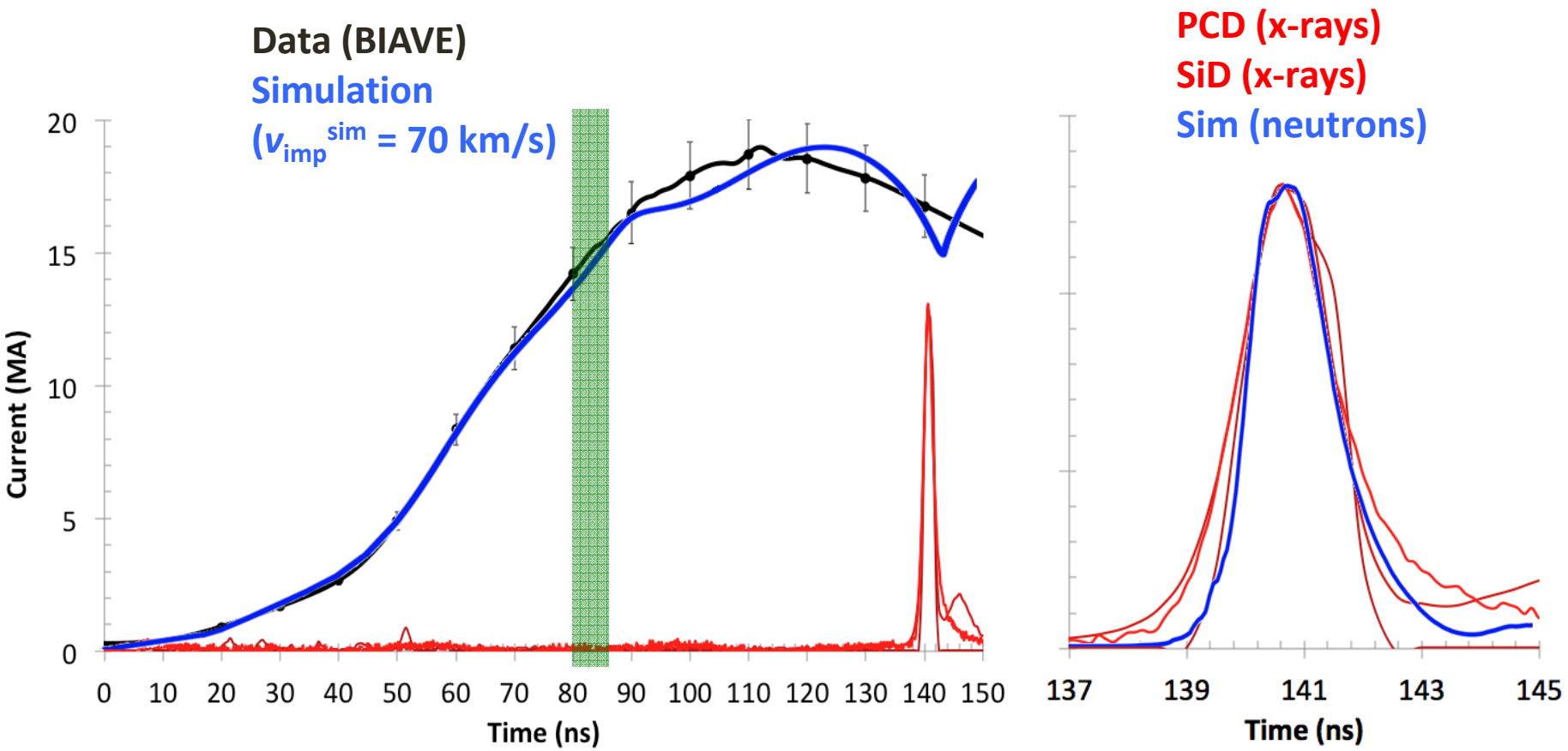

Comparison of stagnation column shape, not accounting for liner instability or opacity

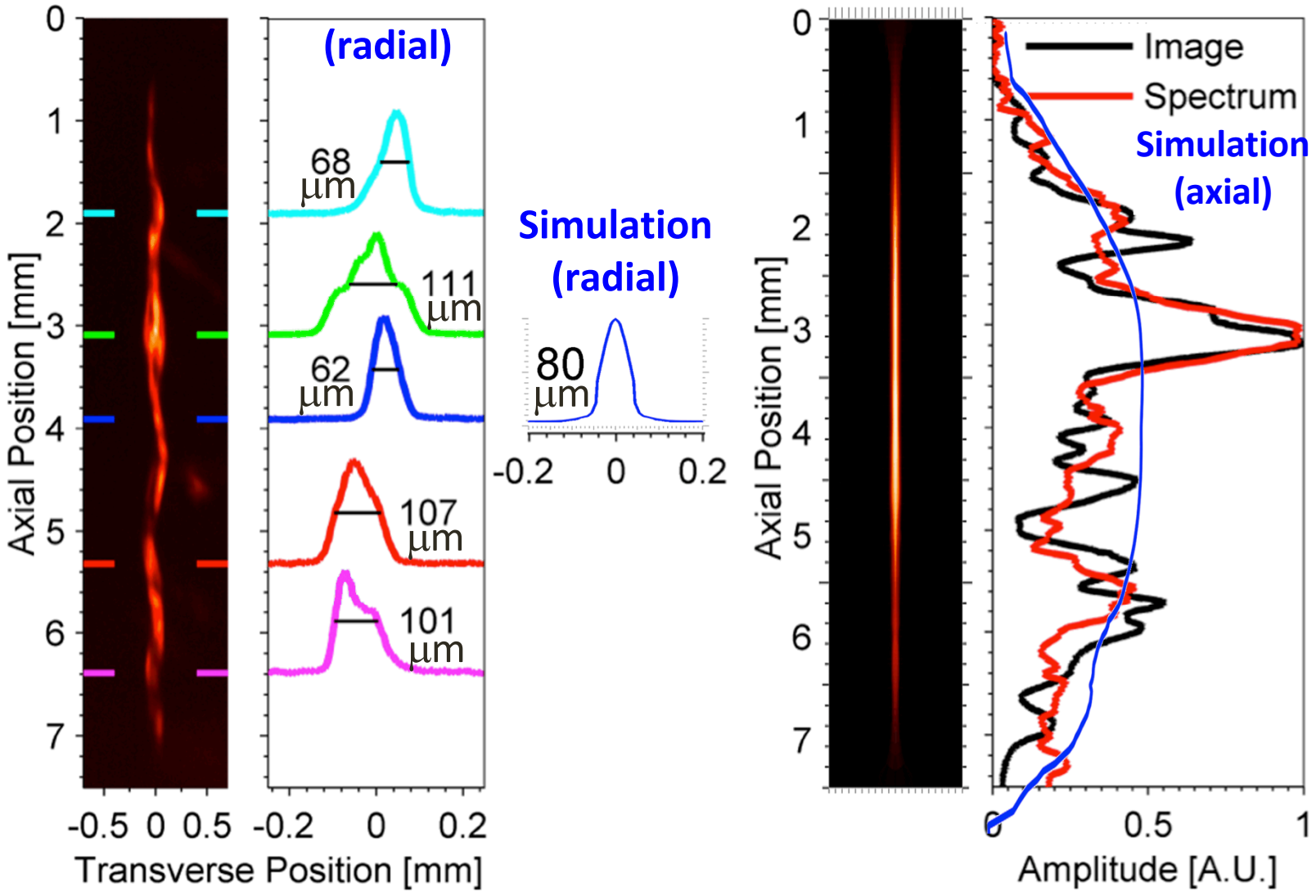

A. B. Sefkow, et. al., *in preparation* (2015).

Variation in self-emission and liner opacity contribute to observed structure

Sandia National Laboratories

Data Example 1

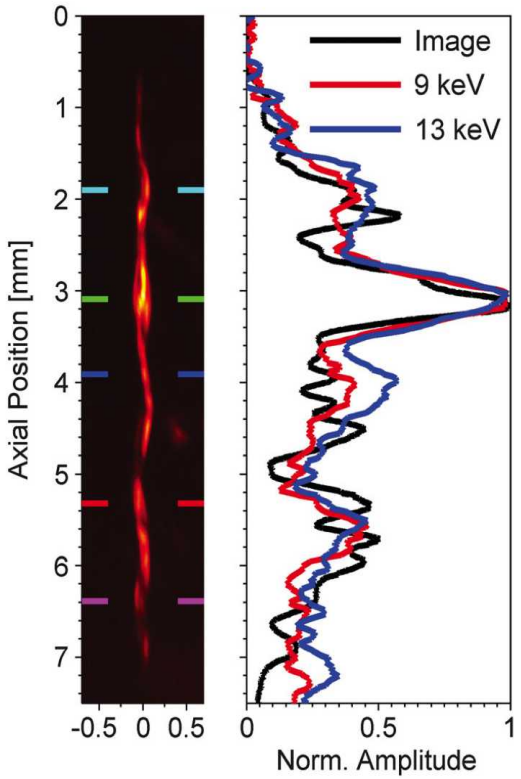

Data Example 2

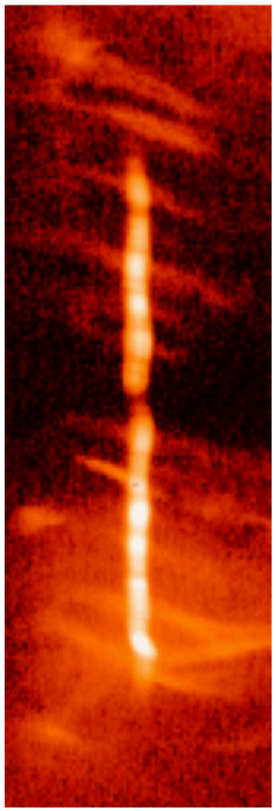

Example 2D simulated radiograph

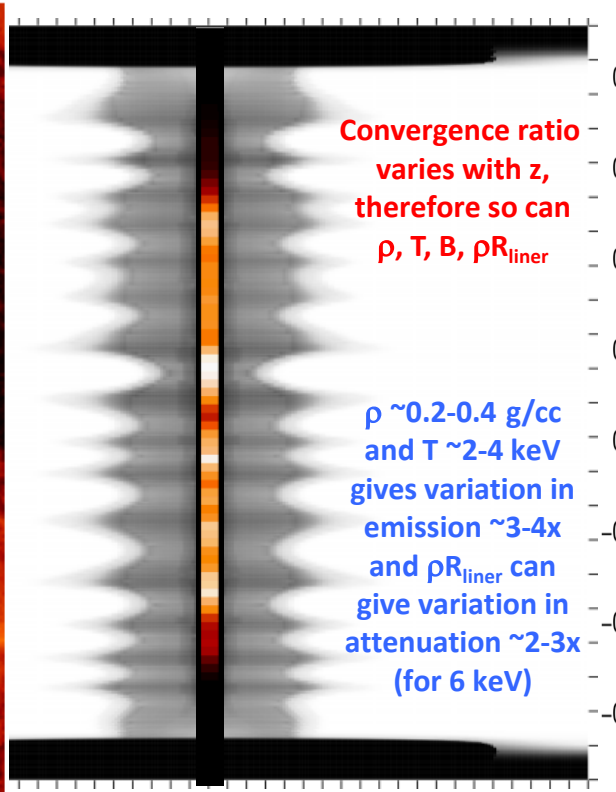

Integrated self-emission accounting for liner opacity and detector resolution

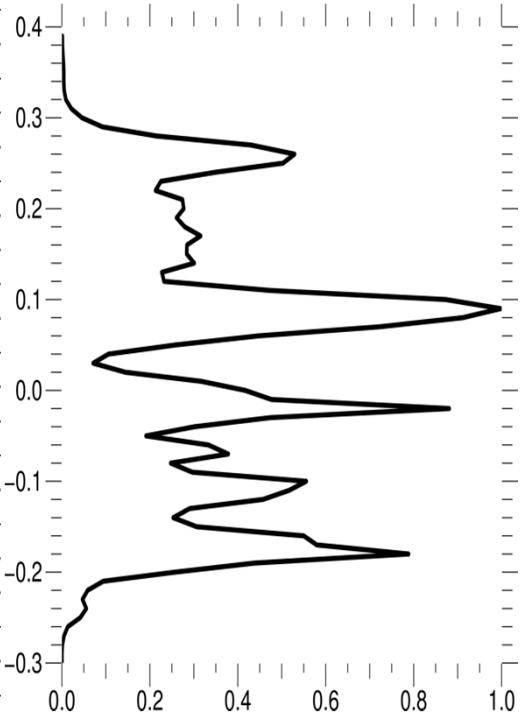

However, helical emission and radiographs require 3D simulations

A. B. Sefkow, et. al., *in preparation* (2015).

In 3D with B_z, simulations show helical perturbations grow as well as improve stability due to m=0 suppression

Exp

Sim

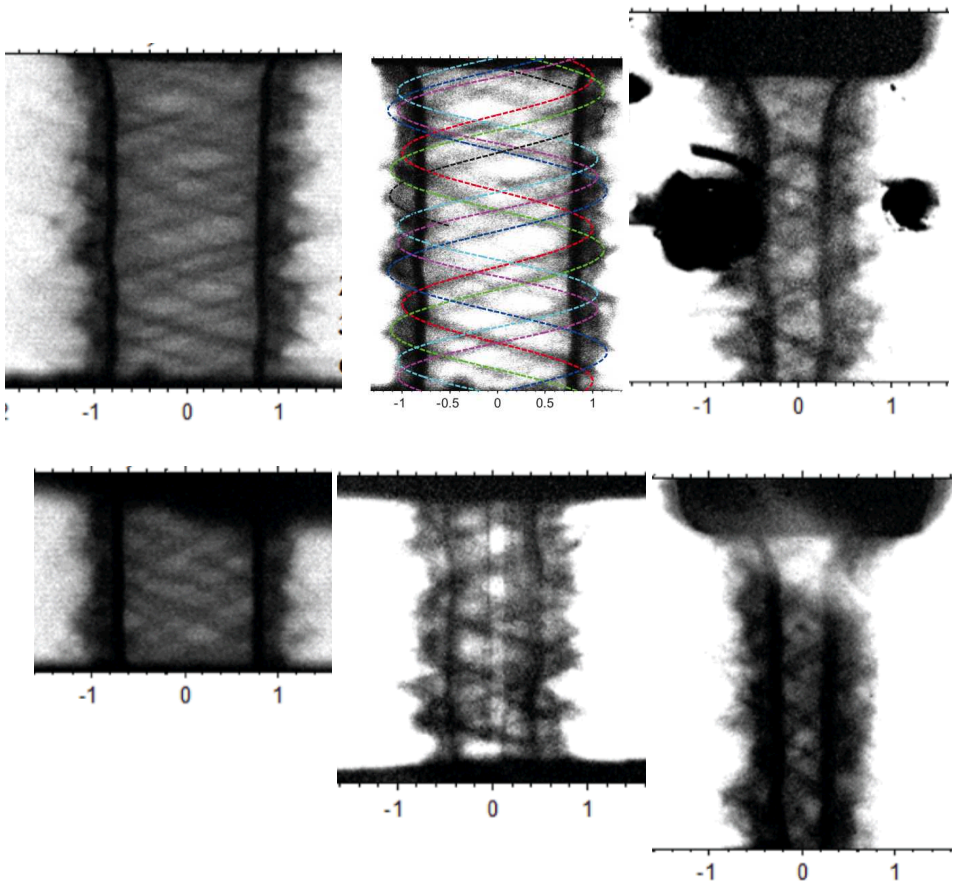

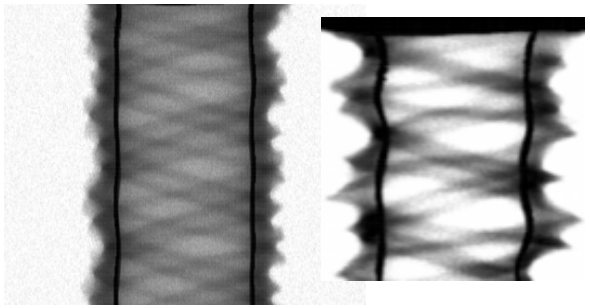

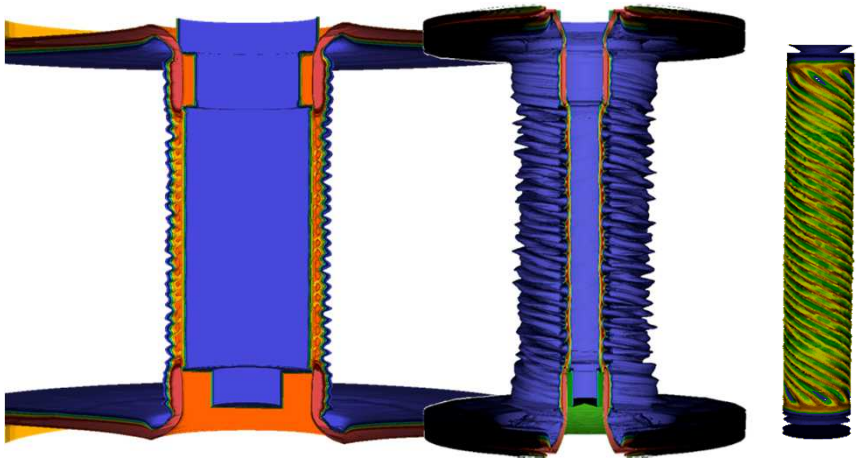

Imposed helical perturbation grows w/ constant pitch and enables high convergence ratio implosions

T. J. Awe., et. al., *Phys. Rev. Lett.* (2013)

A. B. Sefkow, et. al., *in preparation* (2015).

Full 3D with helical instability growth is needed to correctly simulate the stagnation column

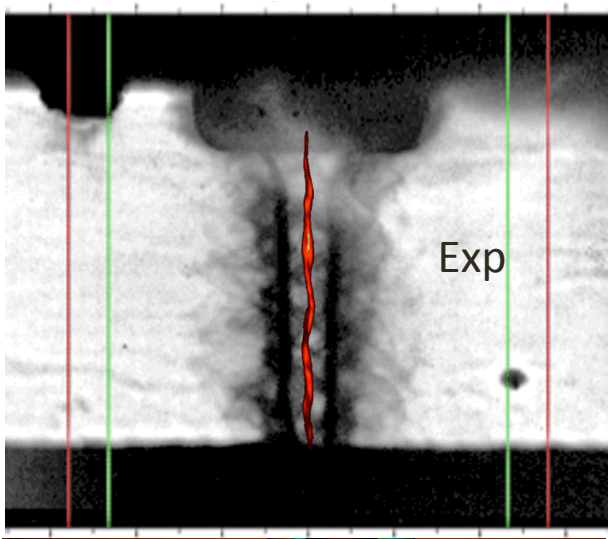

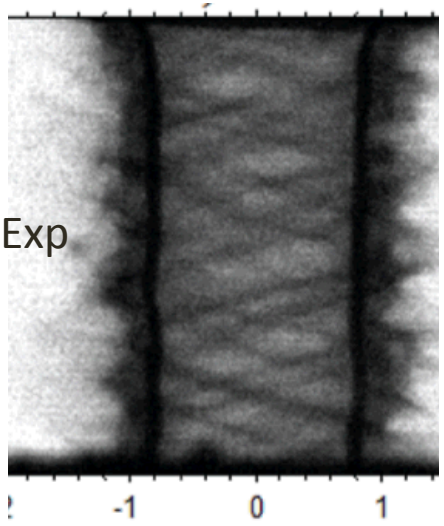

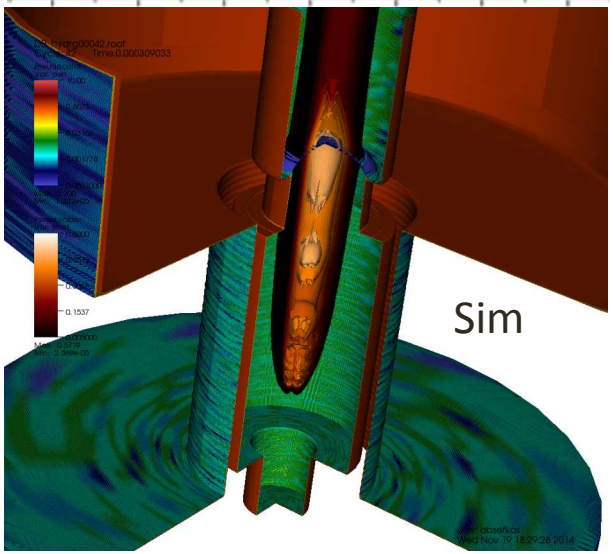

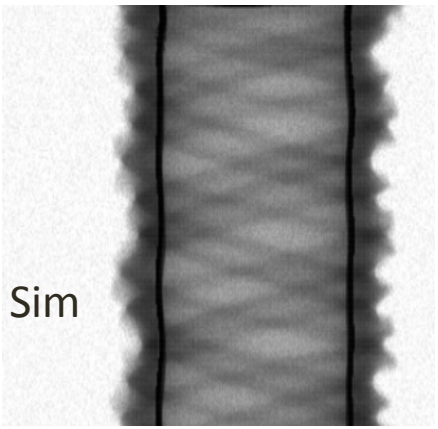

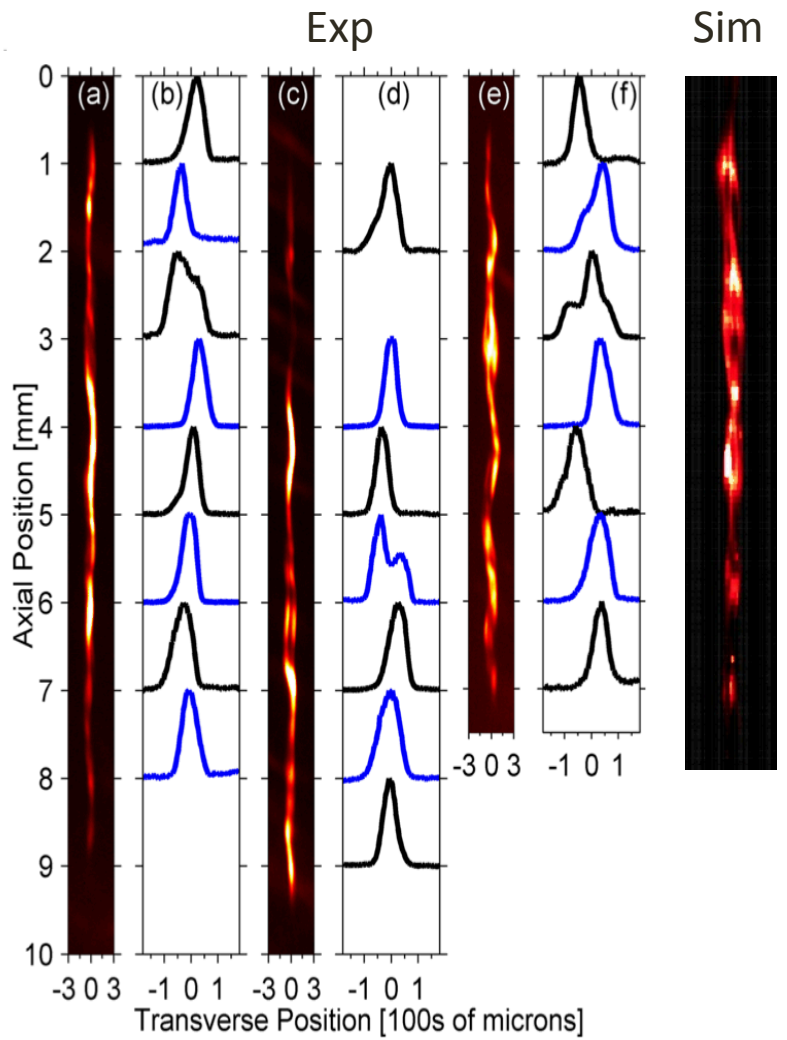

A. B. Sefkow, et. al., *in preparation* (2015).

Trend of helical perturbation with imposed B_z as produced by first principles PIC simulation

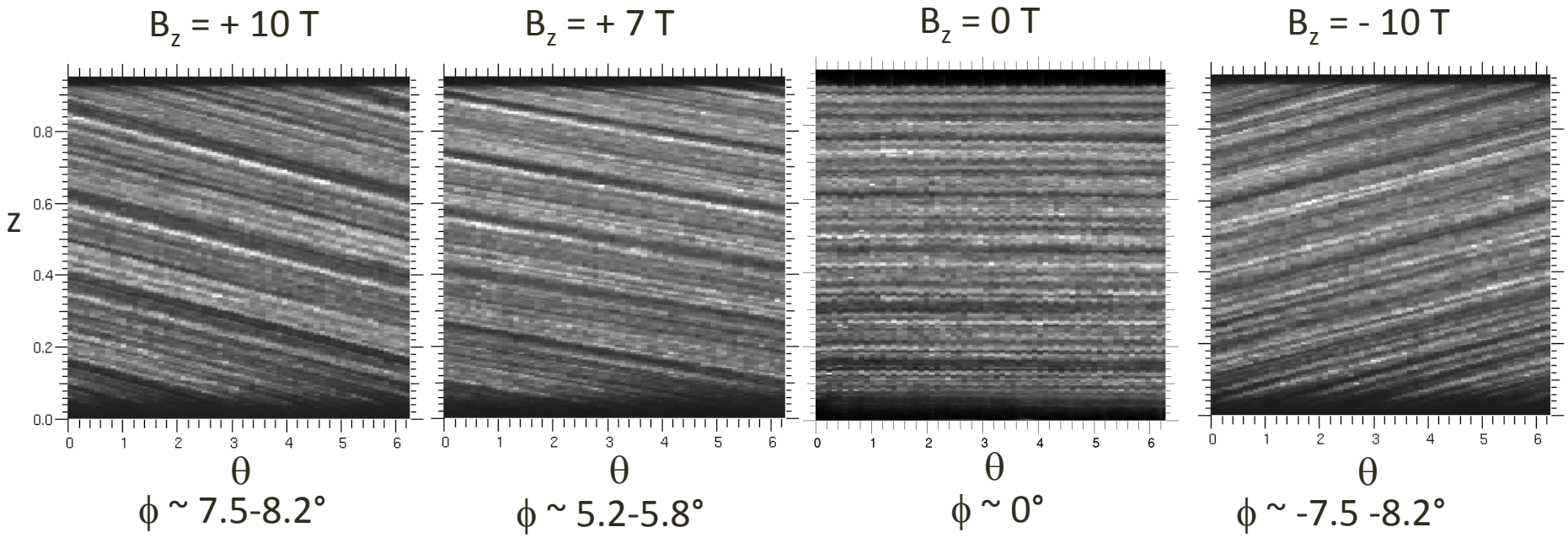

XUV emission on COBRA,
L. Atoyan et. al. (Cornell)
APS-DPP 2014 Poster →

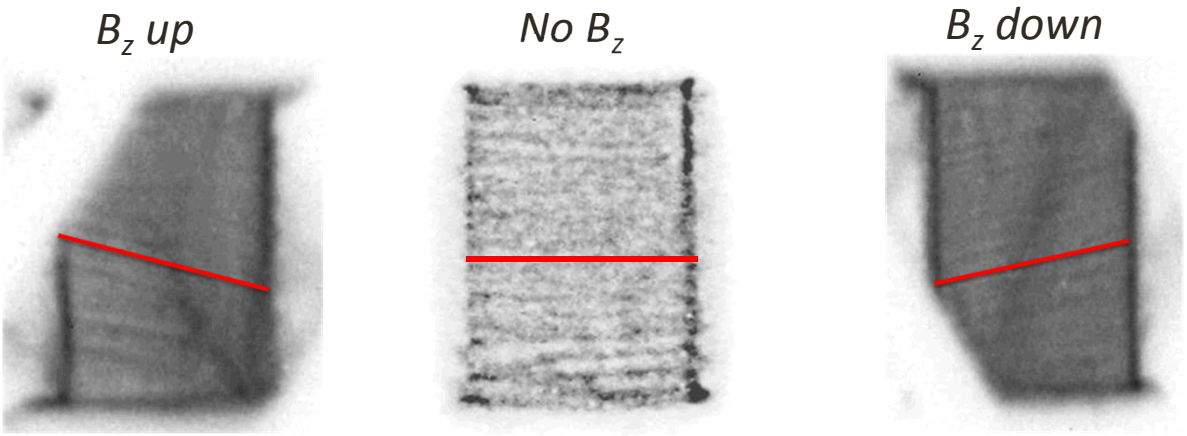

A. B. Sefkow, et. al., *in preparation* (2015).

The ~0.2 and ~1.0 mm modes have implications

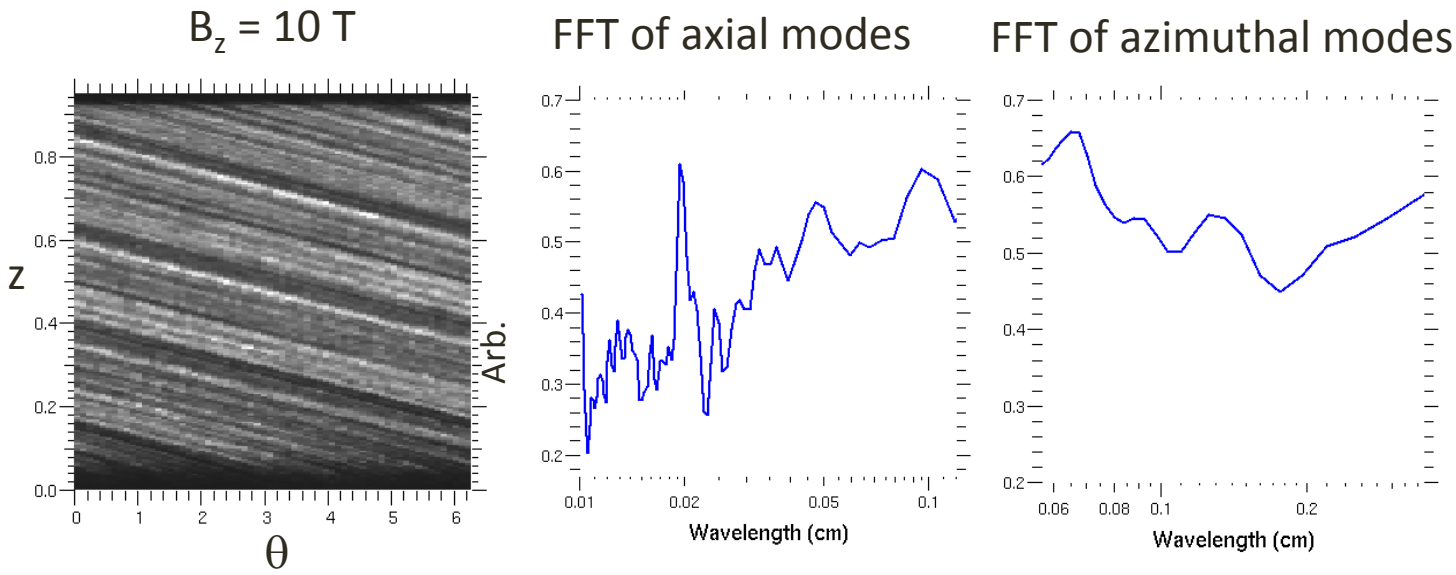

- Short axial λ_z ~0.2 mm mode gives the helical straitions in radiographs
- Long axial λ_z ~1 mm mode imprints at the liner/gas interface and gives the helical self-emission image at stagnation

A. B. Sefkow, et. al., *in preparation* (2015).

Explanation of helical stagnation mechanism

Early-time inner boundary *density*

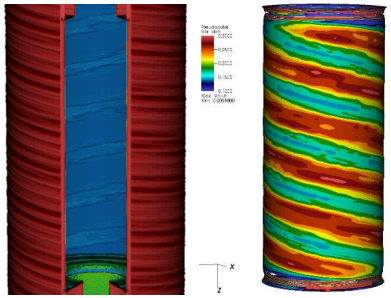

Long axial λ_z ~1 mm is from early-time feedthrough and imprints at the liner/gas interface

Since the interface is magneo-Rayleigh-Taylor stable, the gas is high β, and flux pile-up occurs there, λ_z also imprints on B_z

Inner boundary B_z

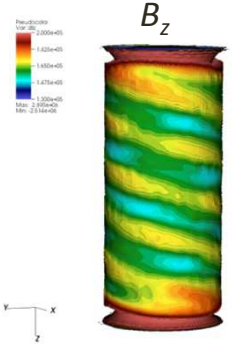

Late-time inner boundary *density* B_z

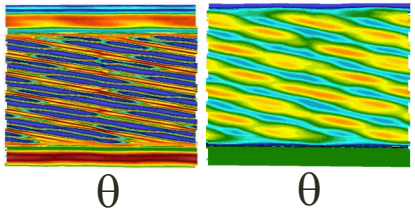

As in helical perturbation on rear side of liner, inner surface helix persists and grows as well

Resulting structure does not strongly modify 2D physics

Exp Sim

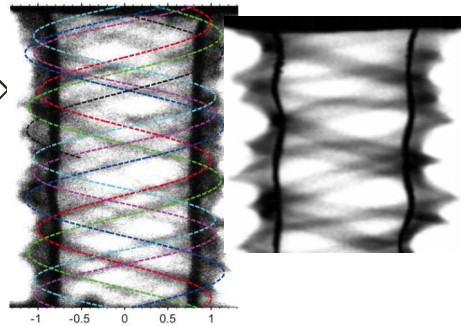

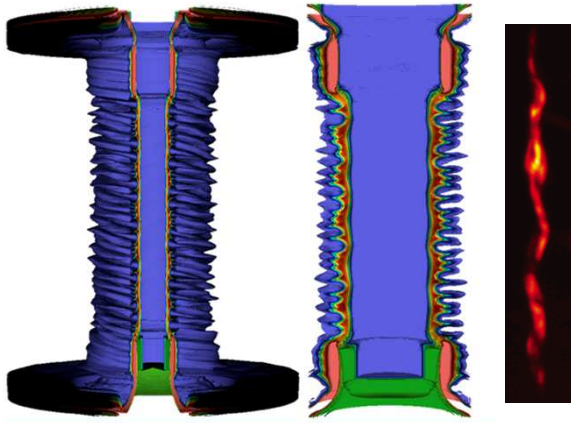

Resulting weakly helical (dr << dz) emitting stagnation column remains quasi-2D such that $P_{stag}^{exp} \sim P_{stag}^{3D} \sim P_{stag}^{2D} \sim 1$ Gbar

When not accounting for variations due to convergence as *f*(z), the averaged quantities may be approximately described even in 1D

A. B. Sefkow, et. al., *in preparation* (2015).

Experimental neutron spectra from z2591

primary

$$D + D \underset{50\%}{\rightarrow} He^3\ (0.82\,MeV) + n\ (2.45\,MeV)$$
$$D + D \underset{50\%}{\rightarrow} T\ (1.01\,MeV) + p\ (3.02\,MeV)$$

secondary

$$D + T \rightarrow He^4\ (3.52\,MeV) + n\ (14.1\,MeV)$$

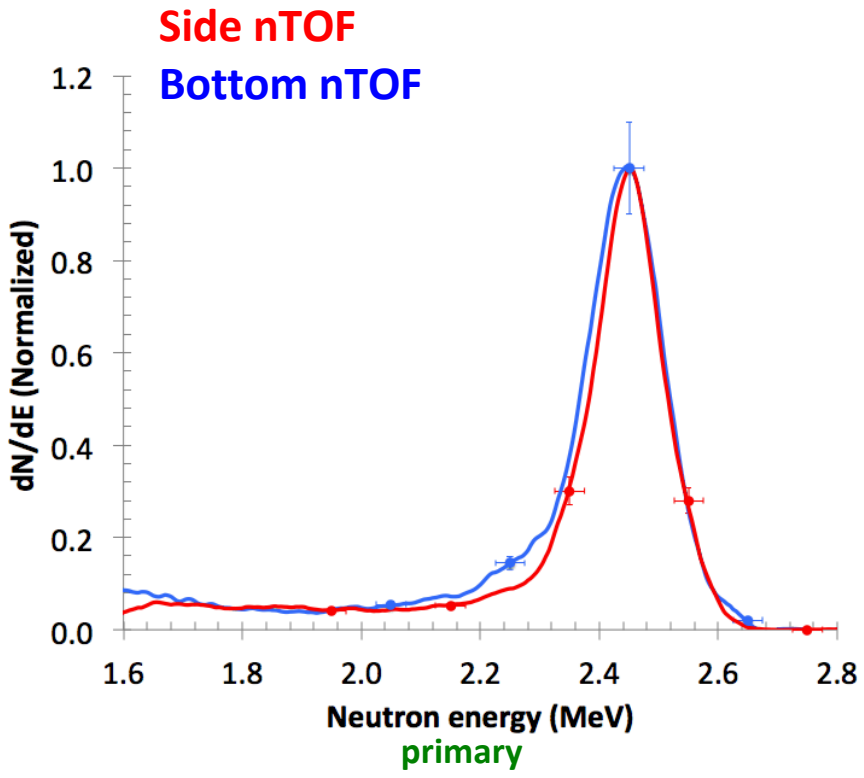

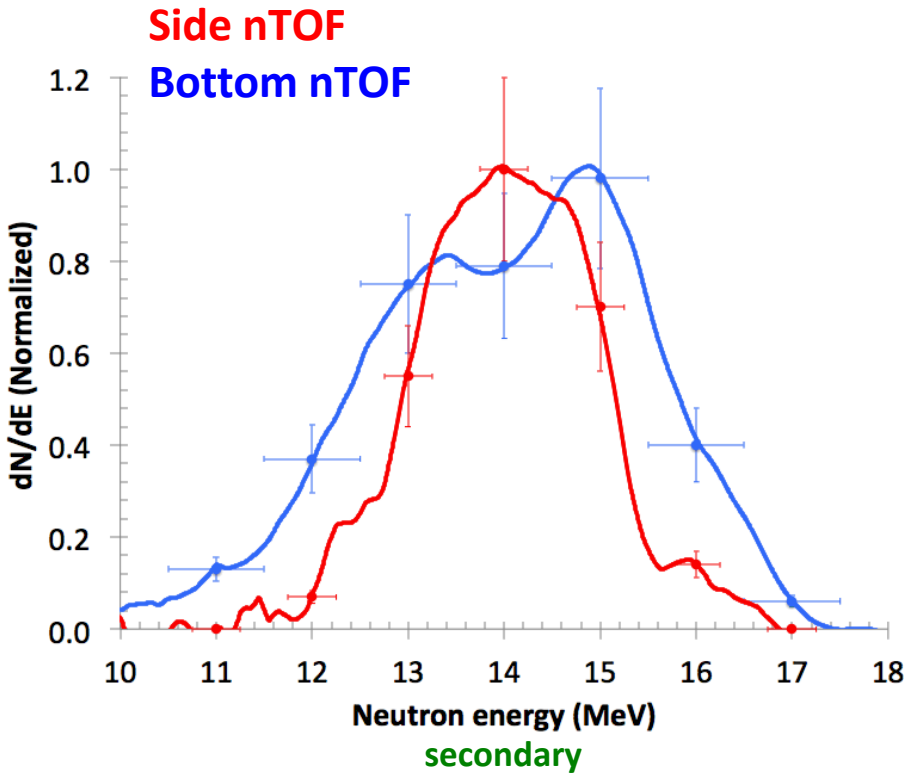

Particle (PIC) simulations are used to generate synthetic neutron spectra

Sandia National Laboratories

LSP simulations are initialized with HYDRA output (n, T, B) just before stagnation, and then run through burn.

All ions are evolved kinetically

$$D + D \xrightarrow[50\%]{} He^3\ (0.82\,MeV) + n\ (2.45\,MeV)$$
$$D + D \xrightarrow[50\%]{} T\ (1.01\,MeV) + p\ (3.02\,MeV)$$
$$D + T \rightarrow He^4\ (3.52\,MeV) + n\ (14.1\,MeV)$$

Synthetic neutron detectors are located to the side, top, and bottom of the stagnation column

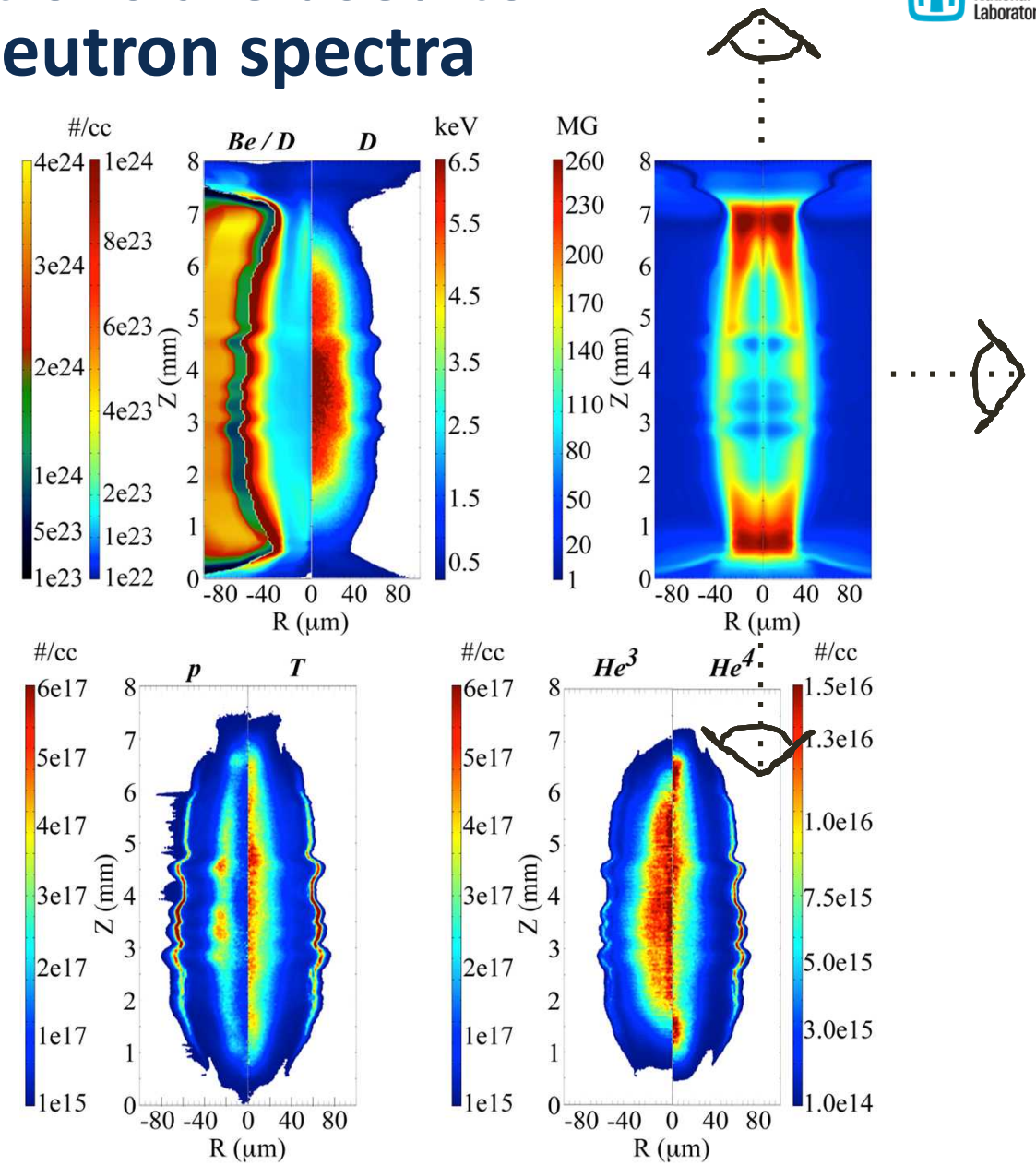

Comparison of neutron spectra

Sandia National Laboratories

primary

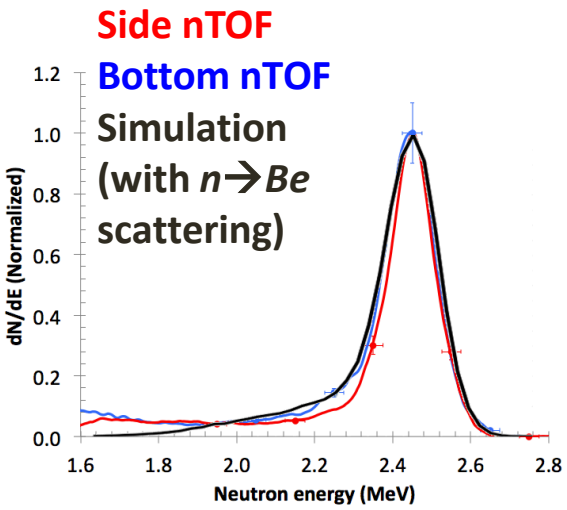

secondary

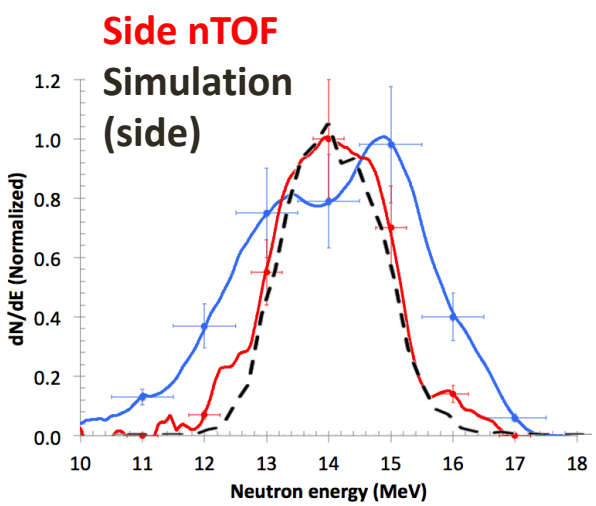

secondary

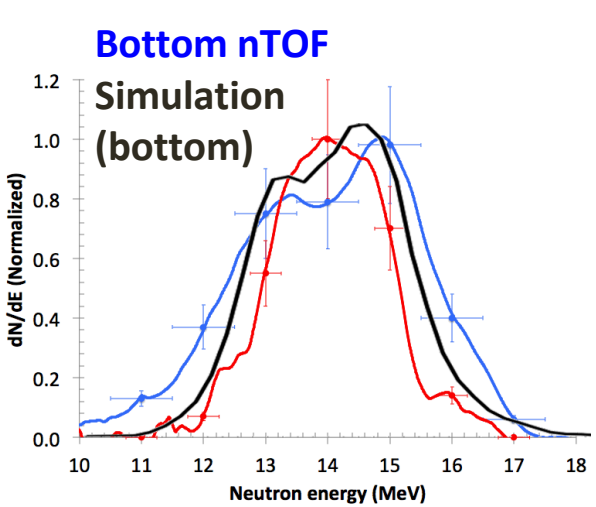

Simulation

$Y_n^{DD} = 2.5e12$

$Y_n^{DD}/Y_n^{DT} = 49$

Experiment

$Y_n^{DD} = (2.0 \pm 0.5)e12$

$Y_n^{DD}/Y_n^{DT} = 40 \pm 20$

Comparison of liner emission

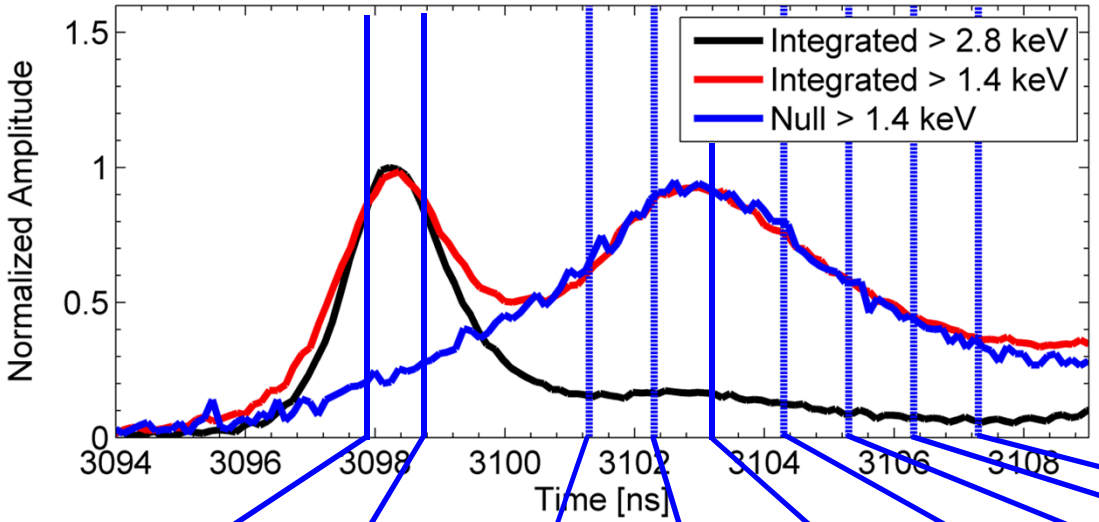

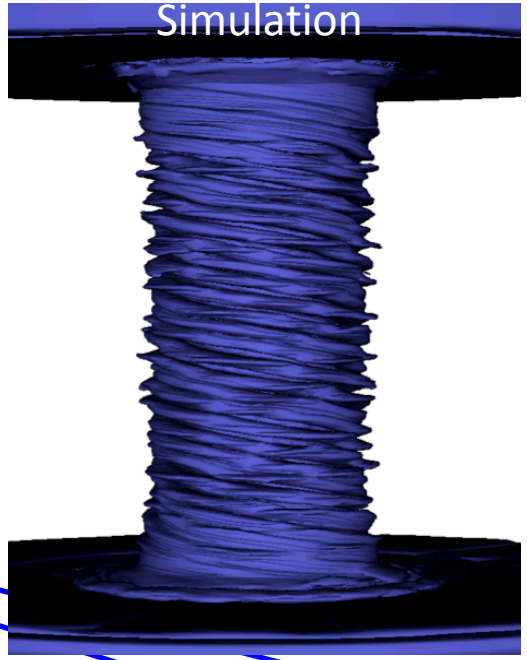

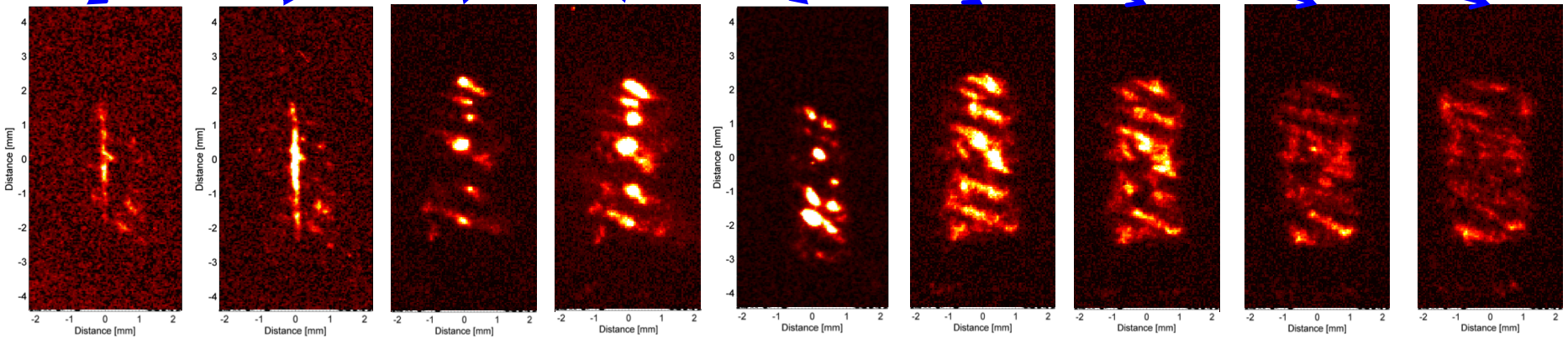

+0 +1 +3 +4 +5 +6 +7 +8 +9

Comparison of liner emission

Sandia National Laboratories

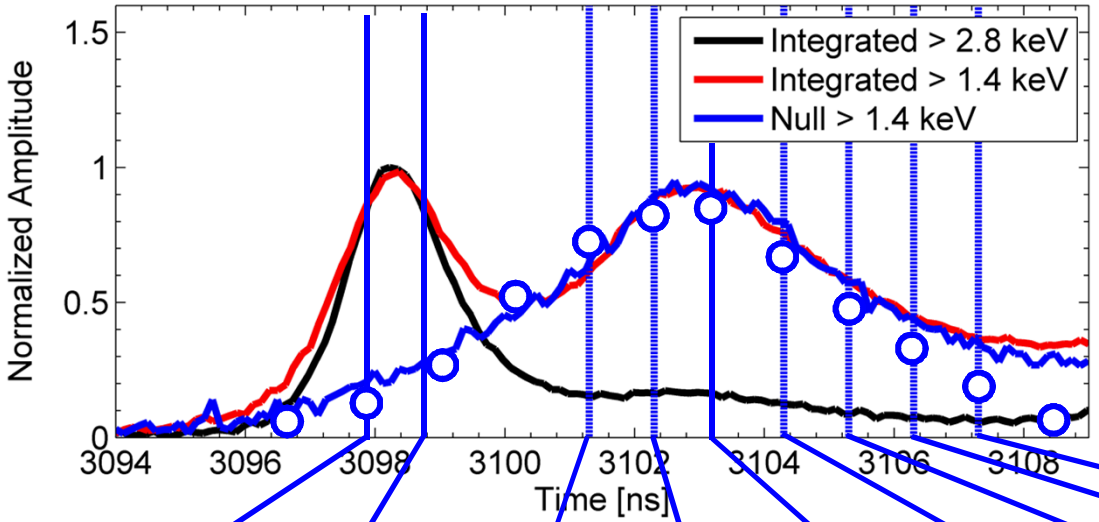

Simulation

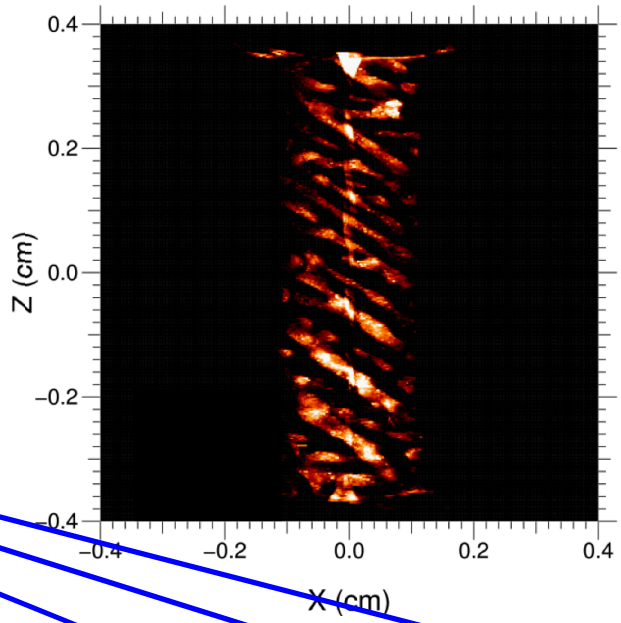

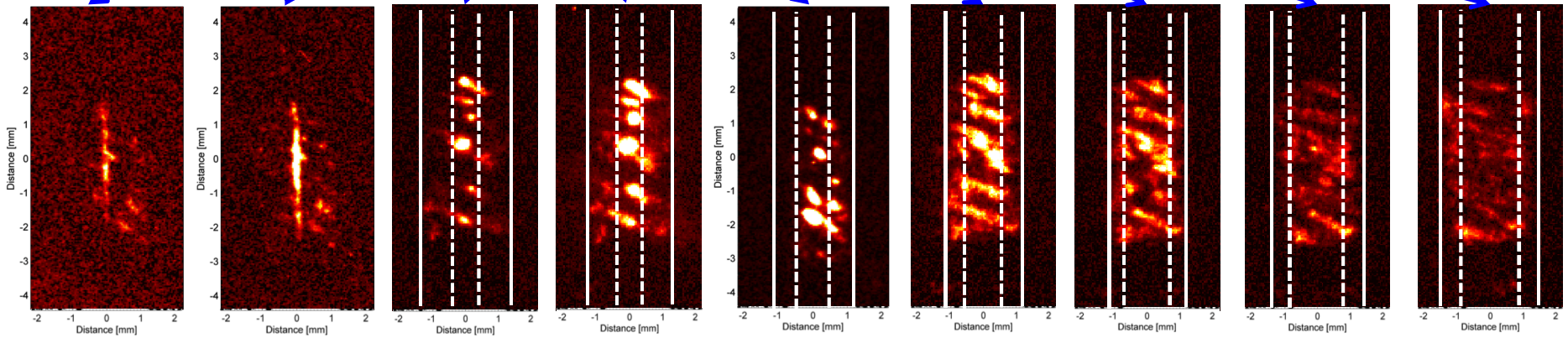

+0 +1 +3 +4 +5 +6 +7 +8 +9

Comparison between observables and post-shot degraded 2D & 3D simulations

Sandia National Laboratories

Parameter	Measured/inferred [z2591]	Post-shot simulations
• I_{max}	19 ± 1.5 MA	19 MA
• t_{imp}^{5MA}	+90 ± 1 ns	+90 ns (~70 km/s)
• r_{laser}	450 ± 150 μm	450 ± 150 μm
• E_{gas}^{abs}	~100-300 J	200 ± 50 J
• r_{stag}^{hot}	44 ± 13 μm	40 μm (r_{stag}^{liner} 53 μm, CR_{2D}^{liner} 44)
• $\langle T_i \rangle^{DD}$, $\langle T_{i,e}^{spec} \rangle$	2.5 ± 0.75, 3.0 ± 0.5 keV	3.0 ± 0.5, 2.7 ± 0.5 keV
• ρ_{gas}^{stag} , m_{loss}	0.3 ± 0.2 g cm^{-3}, ~70%	0.4 ± 0.2 g cm^{-3}, 61%
• ρR_{gas}, ρR_{liner}^{stag}	2 ± 1, 900 ± 300 mg cm^{-2}	2.6 ± 1.0, 900 mg cm^{-2}
• $\langle P^{stag} \rangle$, E_{gas}^{stag}	1.0 ± 0.5 Gbar, 4 ± 2 kJ	1.5 ± 0.3 Gbar, 7 ± 2 kJ
• $\langle B_z^f r_{stag} \rangle$	(4.5±0.5)e5 G cm ($r_{stag}/r_{L,\alpha}$ 1.7)	4.8e5 G cm ($r_{stag}/r_{L,\alpha}$ 1.8) ($\langle B_z^f \rangle$ 91 MG)
• Y_n^{DD}	(2.0±0.5)e12	(2.5±0.5)e12
• Y_n^{DD}/Y_n^{DT}	40 ± 20	41-57
• DD, DT spectra	isotropic, asymmetric	isotropic, asymmetric
• t_{burn}^{FWHM}	2.3 ± 0.6 ns (x-rays) [z2591, Y_n^{DD}=2e12] 1.5 ± 0.1 ns (x-rays) [z2613, Y_n^{DD}=1e12]	1.6 ± 0.2 ns (neutrons and x-rays)
• Liner emission	bounce & peak emission: t_{stag}+5 ns	bounce & peak emission: t_{stag} +5 ns
• Δz_{burn} shape	5 ± 1 mm, asymmetric	Helical shape and emission/attenuation
• mix	0 - 10 %, not ≥ 20%	0% (by design)

Without phase plates or other beam smoothing, we have a "ratty" beam → LPI!

OMEGA-EP
750um DPP

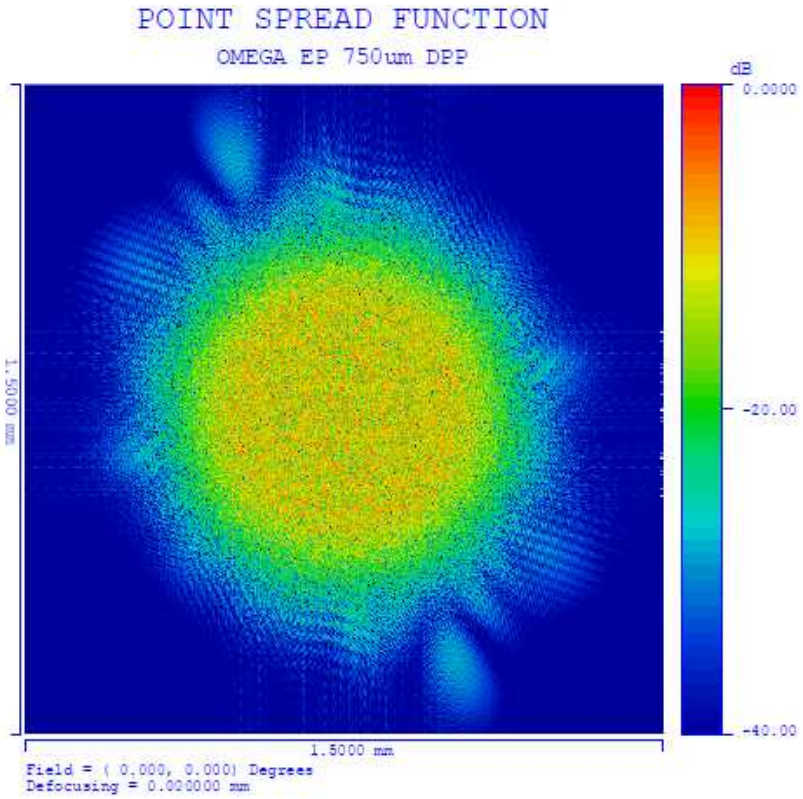

ZBL (Z-Beamlet [NIF prototype])
No DPP (representative)

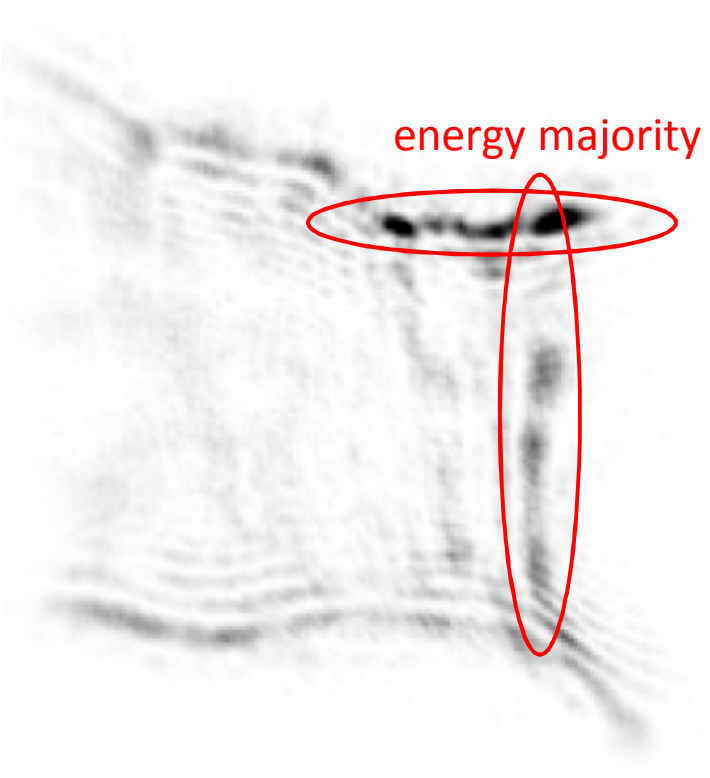

In the beginning, we had to make progress without this critical technology

Four sets of data imply low levels of preheat.

Data set #1: Blastwave measurements via VISAR

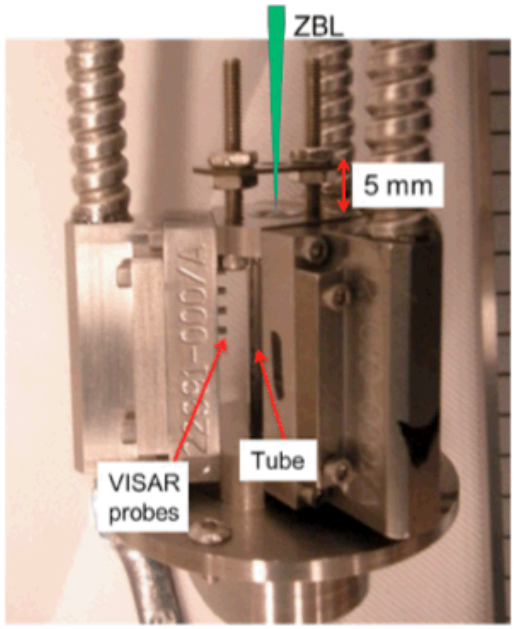

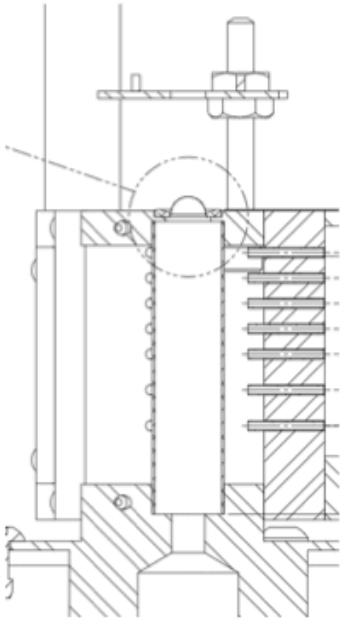

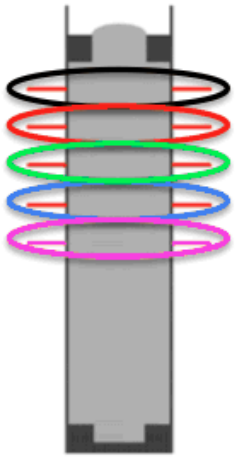

Dashed: Data
Solid: HYDRA simulation

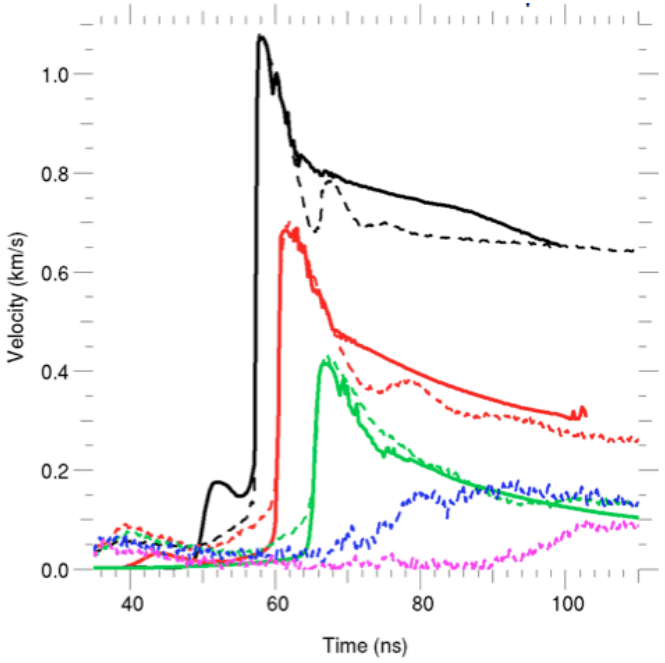

Inferred: 330 J or less coupled to the gas (of ~2.8 kJ)

Four sets of data imply low levels of preheat.

Data set #2: Calorimeter measurements

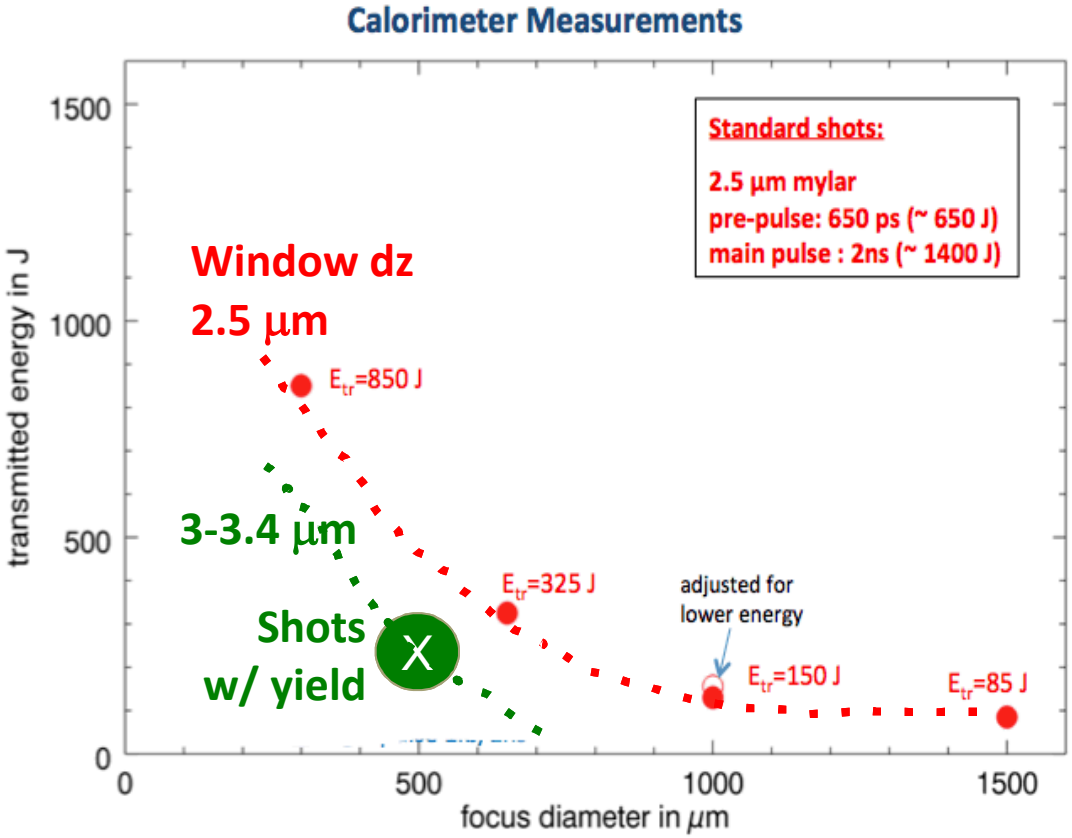

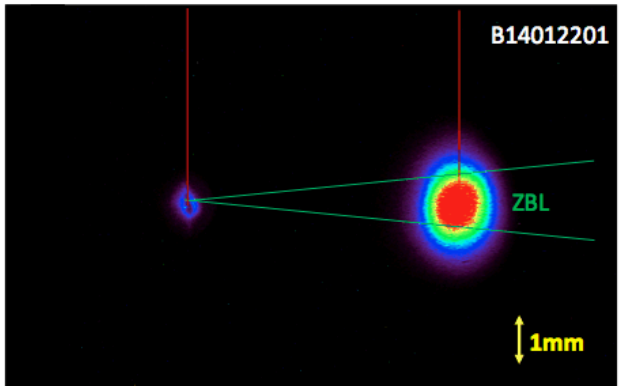

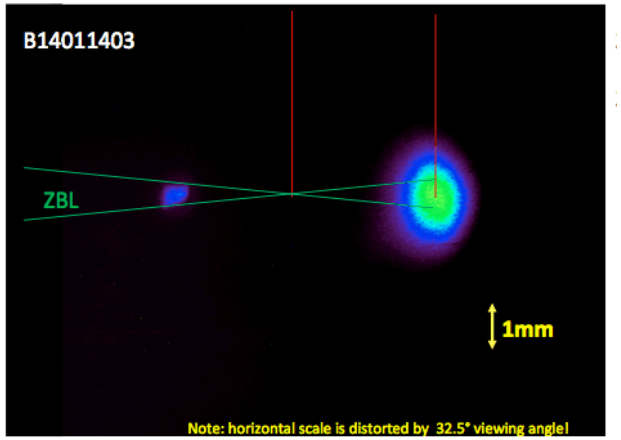

Inferred: ~200-300 J coupled through 3-3.4 μm foils

Four sets of data imply low levels of preheat.

Sandia National Laboratories

Data set #3: Shadowgraphy of blastwave (~600 J*)

Shadowgraph measurements
Ne 250 Torr gas-cell shot, 10/6/2014

ZBL: 1.8kJ/2ns, 300J prepulse, 1mm dia. focus
Target: scale-2 gas cell, 1μm-thick Mylar LEH, 250 Torr neon gas fill

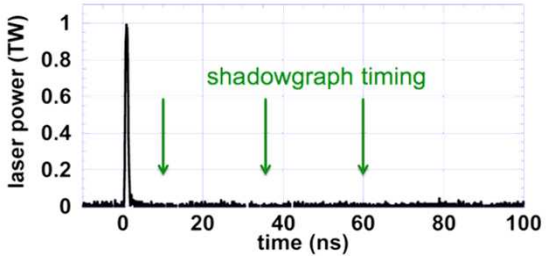

Shadowgraphs appear to measure the plasma's index of refraction $n \sim n_e^{0.5}$, which stays ~constant and captures shock and fuzzy edge radiation feature (whereas ρ, T_e, etc., vary and do not always capture features).

The $n_e^{0.5}$ profile tracks the plasma pressure very well, so the shadowgraphs are indeed measuring the laser absorption (the edge of where the plasma is hot).

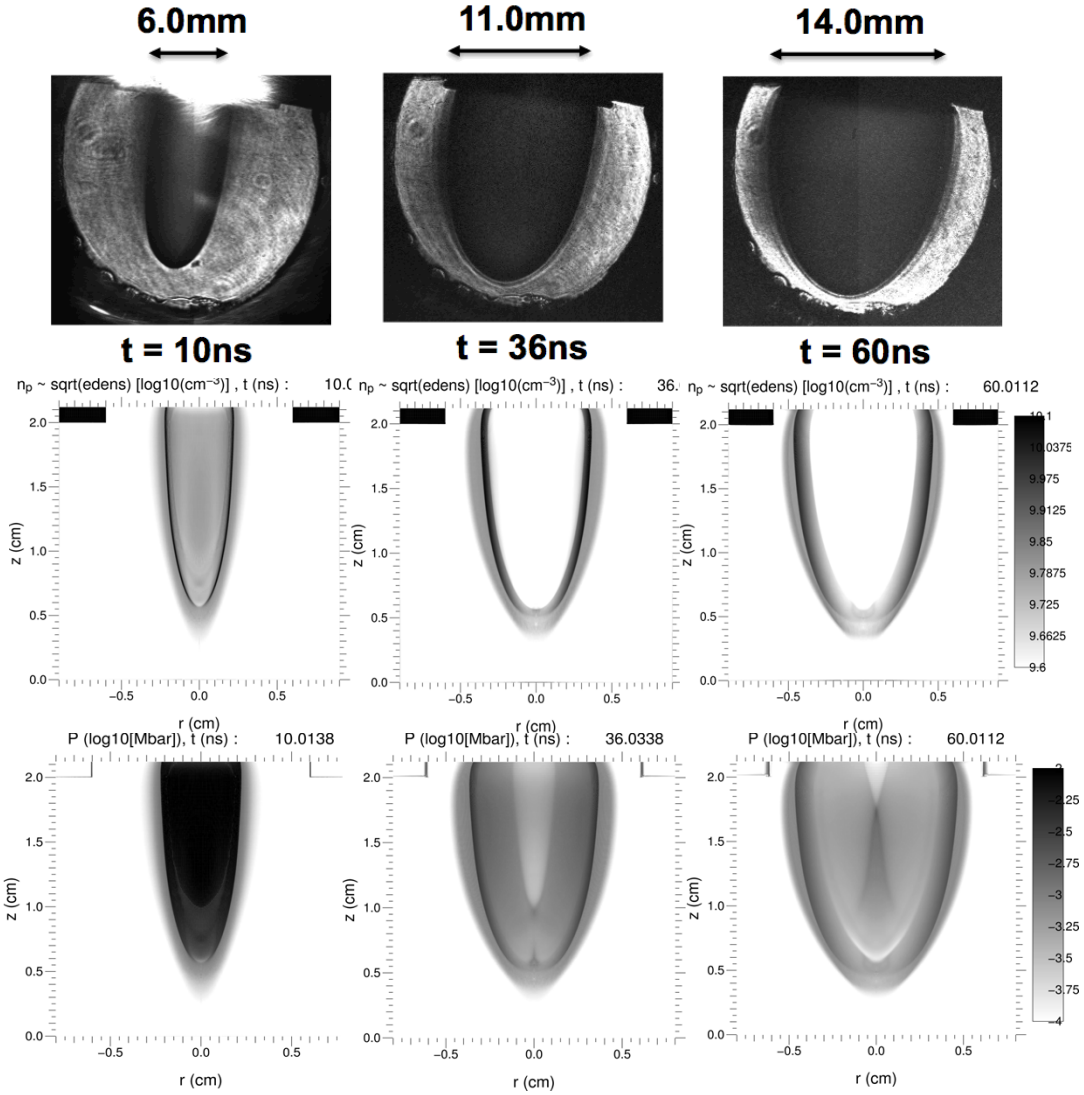

Four sets of data imply low levels of preheat.

Data set #4: Laser with B_z shots in Z chamber

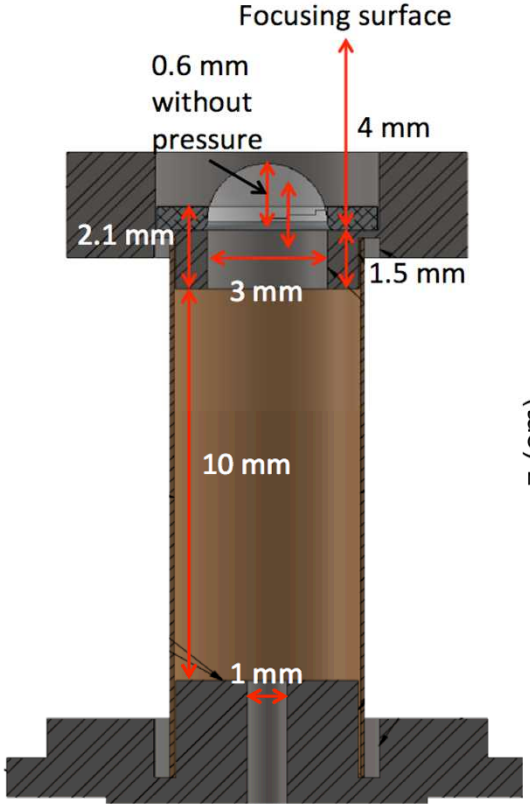

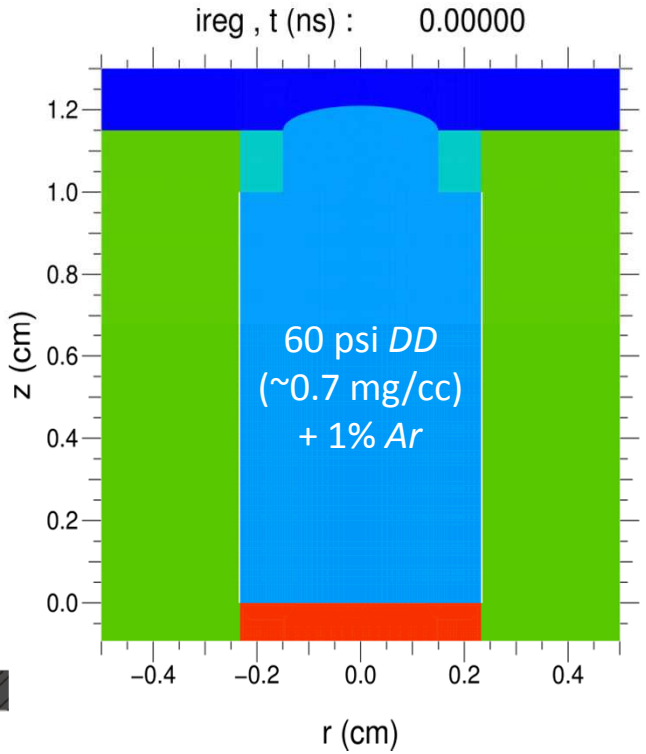

Transmission through body only

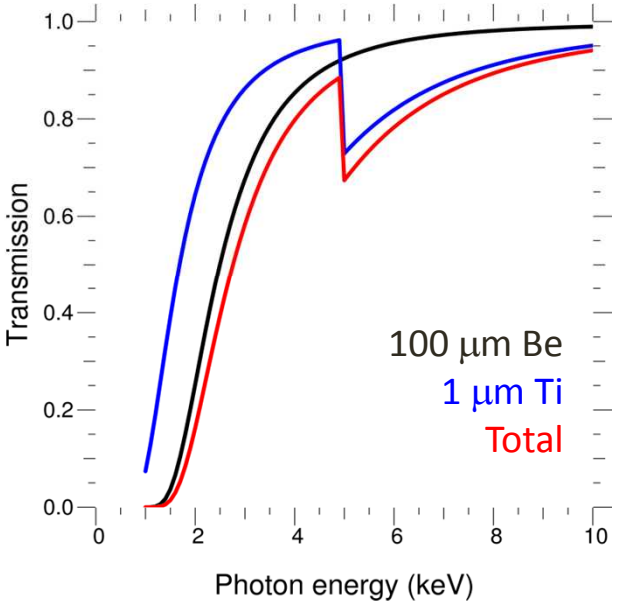

- B_z = 9.8 T
- 1.89 µm polyimide stretched to 1.55 µm
- 100 µm thick *Be* liner + 1 µm thick *Ti* foil
- *KI* solution on top SS endcap
- 1 µm thick *V* foil + $CaCl_2$ solution on *Al* bottom endcap

- E_{las} = 497 J (pre) + 2405 J (main)
- no phase plate
- D_{las} ~450-550 µm on window (guess)

Two separate diagnostics confirmed heating

Inferred peak T_e~500 eV (equilibration value lower)

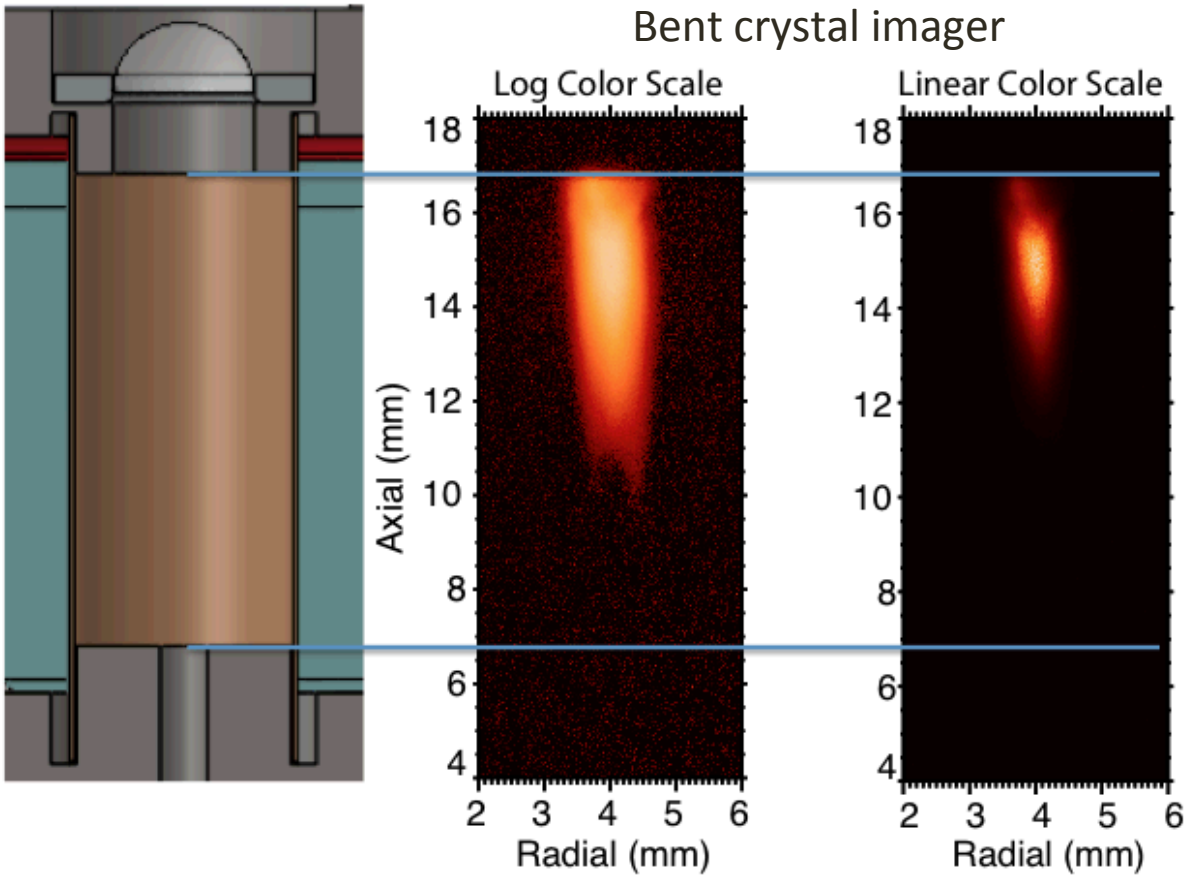

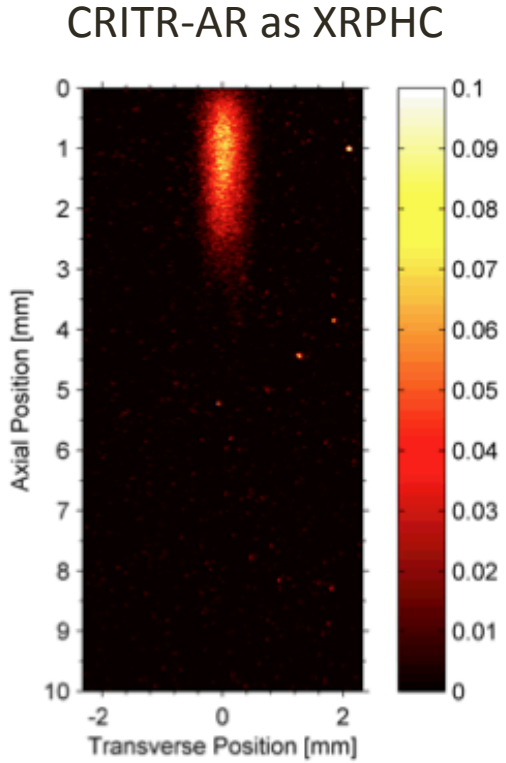

Simulated spatial distribution at peak T_e for ~200 J absorbed in gas

Peak T_e
from 0 to 640 eV

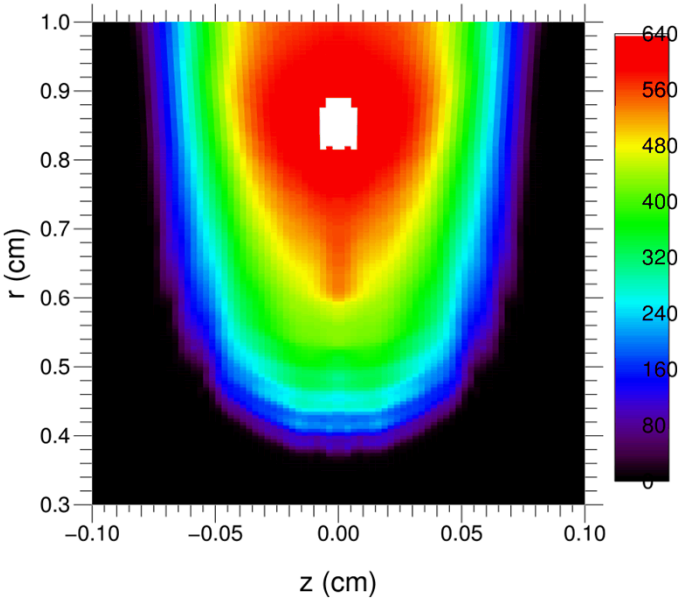

Peak T_e
from 400 to 640 eV
(observable transmission through target body)

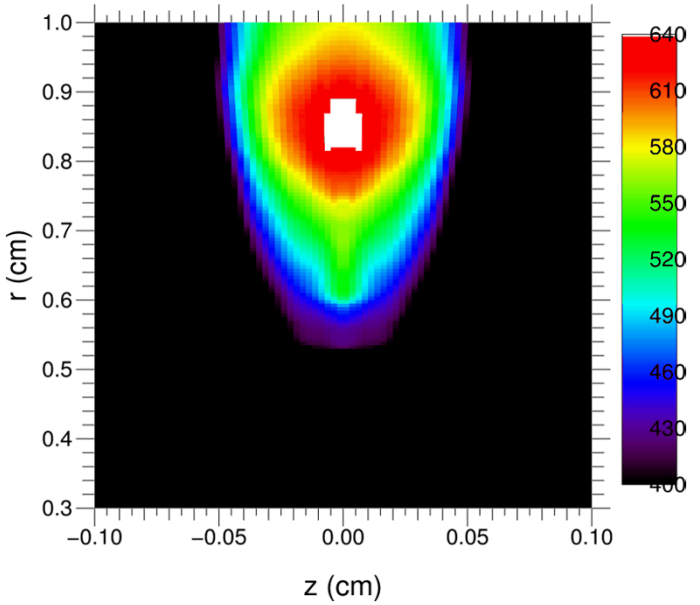

- Peak of emissivity-weighted $\langle T_e \rangle$ ~ 500 eV at end of pulse
- Only 185 J absorbed in gas leads to these temperatures and sizes
- D_{las} in gas closer to ~1.5 mm, not ~0.45-0.55 mm on window from estimates
- Tough to detect below ~400 eV
- No deposition beyond dz~6 mm in imploding region

Radial and axial extents of heated plasma region match up on both linear and log scales

Linear experimental transmission

Linear simulated transmission

Log experimental transmission

Log simulated transmission

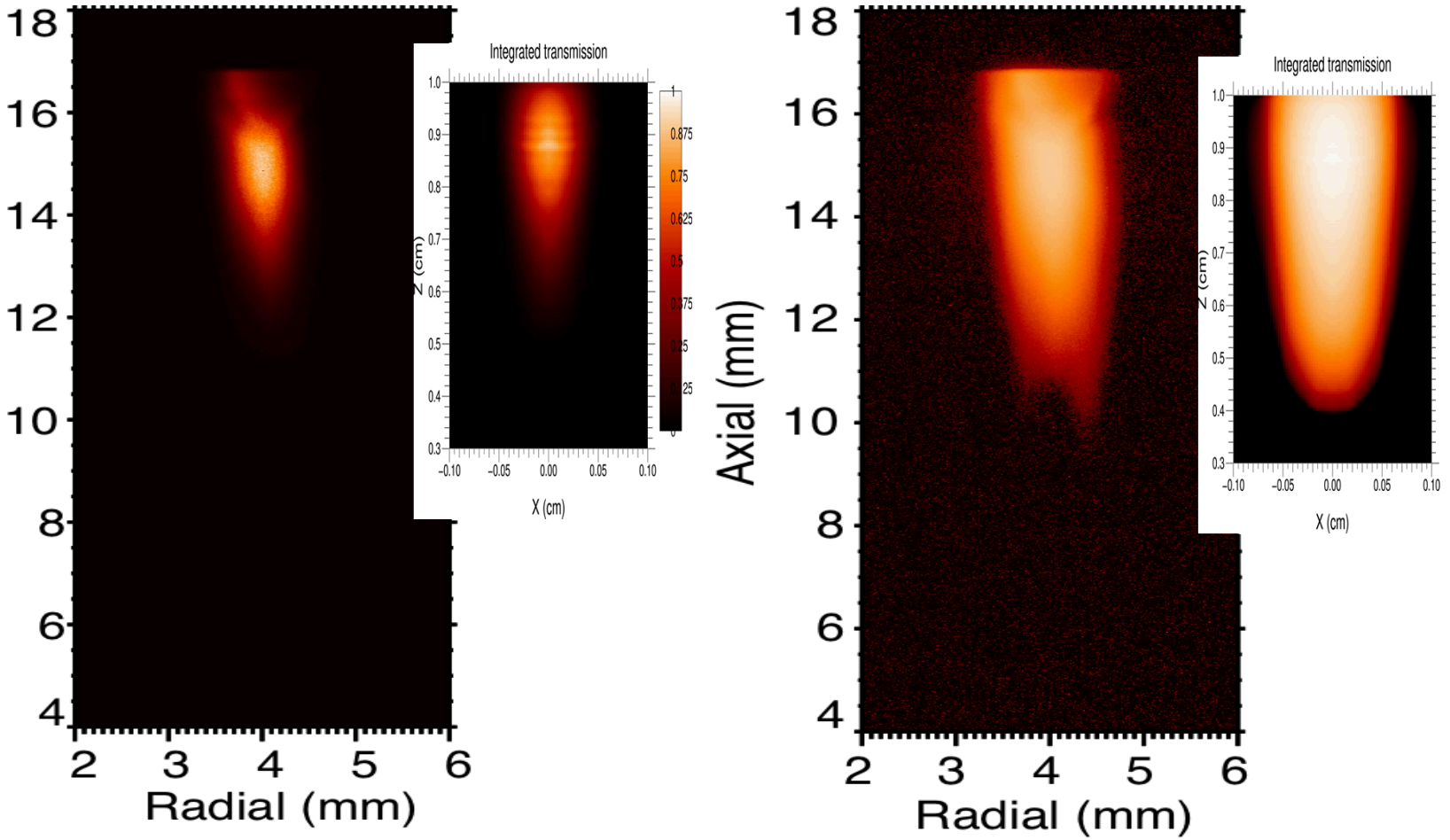

Normalized x-ray images from two diagnostics compare favorably to calculated distribution

Sandia National Laboratories

Simulation

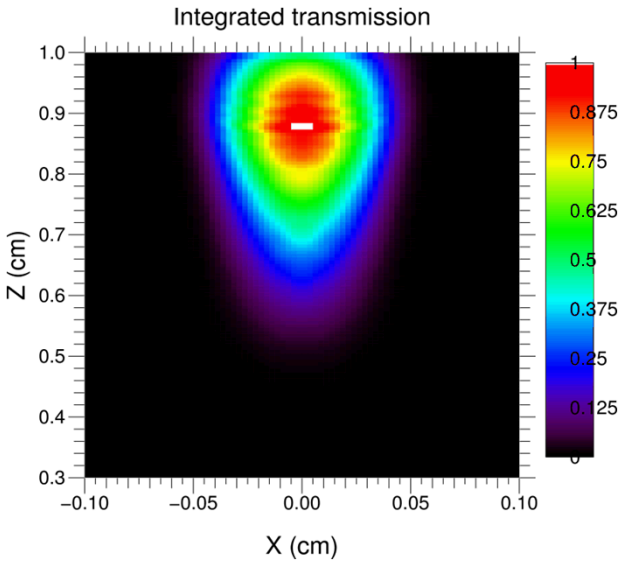

Ar Imager

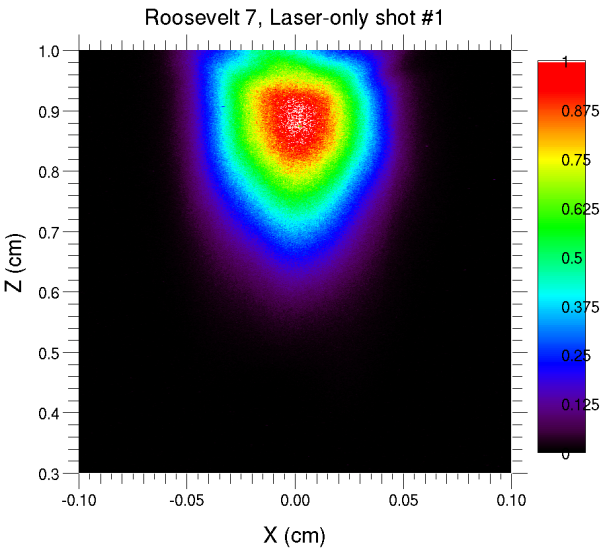

CRITR-AR as XRPHC

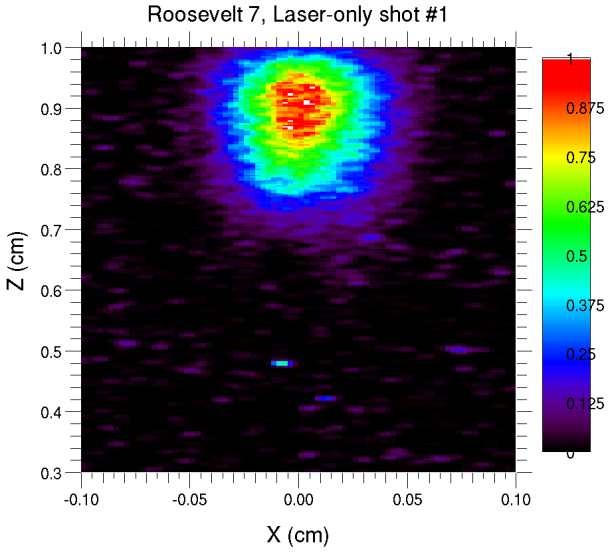

Inferred: ~200 J coupled through 1.5* μm foils (of ~2 kJ)

What happens when a phase plate is added in order to improve the beam quality?

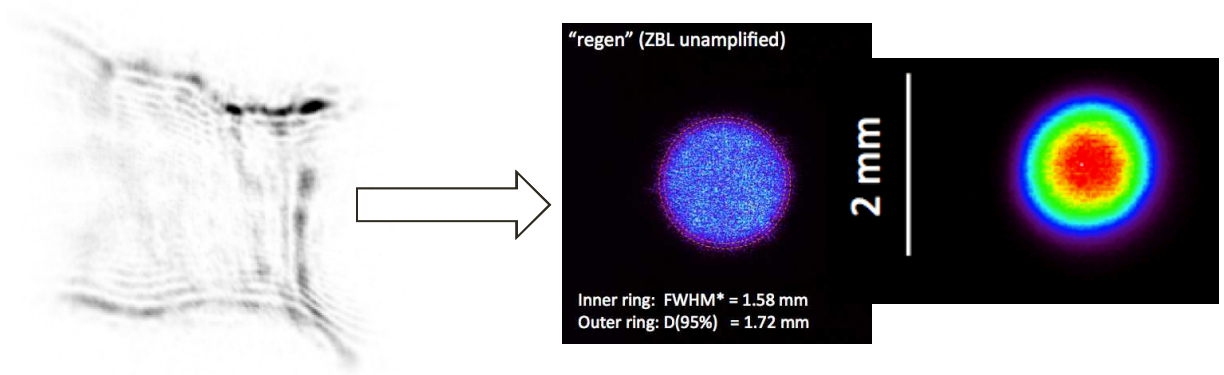

Vacuum window transmission shots (no gas, no B_z) appear to now agree with simulation, indicating ~1.0 kJ transmitted out of ~2.7 kJ incident on a 1.6 μm window.

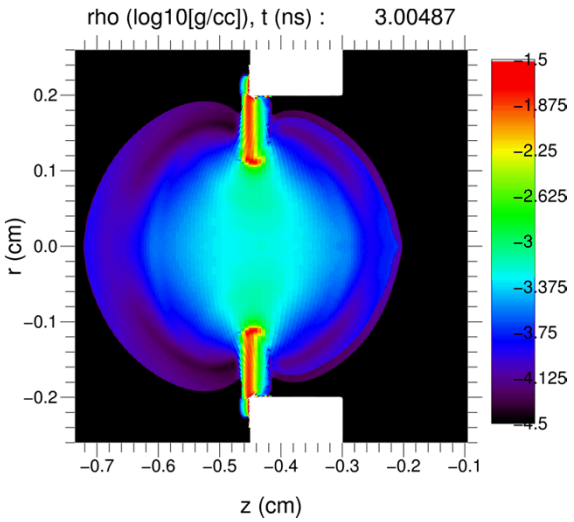

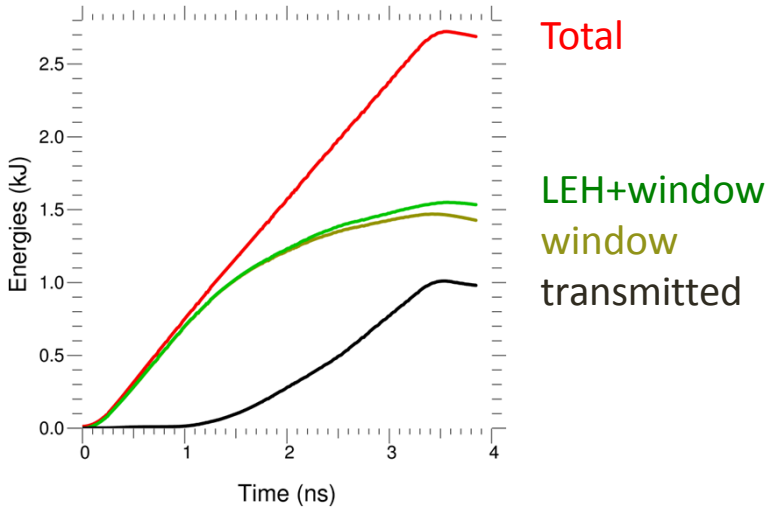

However, simulations believe the presence of gas and B_z alters the transmission, and possibly introduces mix

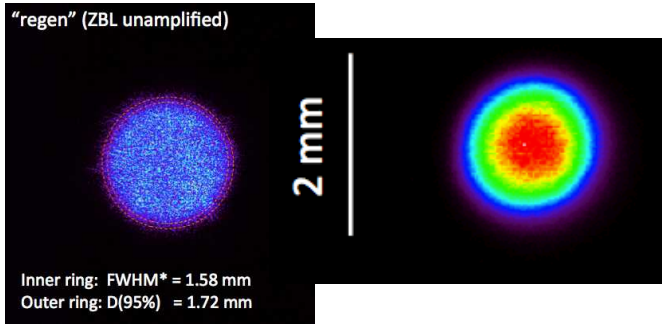

With 60 psi D2 and B_z=10 T, the window gets hotter and transmission increases to ~1.7 kJ. In high-resolution sims, mix threats from window and LEH appear to increase from radiation ablation, and window material moves into the gas quickly.

dr ~ 350 μm of inner LEH material ablated, interacts with blastwave

window material jets forward into gas

dr ~ 100 μm of inner liner wall ablated

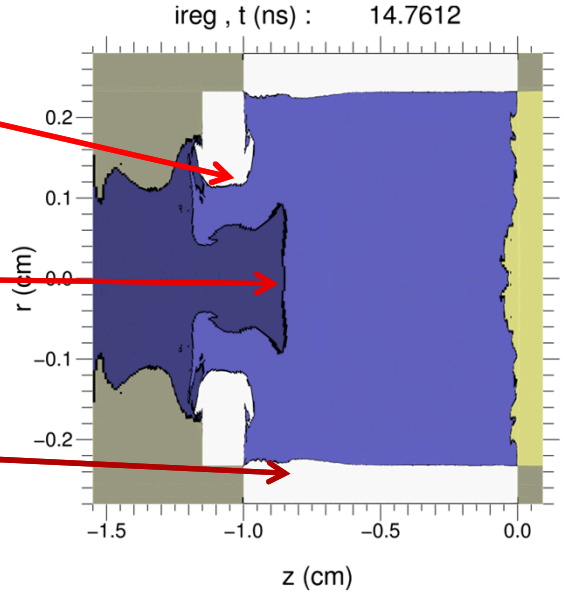

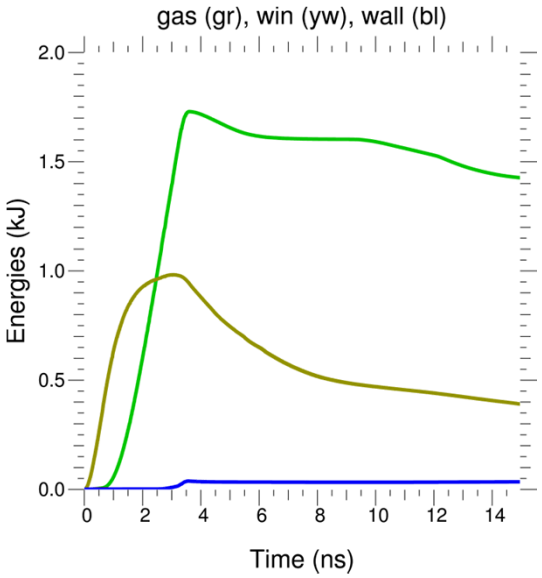

Pinhole imager data collected in recent preheat series: relative signal strength suggests *significant* window mix

All pinhole images have similar intensities above washer

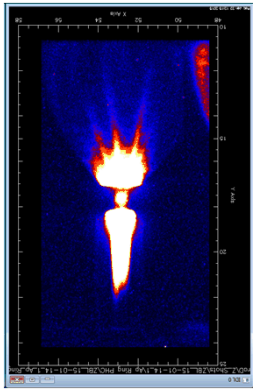

H19
45 psi, 0.5% Ar

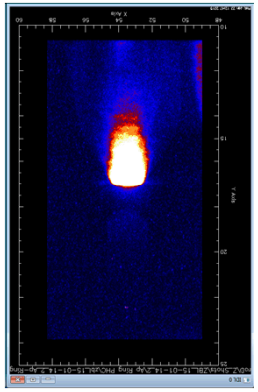

H20
50 psi, Pure Ne

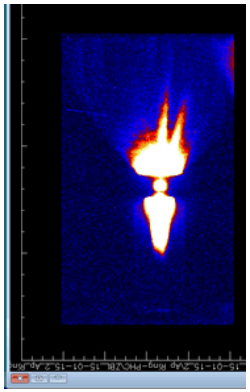

H22
60 psi, 0.5% Ar

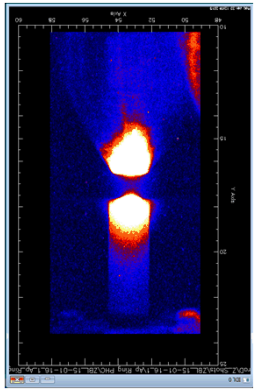

H23
60 psi , 5% Ar

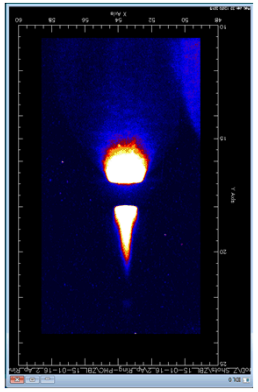

H24
60 psi, pure D2

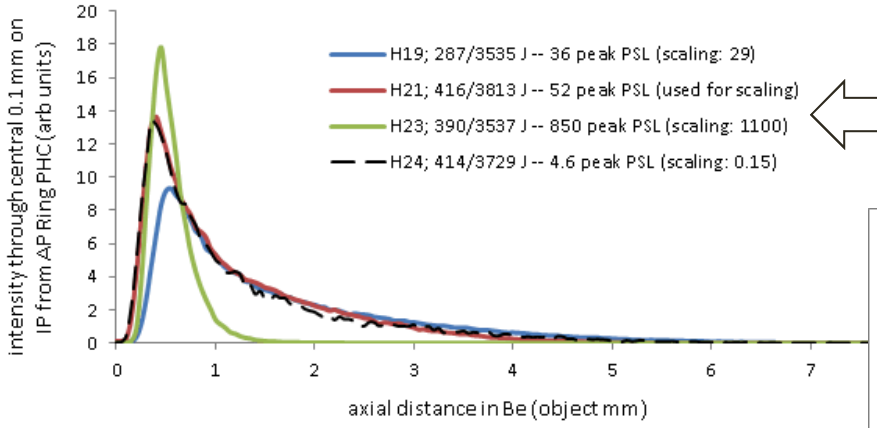

Axial lineouts below washer show similar profiles for low dopant fractions, with intensity scaling that suggests 10% carbon mix in pure D2 case (H22)

XRS3 spectra indicate fill temperatures of 0.6 – 0.8 keV, small (~0.02%) Cl mix fractions, and significant (>20%) low-Z mix

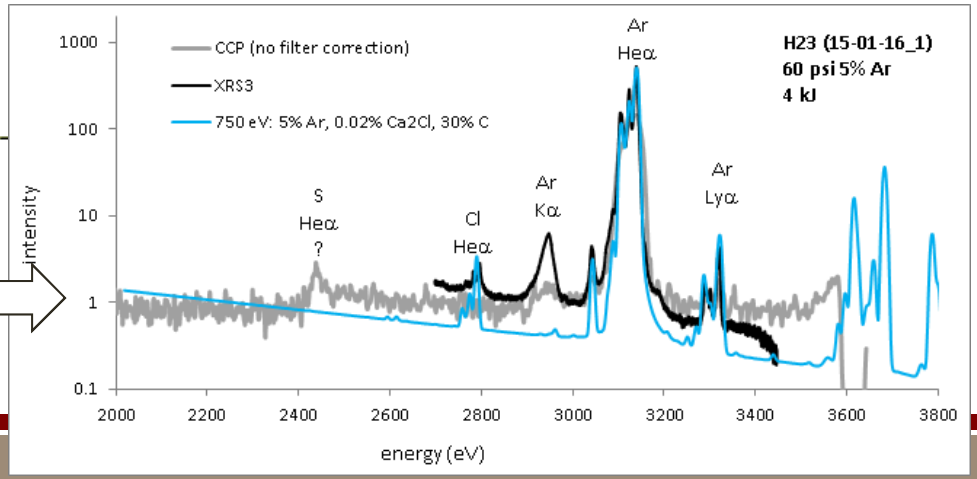

To date, increased laser energy has reduced yield, consistent with *Z*>1 mix from the window and LEH

Simulations:
Increasing laser energy (E_{laser}) from 200 J absorbed to > 1 kJ should *dramatically increase* yield (in absence of mix)

Experiments to-date:
Target changes thought to *increase* laser absorption into gas have all *decreased* the yield.

Laser-produced mix (direct or indirect via blastwave of radiation) appears to be the culprit.

Must stay unmixed for ~50 ns!
We can dud the top of the stagnation plasma!

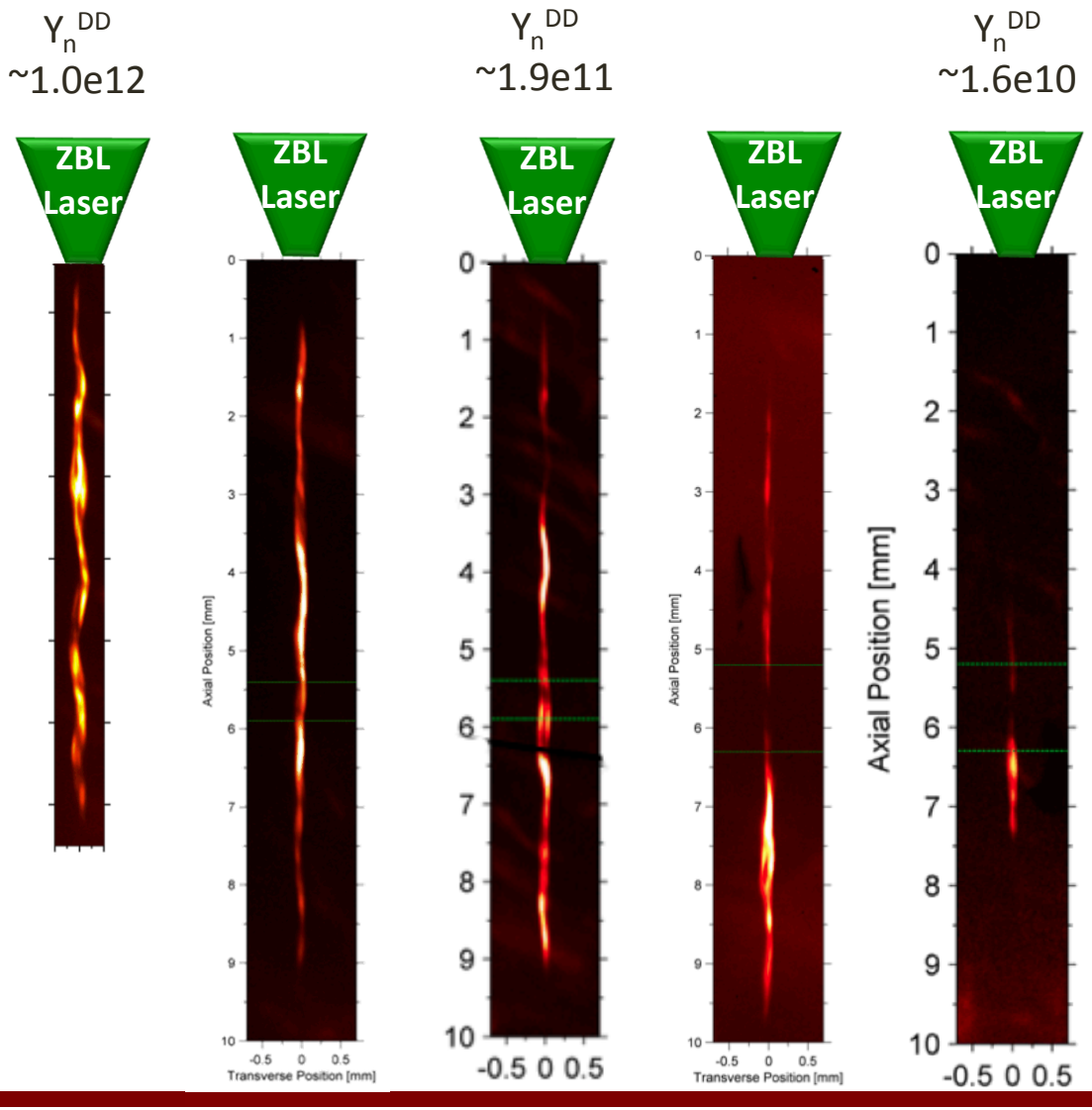

Upcoming experiments (July 2015) will test a redesigned target meant to reduce laser-produced mix

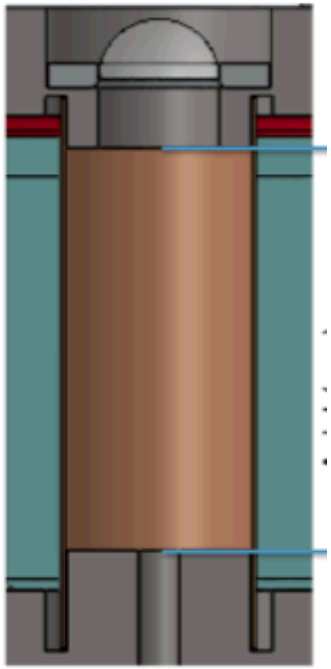

Old target:	New target (cryo):
1.5 mm standoff between window and imploding region	5.0 mm standoff (window has to move farther to mix)
1.5-3.5 micron window thicknesses	0.25-0.4 micron (3-9x mass reduction)
3 mm ID LEH	4.6 mm ID LEH
CH and/or *Al* components in LEH and beam dump	None (laser only sees *Be*)
Either no phase plate or 1.8 mm phase plate	0.7 mm phase plate

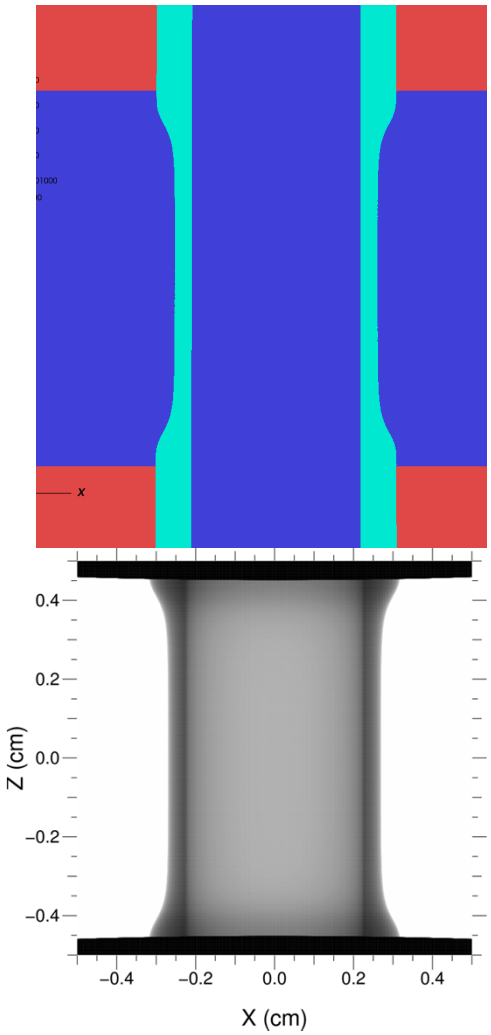

Outline

1. Magnetized Liner Inertial Fusion (MagLIF)
2. Comparisons of MagLIF-related experiments to simulations
3. OMEGA-EP laser-heating experiments
4. Magnetized hohlraum experiments at OMEGA
5. Mini-MagLIF at OMEGA

OMEGA-EP at Laboratory for Laser Energetics

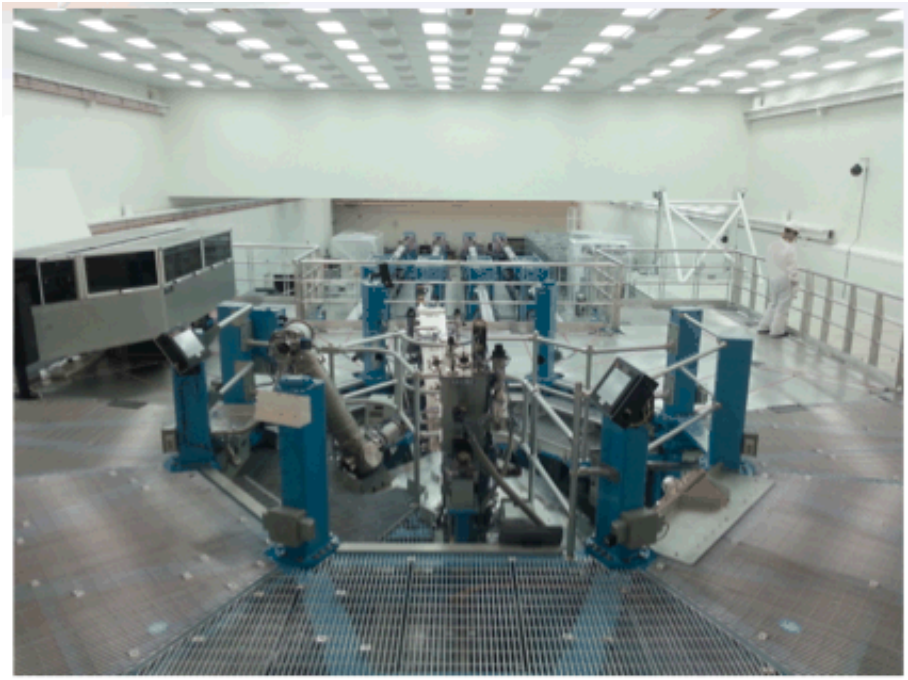

We are currently investigating laser preheating on a number of different facilities:
PECOS (Z-Beamlet), OMEGA-EP (LLE), OMEGA (LLE), Z-Beamlet (on Z), and NIF

OMEGA-EP

- Excellent diagnostics
- B field capability using MIFEDS
- Similar laser energy and pulse shapes to ZBL
  - Although 3ω, not 2ω
- Well characterized, smooth beam profiles
- Same scale targets as Z experiments

- How do lasers deposit energy into under dense gasses through an LEH and what factors affect this?
  - Beam smoothing, magnetization, LEH design
  - Laser-induced mix and mitigation strategies
- How well does an applied B field suppress electron thermal conduction at MagLIF-relevant conditions?
  - Temperature measurements of laser-heated D2 plasma both during and after heating
  - Measurement accuracy sufficient to constrain simulations

Data is required to constrain and improve models in simulations

Each facility has unique capabilities that are required to study MagLIF preheating. Experiments at each facility are designed to complement each other.

We have several objectives for the Omega EP campaign

Sandia National Laboratories

First experiments

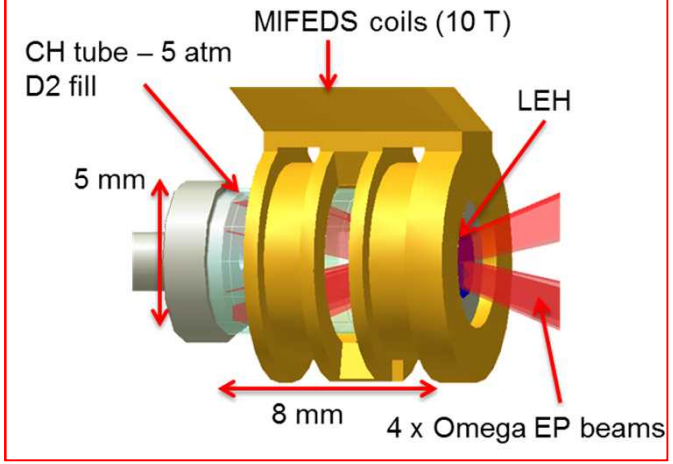

Second experiments

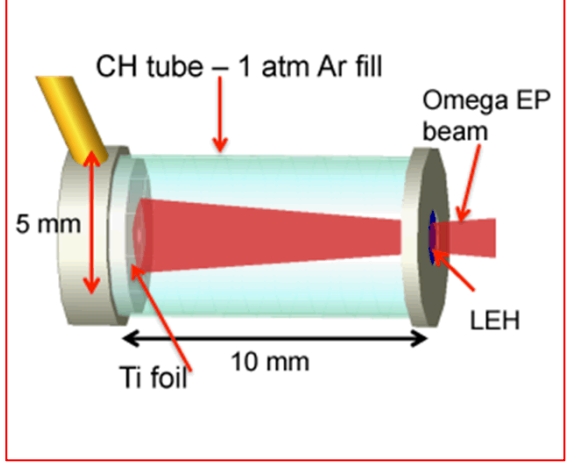

Third experiments

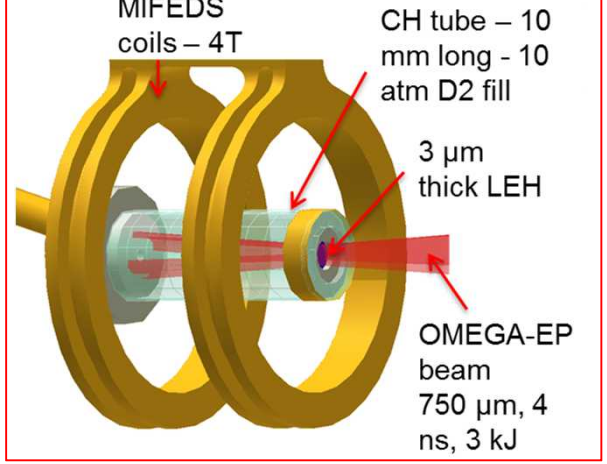

- Study laser deposition in a MagLIF-relevant D2 gas
  - (n_e=0.05-0.1n_c), magnetization (ωτ~2-5), scale length (10 mm), and $I\lambda^2 \sim 10^{14}$ W μm^2 /cm^2
- Investigate the effects of magnetization on electron thermal conduction
- Evaluate impact of beam smoothing on propagation and energy coupling
- Test simulation code predictions at conditions expected to minimize LPI effects
  - 3ω, smooth beams, and low intensity

D2 5atm

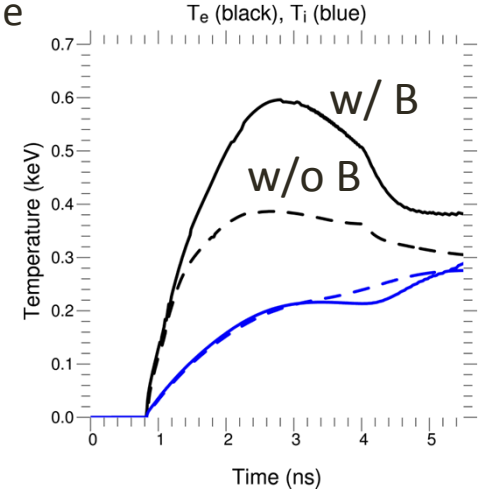

D2 10atm

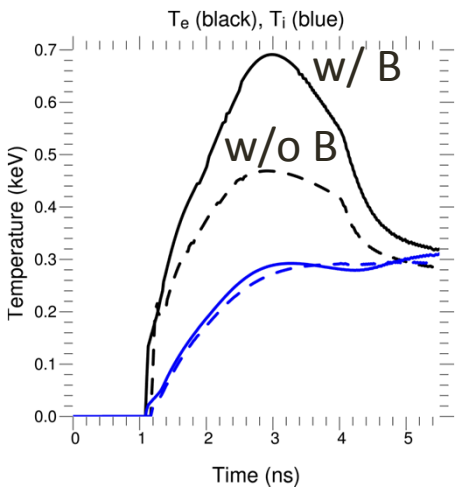

First experiments: platform development

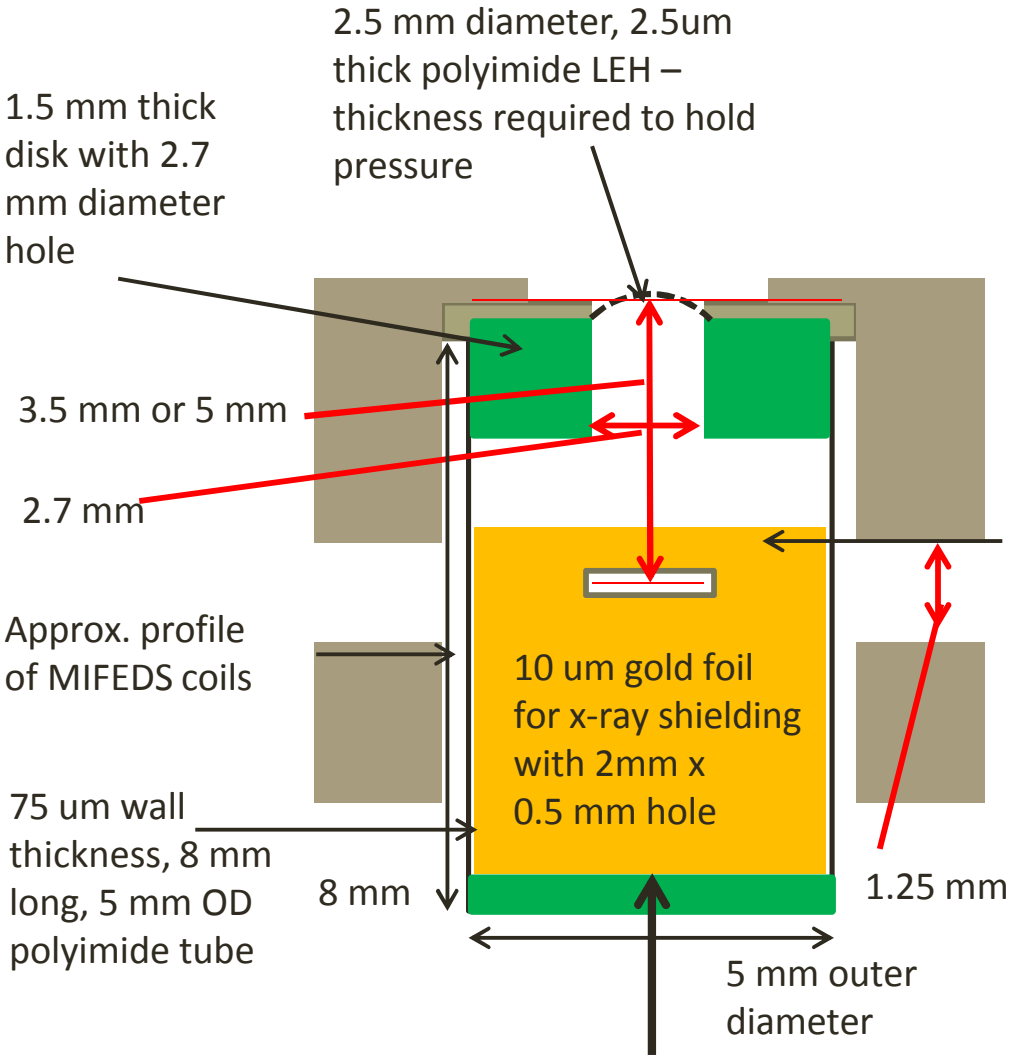

Gas fill using crimp/sealable tube - 5 atm (74 psi) D2 gas 0.1% Ar dopant by particle number or 15 psi Ar dopant

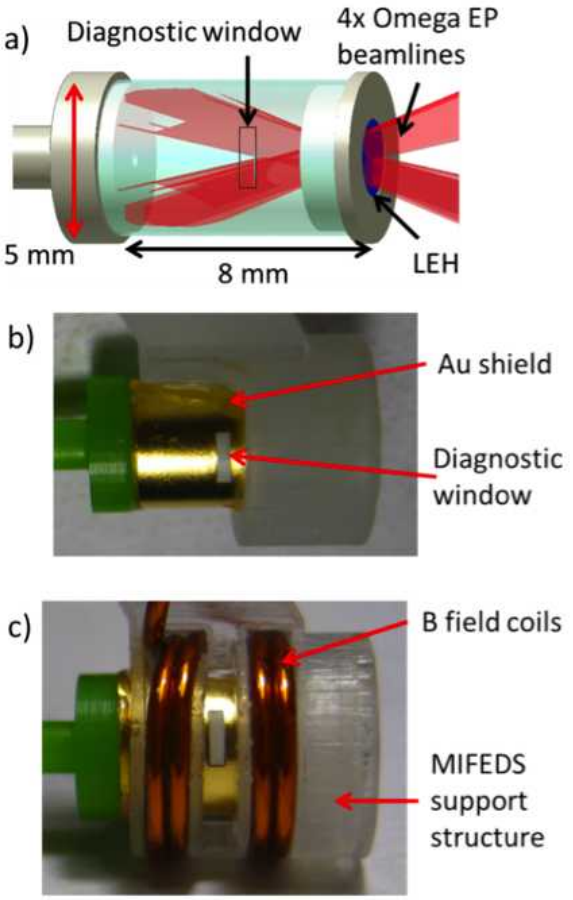

Figure 2a) VISRAD model of the tube target without surrounding MIFEDS coils and b) a photograph of the unmagnetized and c) magnetized targets showing the gold foil with diagnostic window and the surrounding MIFEDS coils and support structure.

Targets used four OMEGA EP beams

First shots were unmagnetized targets

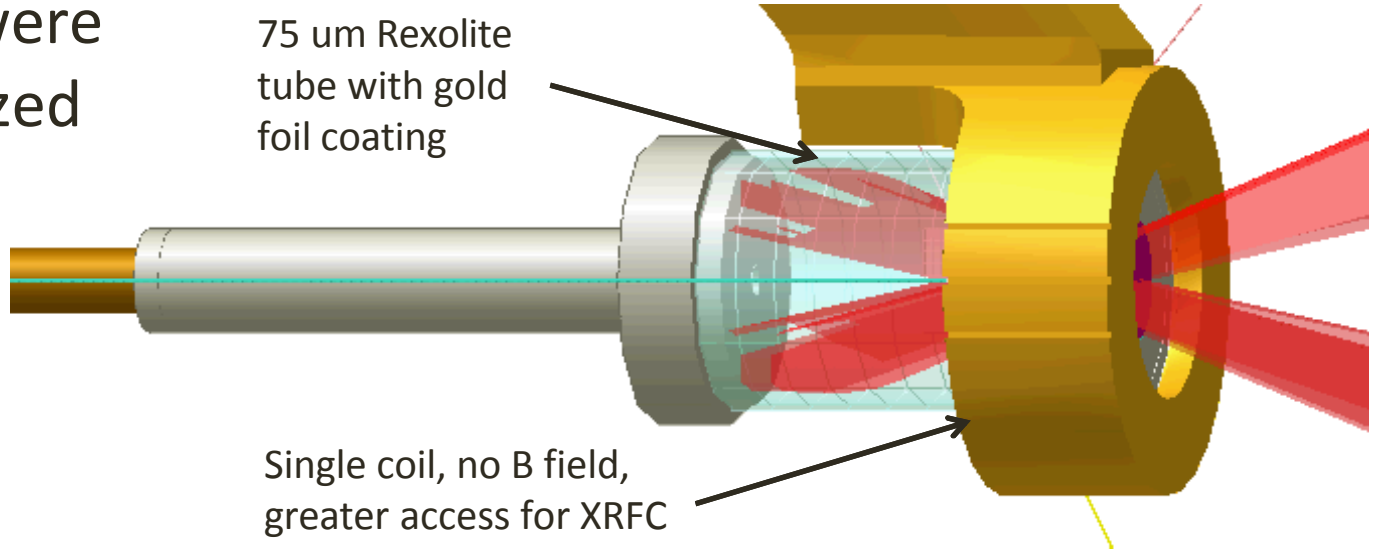

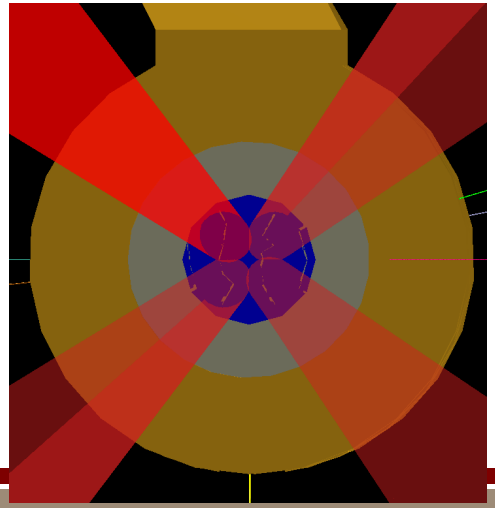

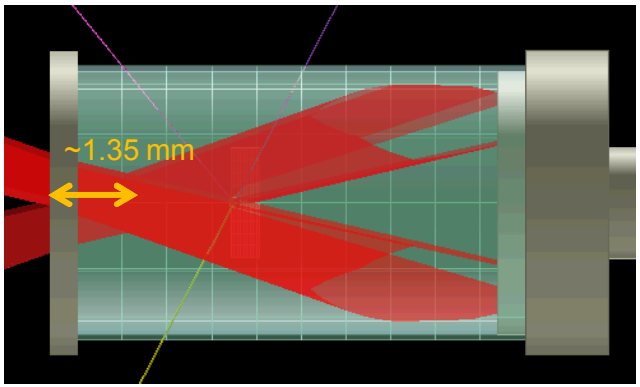

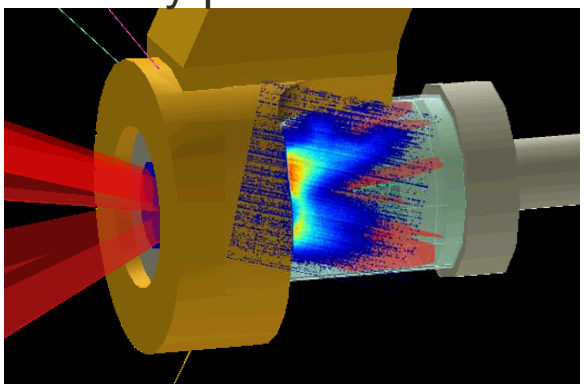

Simulation initialization

XRPHC target view

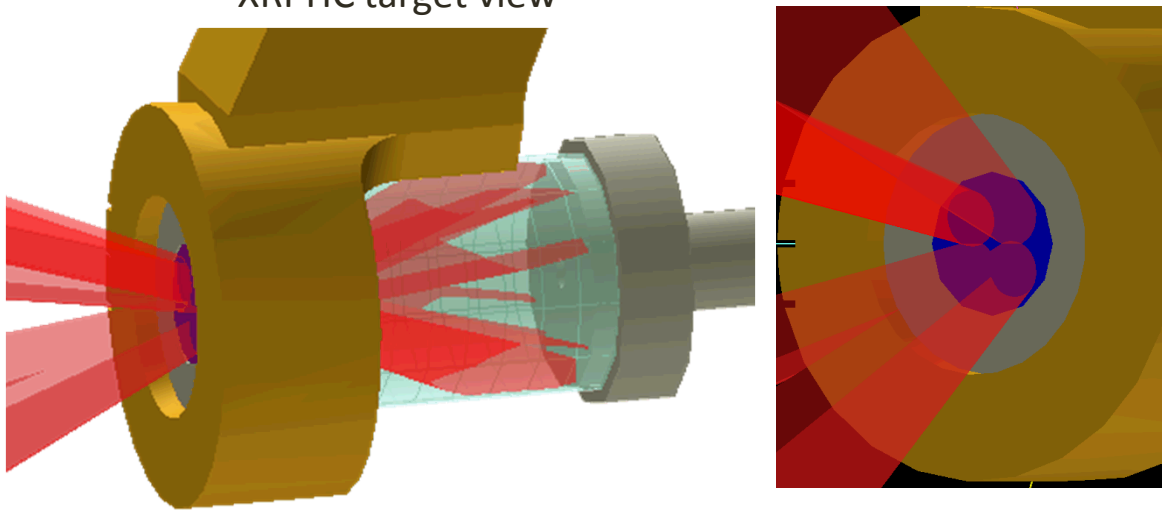

HYDRA simulation setup

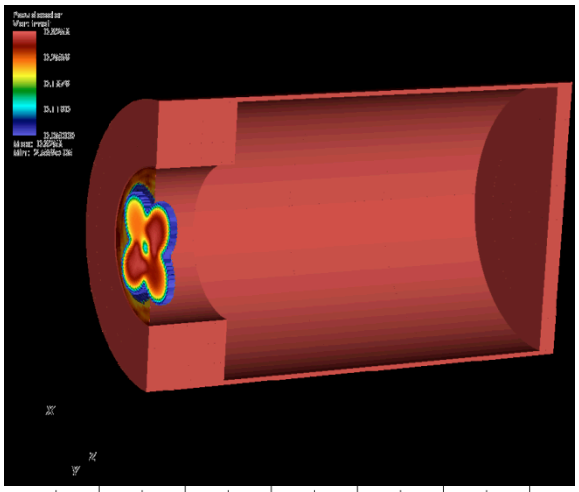

4 beams, f/6.5, ~23 deg

- 3D HYDRA modelling of 1 atm unmagnetized Ar target shows good agreement with deposition
- Actual beam energies and spot sizes used (1.7-2.5 kJ, 4 ns, square pulse, 750 um spot size)
- 4 laser spots are not of equal energy – sims. include this and match observed asymmetry

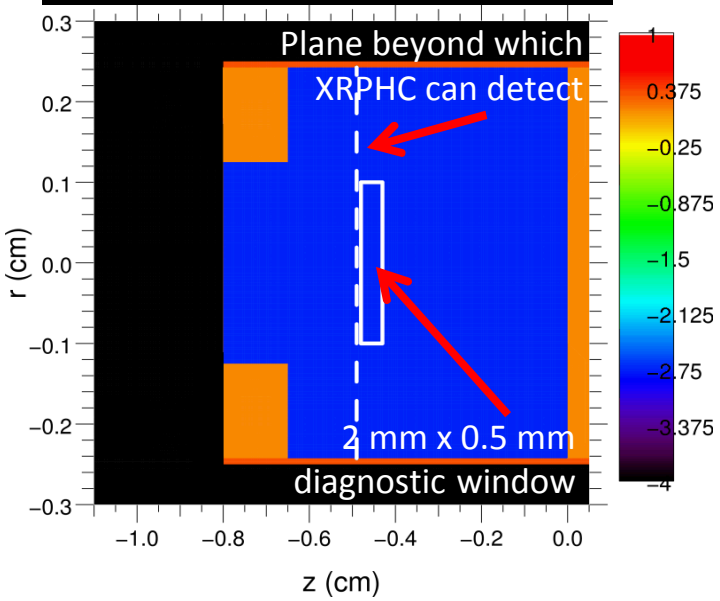

Simulation of XRPHC from pure Ar gas fill

x-ray pinhole camera
pure Ar shot

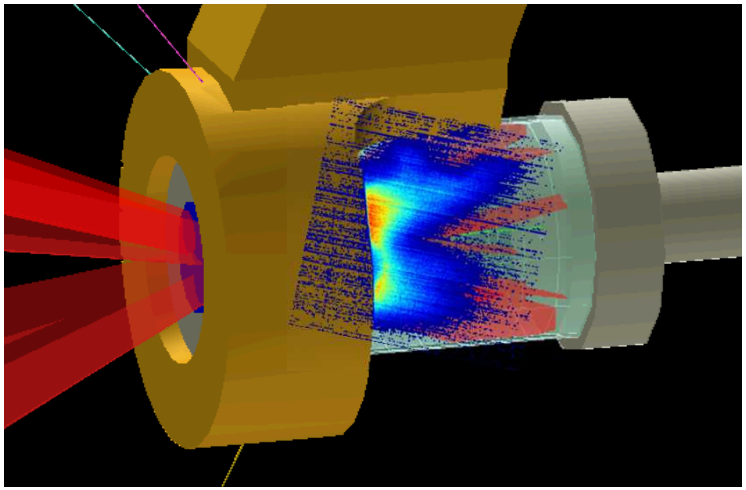

Exp

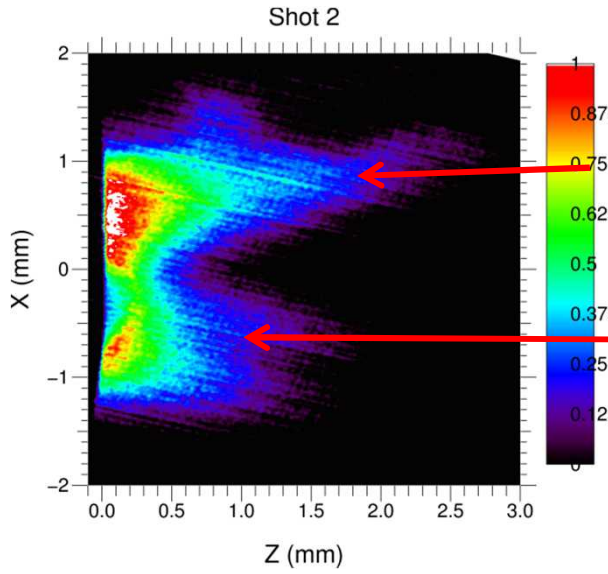

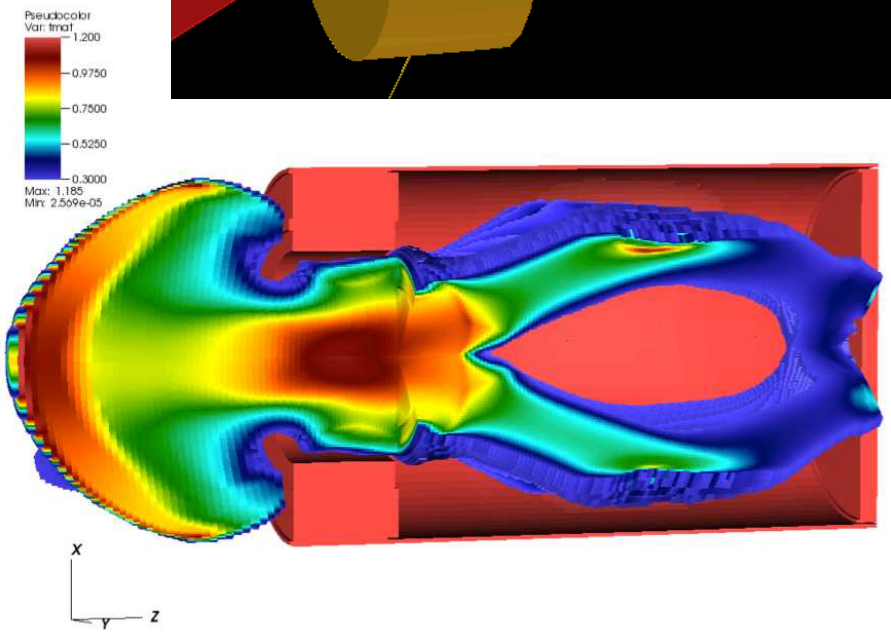

Sim

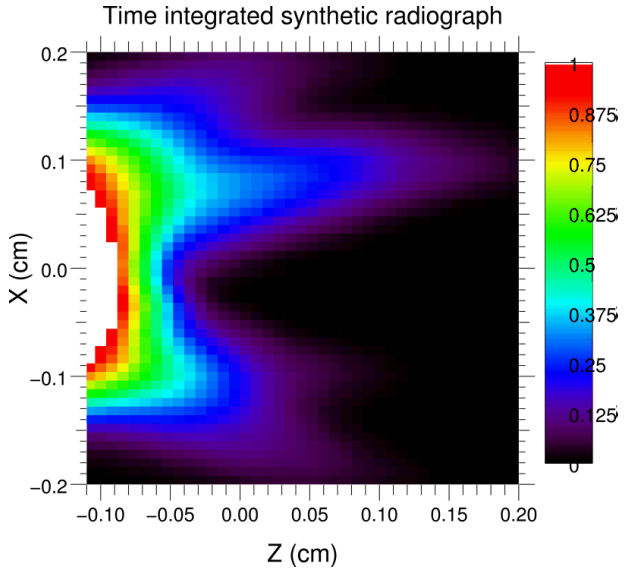

Comparison of magnetized vs unmagnetized D2

+0.1% Ar (optically-thin dopant)

Shot no.	Gas fill	Magnetized?	SSCA results	Notes
18054	74 psi D2	Yes	Good signal	
18056	74 psi D2	No	No signal	No emission observed on XRPHC or spectrometer – but did detect neutrons

74 psi ~0.9 mg/cc (on the low end for MagLIF and several kJ of E_{laser})

4 ns, ~8.8 kJ →

4 ns	1900 J	1900 J	2500 J	2500 J

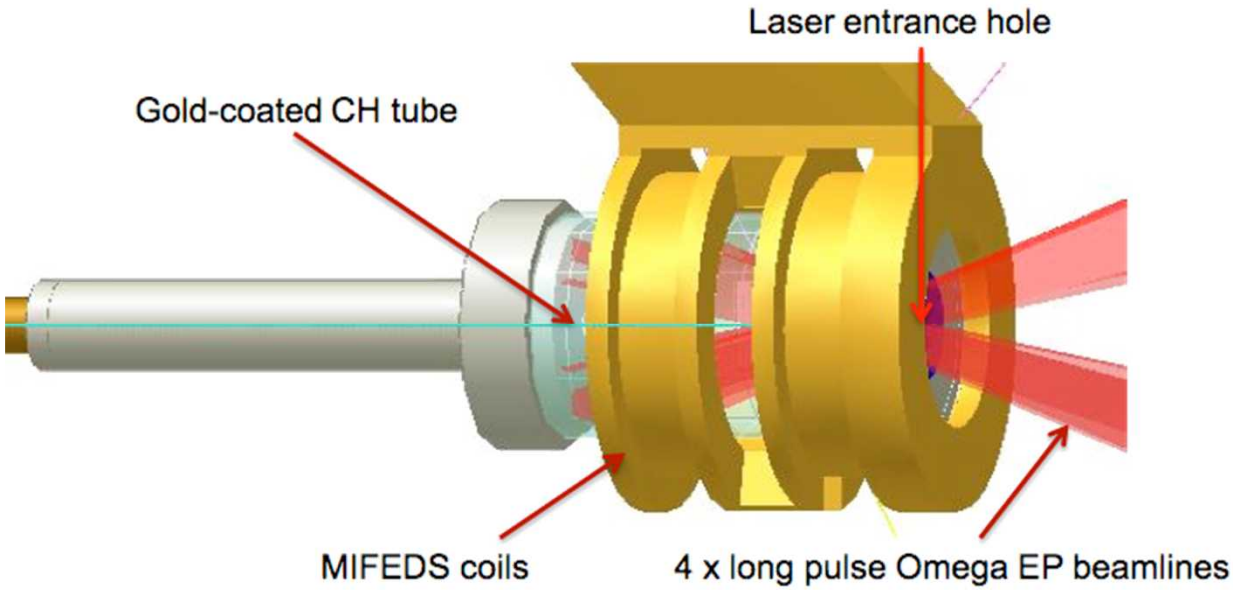

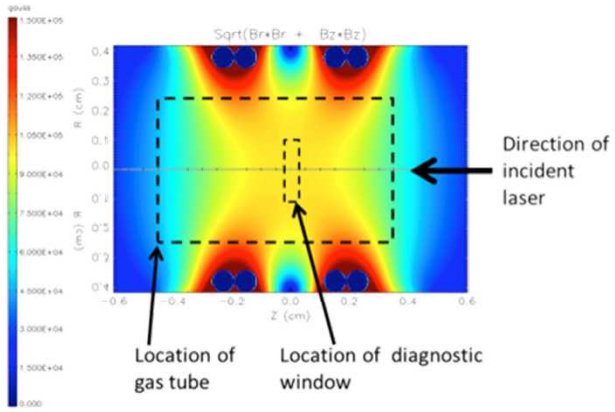

Figure 3: simulation of the magnetic field distribution produced by the MIFEDS coils. The dashed lines show the location of the target and the diagnostic window within the coils.

Comparison of magnetized D2 shots

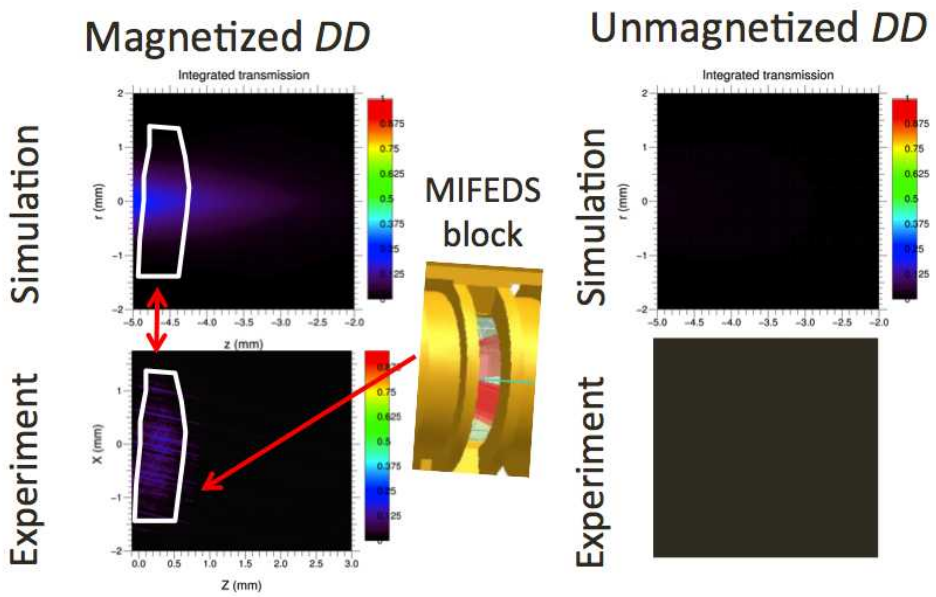

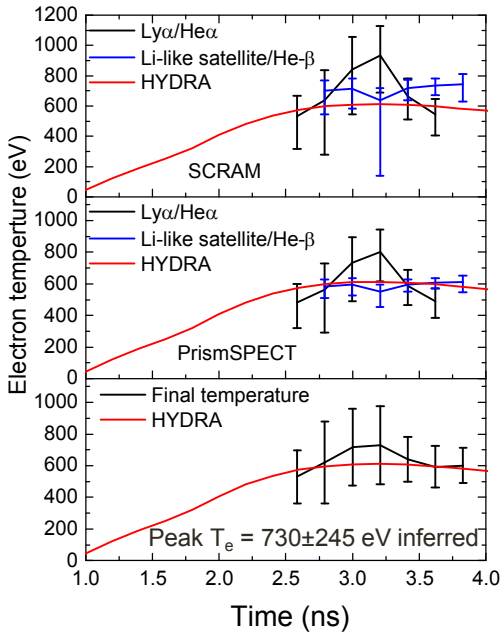

This was "platform development".

Improved designs are being fielded in 2015/16.

Allowable gas pressure too low (~5 atm) until recently (~10-20 atm).

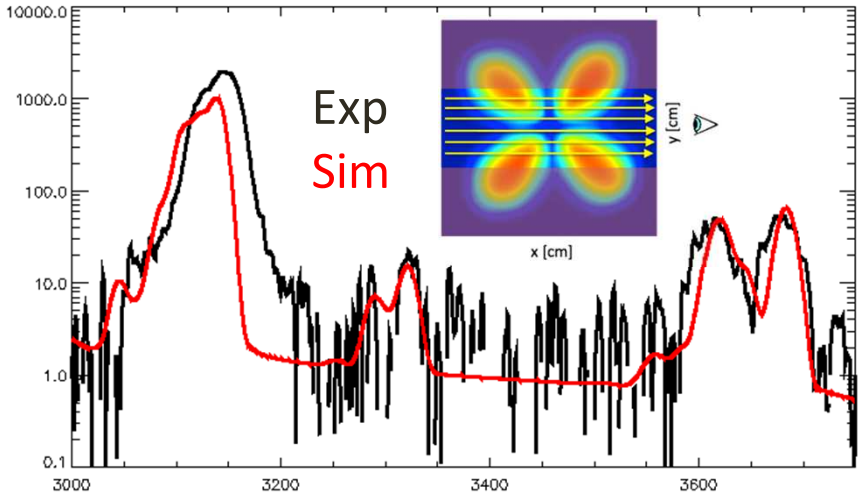

Window shocks (~1-2 keV) produce D-D fusion neutrons

Exp: Y_n^{DD} ~ 1.0-3.0*10^8

Sim: Y_n^{DD} ~ 0.8-1.5*10^8

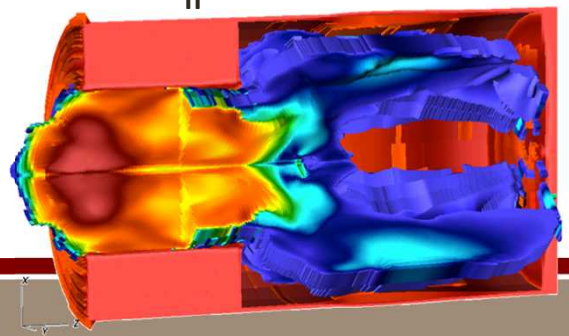

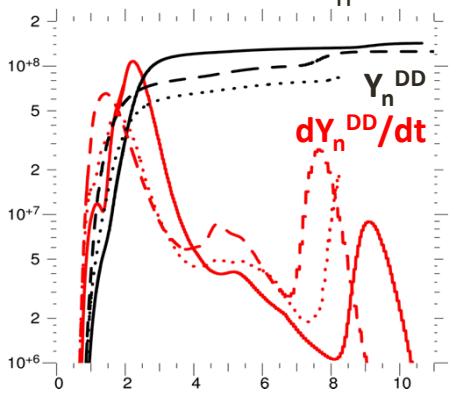

Second experiments: unmagnetized propagation dependence on laser energies/powers and windows

- Argon gas (~ 1 atm, n_e=0.048n_c) filled plastic tube (10 mm long, 5 mm diam. 75 µm wall thickness)
- Laser entrance hole polyimide window (1.7 mm diam., **1 or 2 µm thick**)
- 1 µm thick Ti coating on end plug

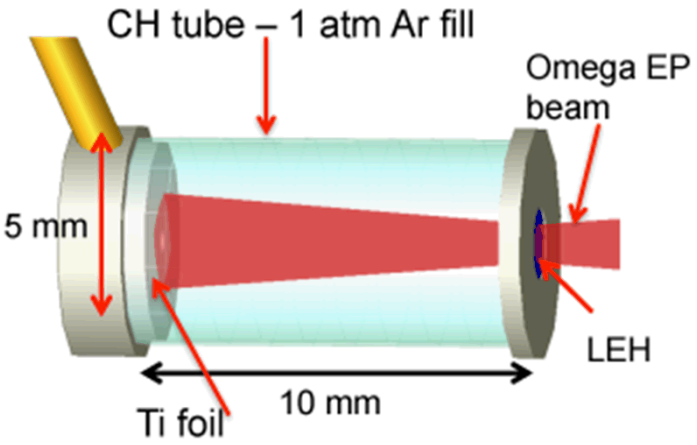

- Main interaction beam (aligned to the tube axis) with **different pulse durations/powers**
  - 2 ns (2. 2 kJ, 1.1 TW)
  - 4 ns (3 kJ, 0.75 TW)
  - 10 ns (4.5 kJ, 0.45 TW)
- Interaction beam **w/ and w/o DPP** (750 µm)
- Prepulse 0.25ns (250 J), 1 ns before main beam

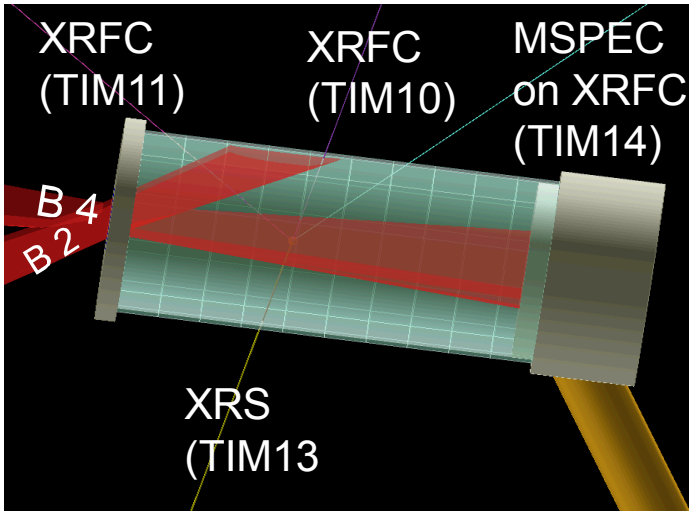

E_{laser} ~ 2.2 kJ with 2 ns duration

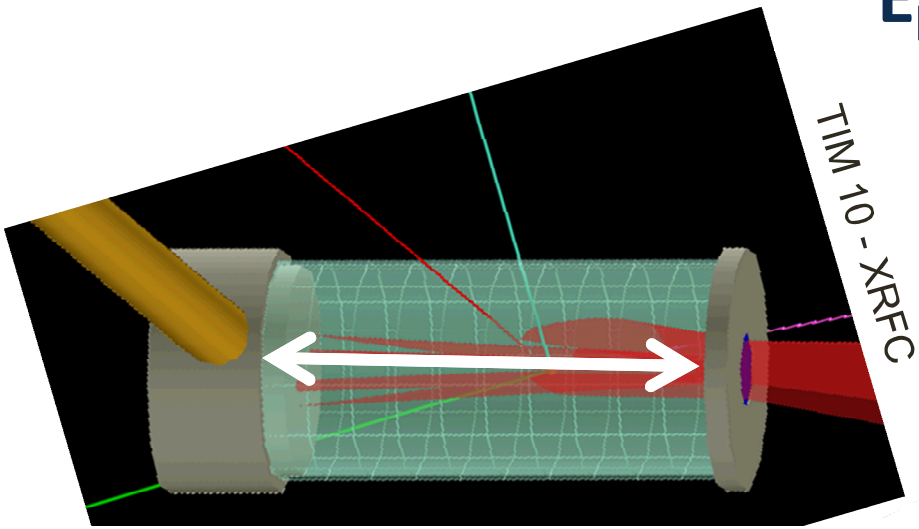

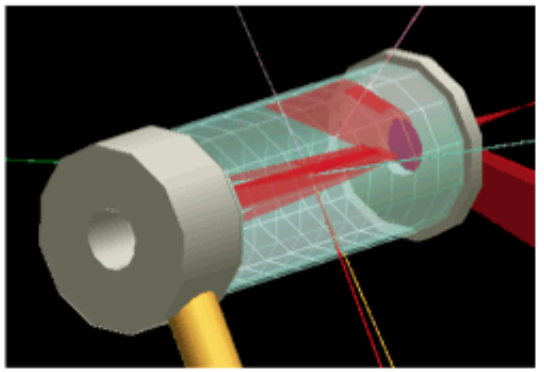

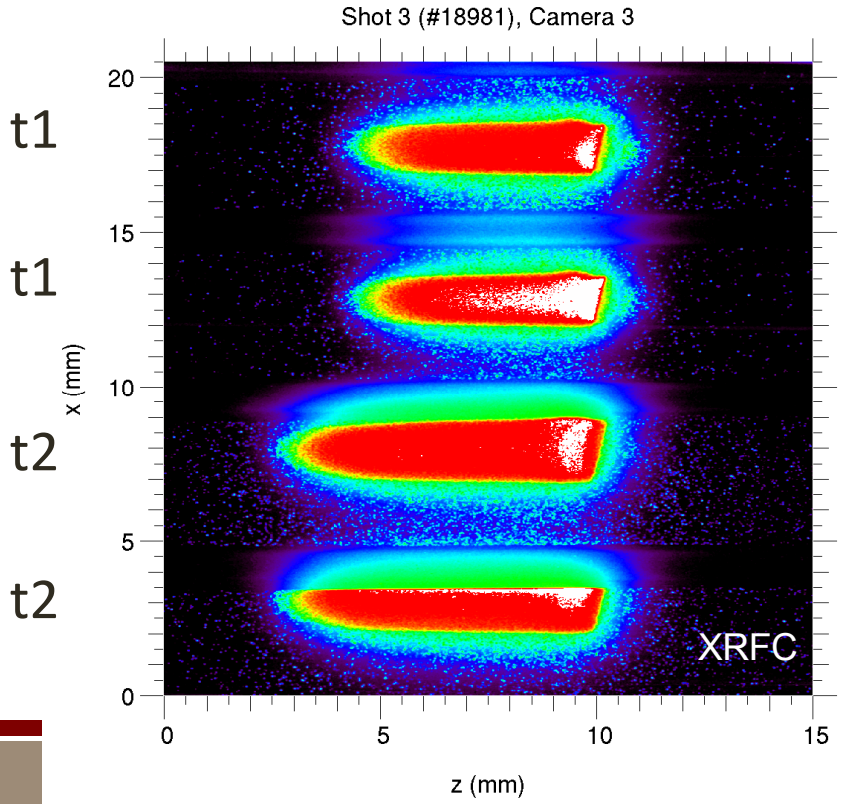

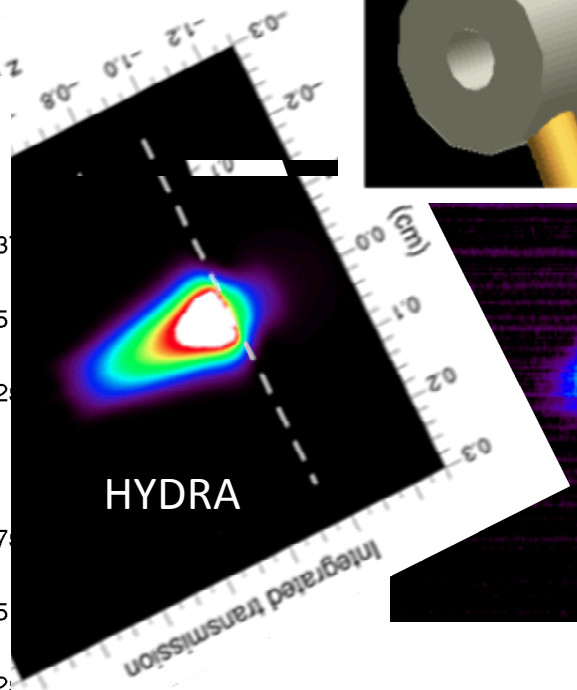

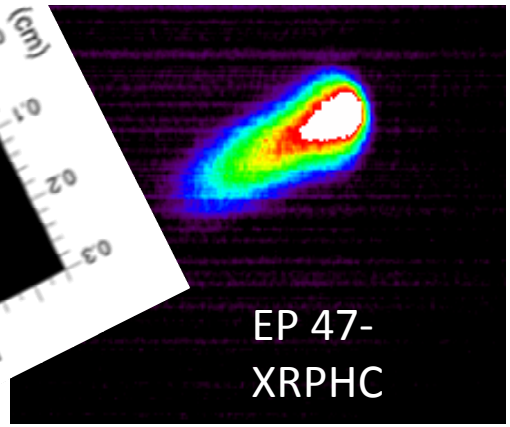

E_{laser} ~ 3.1 kJ with 4 ns duration

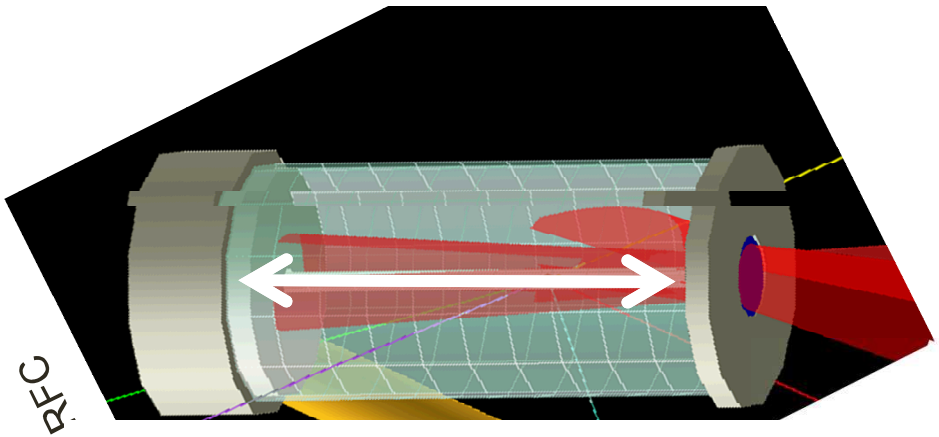

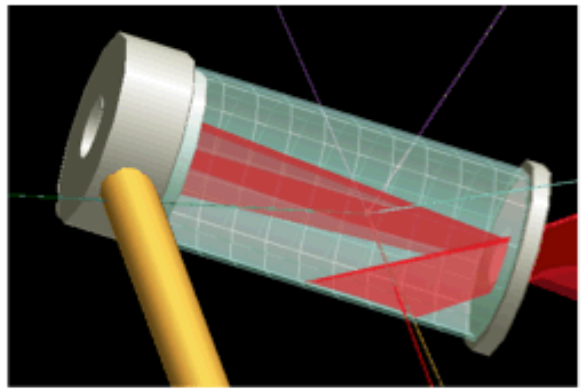

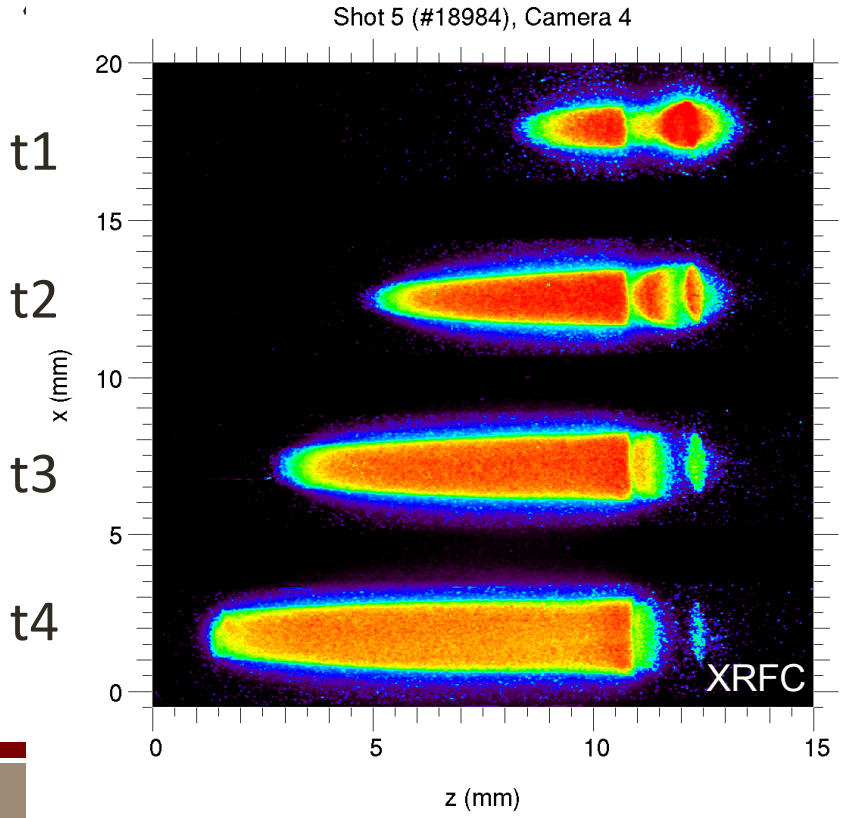

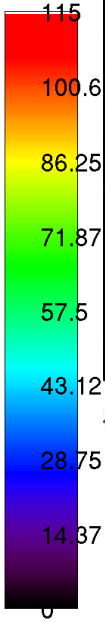

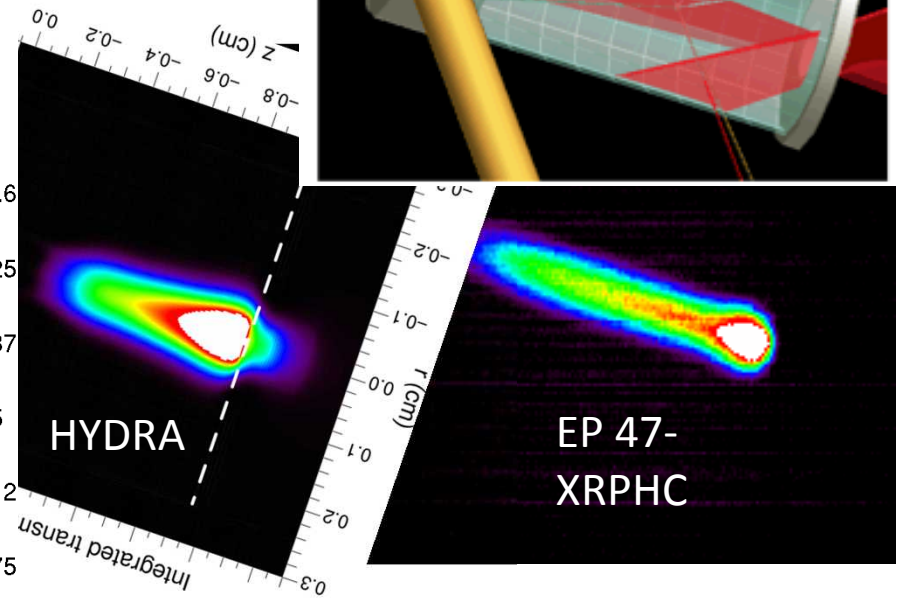

E_{laser} ~ 4.9 kJ with 10 ns duration

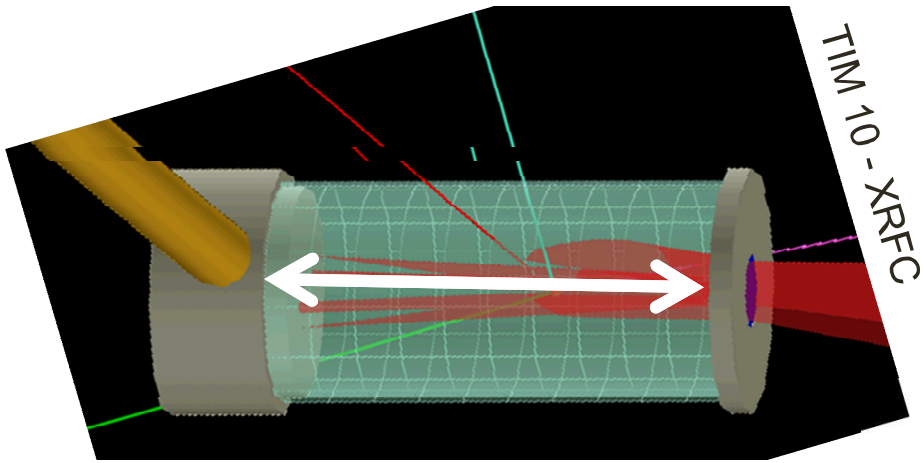

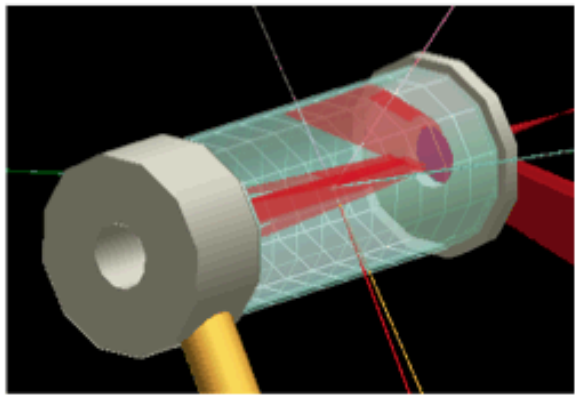

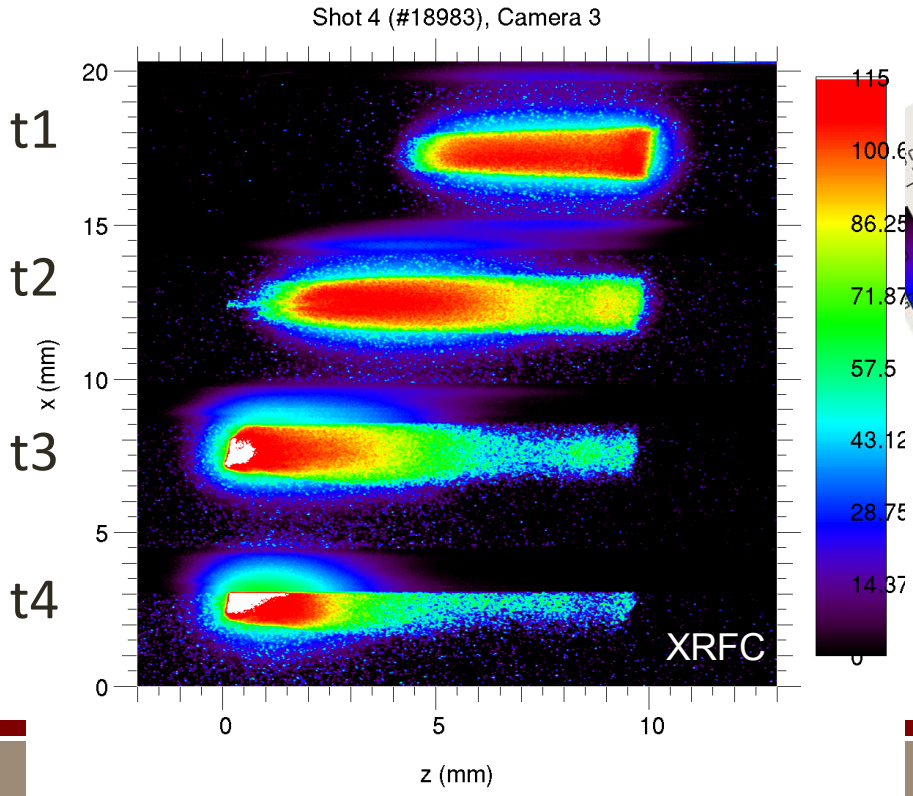

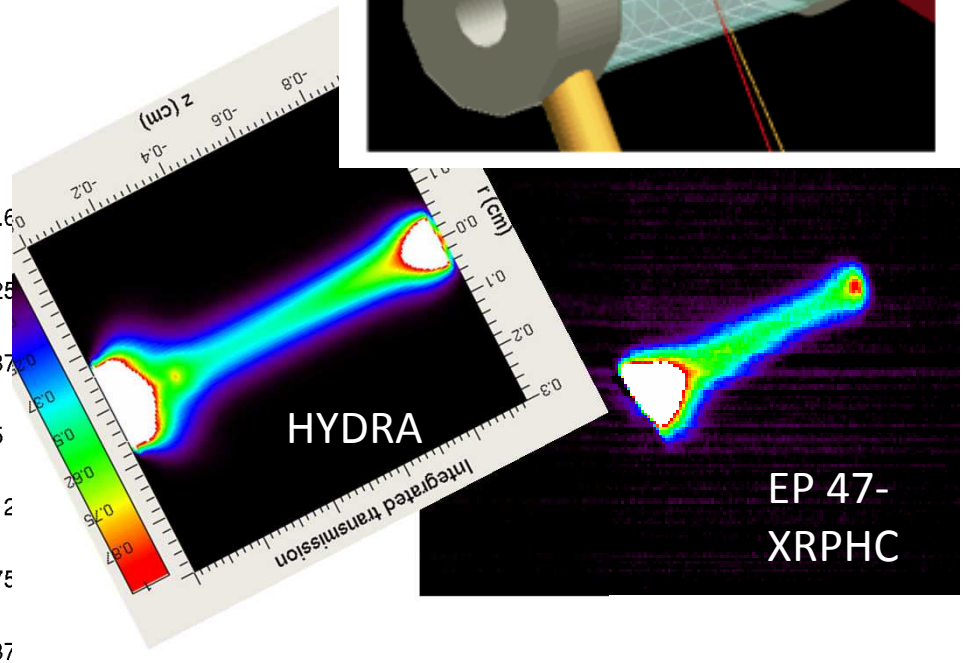

Known leaky target

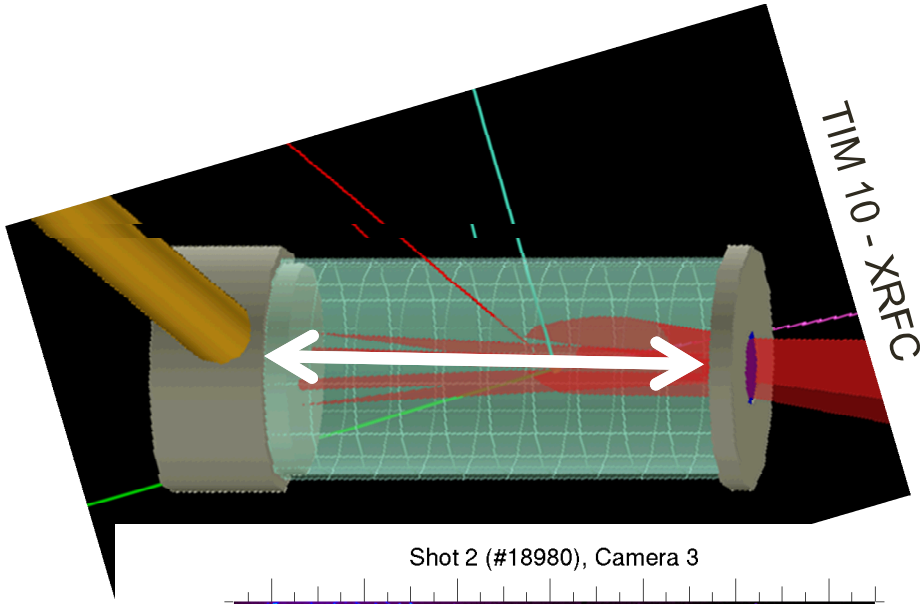

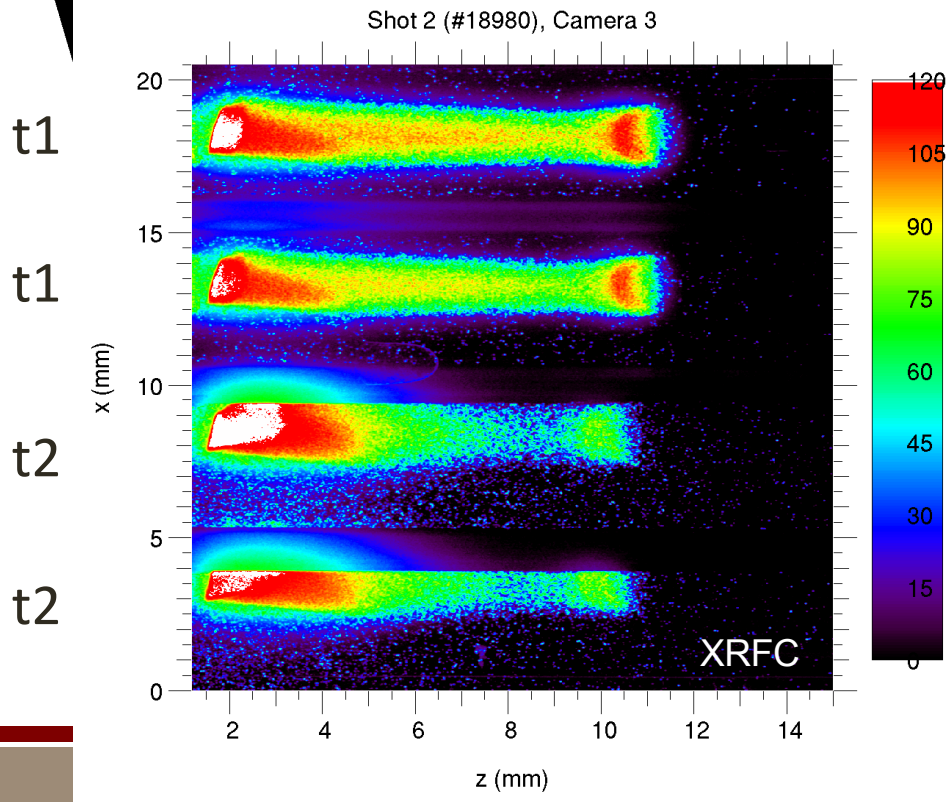

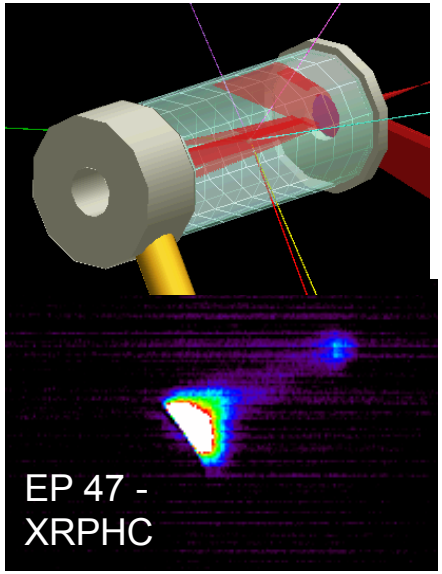

Agreement is observed for laser propagation/plasma heating with a smooth beam and no pre-pulse

Sandia National Laboratories

Experiment with 4 ns heating beam

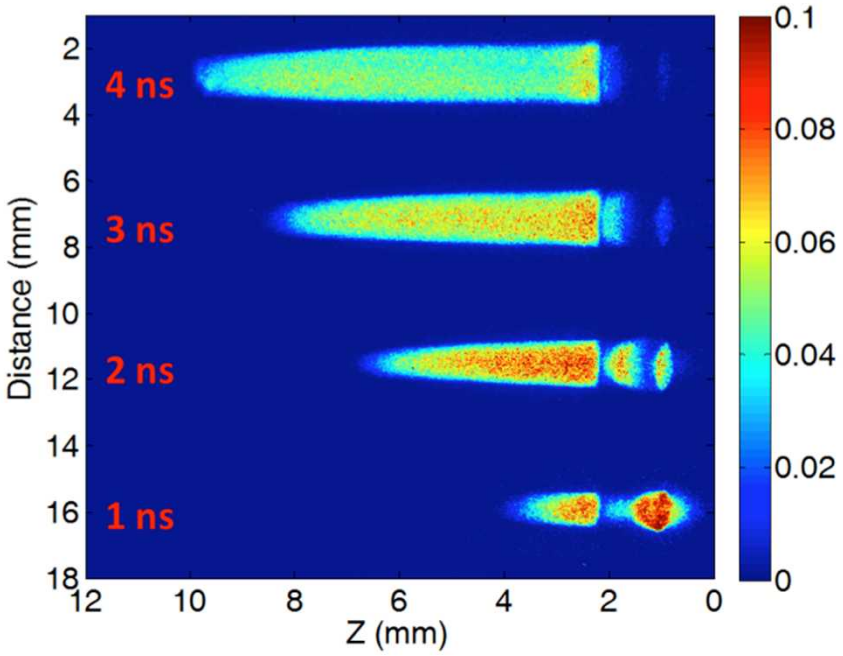

Simulation

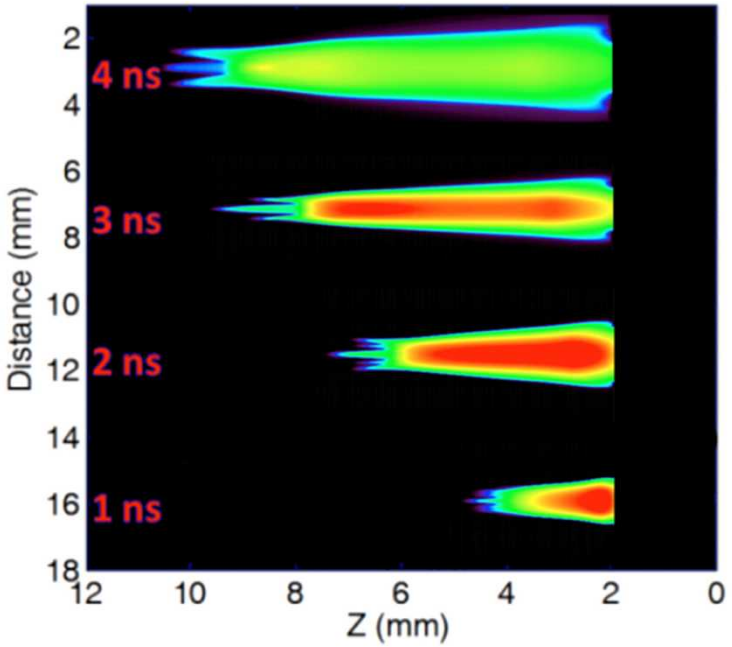

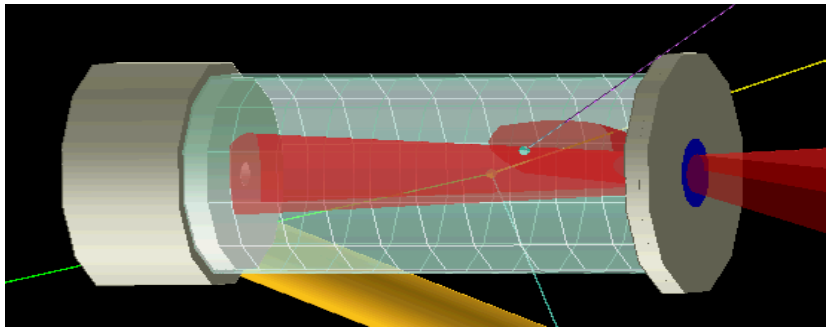

We are also evaluating power/energy scaling with different window thickness

Sandia National Laboratories

2 ns/2.2 kJ, 1 μm LEH, no prepulse

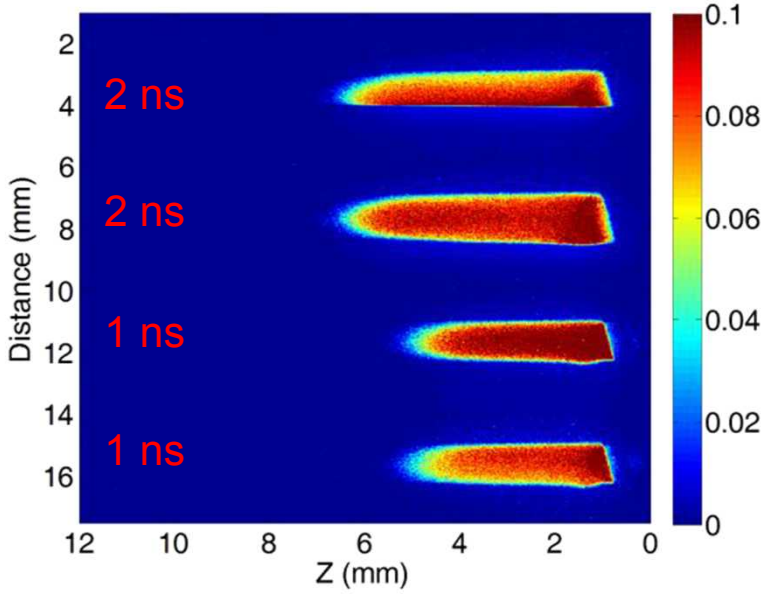

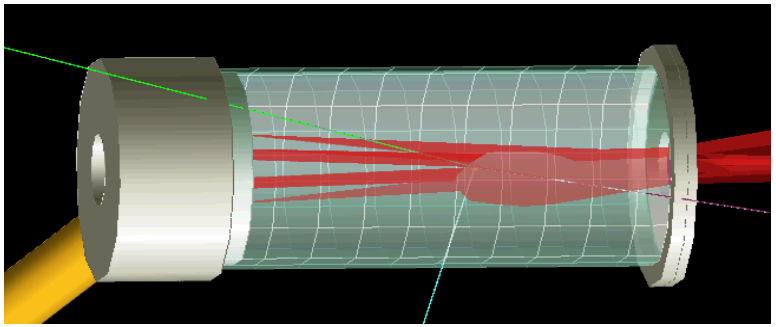

4 ns/3.1 kJ, 2 μm LEH, no prepulse

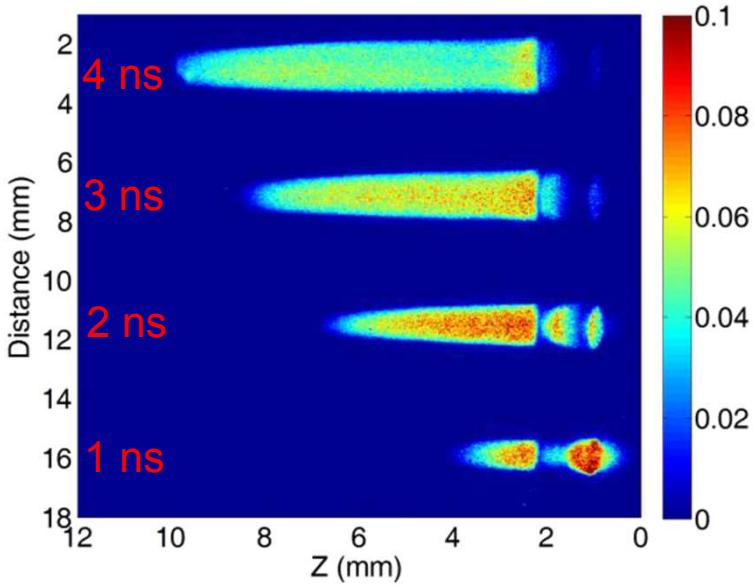

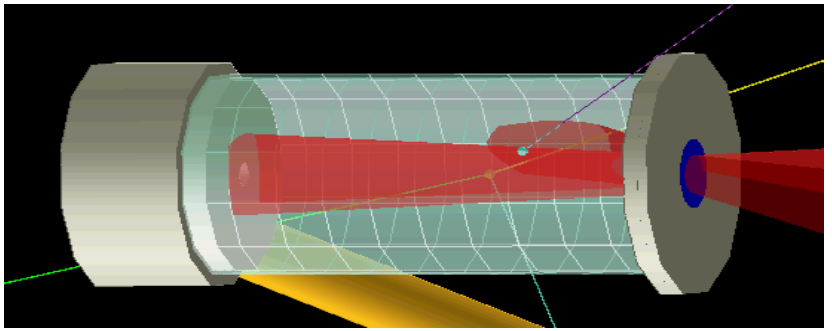

Unsmoothed beams exhibit shorter propagation distance and greater nonuniformity

Sandia National Laboratories

4 ns/2.93 kJ, 2 μm LEH, no prepulse
without DPP

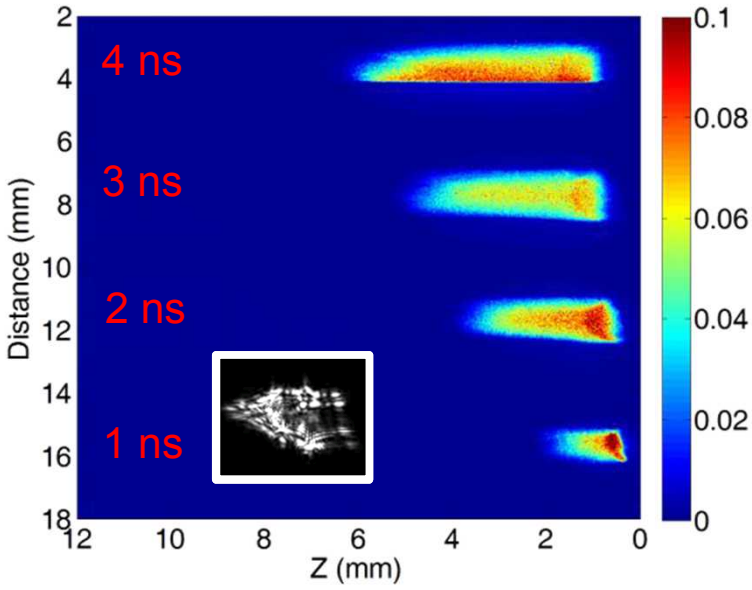

4 ns/3.1 kJ, 2 μm LEH, no prepulse
with DPP

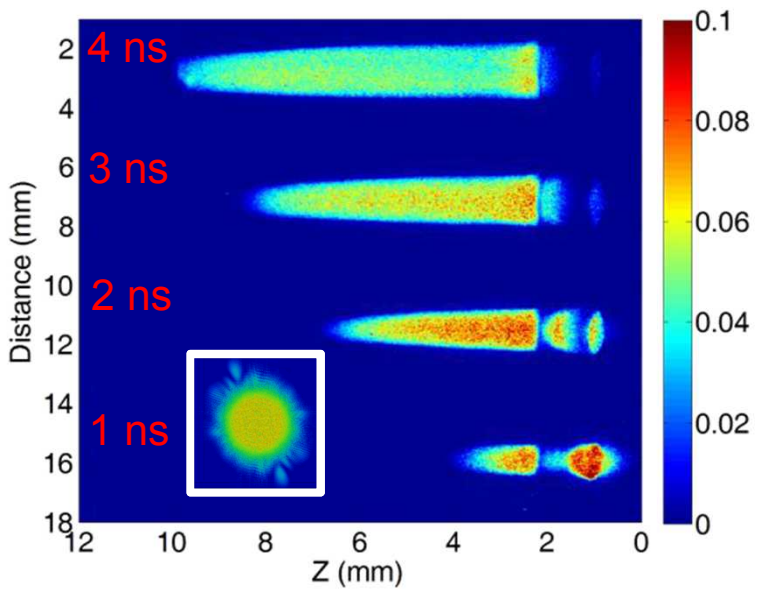

1 micron window
No prepulse, no DPP

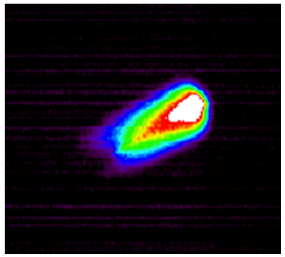

- Removing DPP likely leads to greater filamentation and LPI inhibiting propagation
- Results motivate need for phase plates on ZBL
- Is additional beam smoothing necessary?

1 micron window
No prepulse, DPP

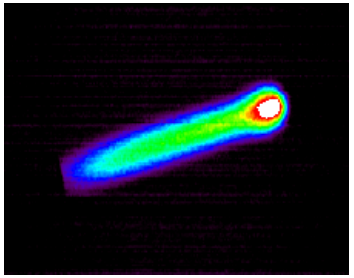

Third experiments: Improve magnetized D2 results

(simplify geometry, increase gas density, and better diagnose laser heating)

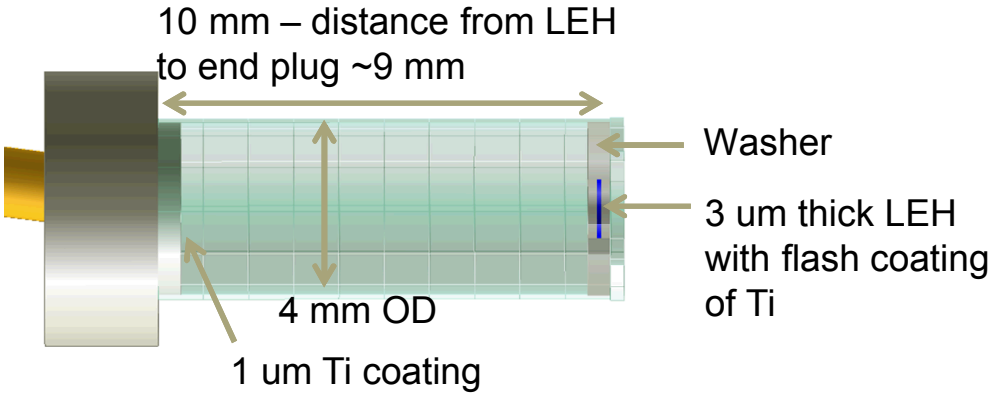

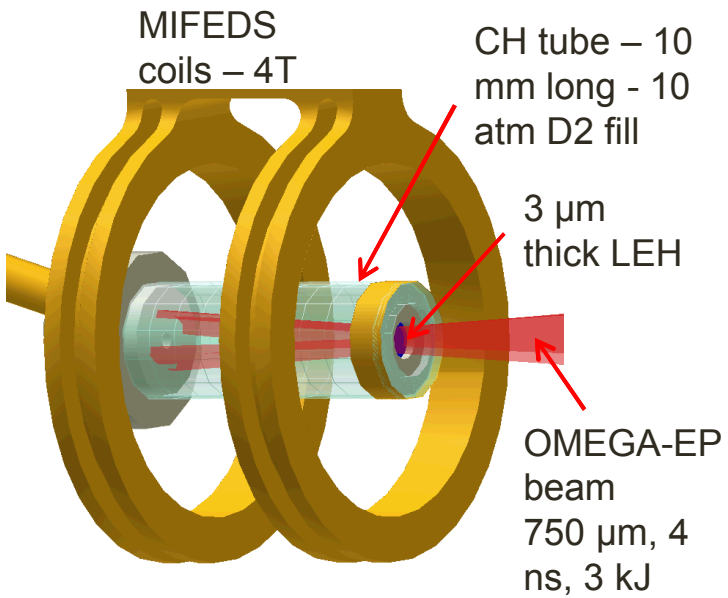

- MIFEDS design allowed for improved access but reduced B field to 4 T ($\omega\tau$~2)
- Improved target design enabled high pressures (10 atm D2 with 0.5% Ar dopant (n_e=0.058n_c)
- 1.3 mm diameter LEH window – 3 um thick
- Ti tracer layer on inside of LEH to view propagation of window material
- Single 4 ns heating beam (2 ns in some shots), 750 um DPP spot size, ~3.2 kJ energy
- Targets used pressure transducer on EP for first time – gas fill pressure is known accurately

Magnetization increases propagation length, as predicted in integrated MagLIF simulations

Sandia National Laboratories

4 ns beam no B field

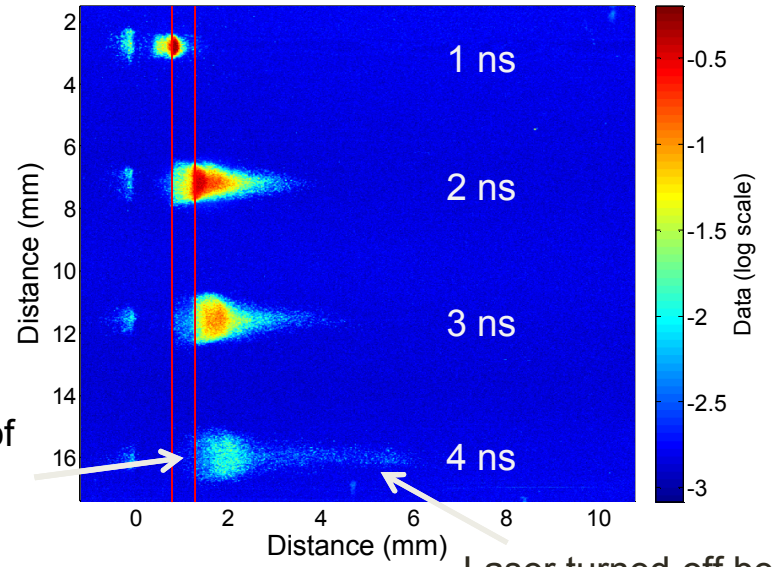

4 ns beam with B field (4 T)

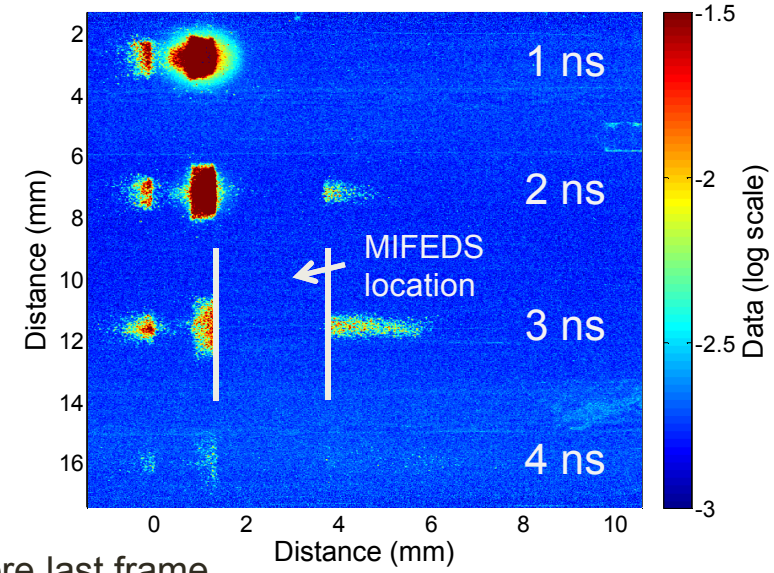

Edge of Ti foil fiducial

Laser turned off before last frame

- Initial qualitative analysis indicates excellent agreement with simulations
- Emission decays rapidly after laser turns off, final frame just after laser has low signal
- We are exploring using crystal imager to increase imaging sensitivity
- Need to further estimate and compare cooling rates

XRFC view of target

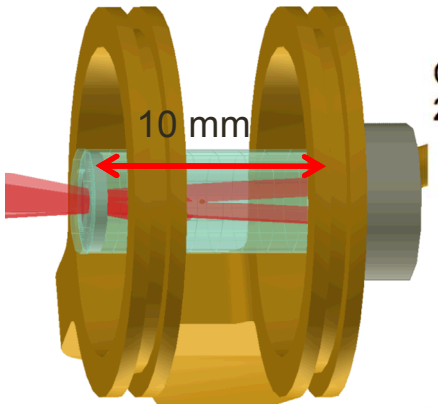

New design for 20 atm pressures, 7T fields

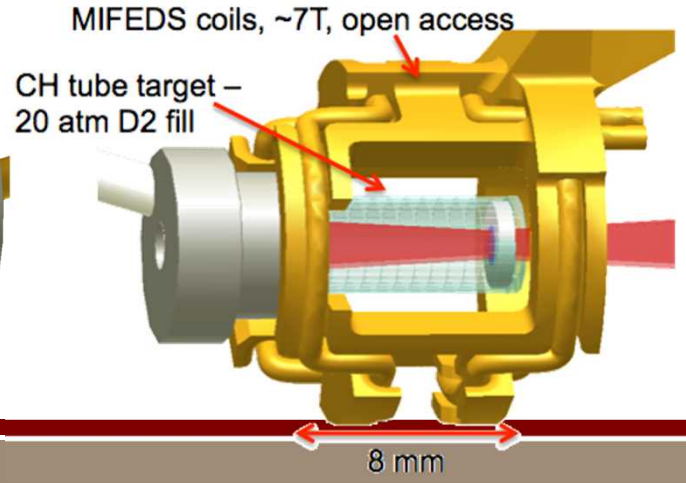

Evidence suggests that some LEH window material is propagating into the fuel region

MSPEC target view

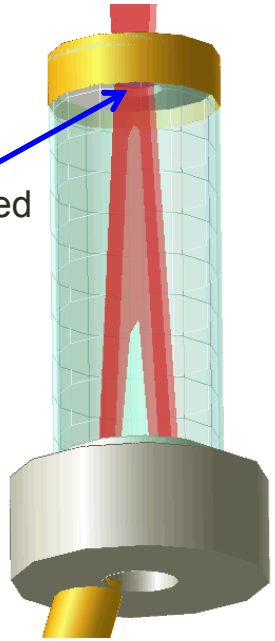

Spectrum from unmagnetized target at 2 ns into heating pulse

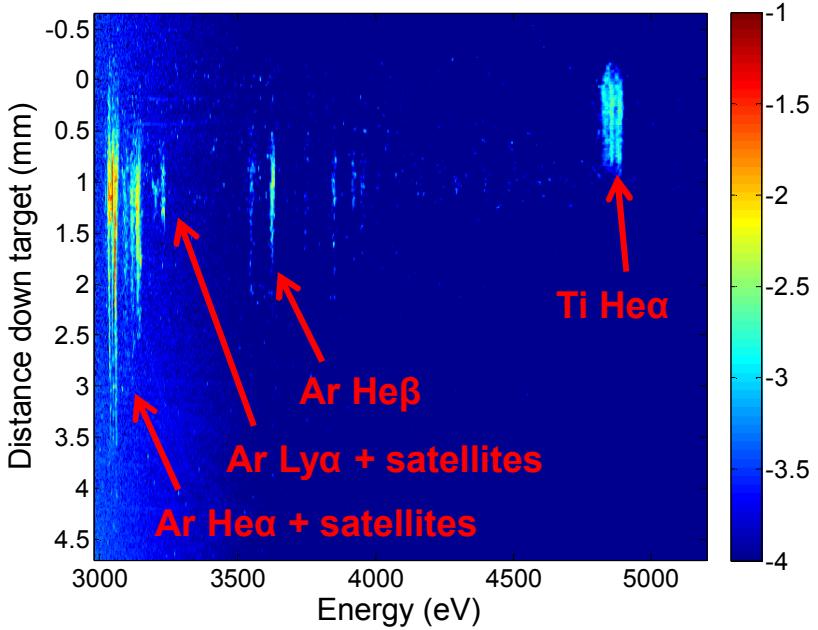

- 10 atm D2 gas fill with 0.5% Ar dopant (n_e=0.058n_c)
- 1.3 mm diameter LEH window – 3 um thick
- Simulations predict window can mix a few mm into target
- MSPEC shows heating of gas and propagation of Ti coating
- Still need to examine magnetized case and thinner windows

Work is in-progress and more shot days are planned
OMEGA-EP has a critical role in our magnetized fusion program
Similar NIF shots scheduled for Jan. 2016– "Next step" heating

Sandia National Laboratories

E_{las}~2.2 kJ in 2 ns

E_{las}~3.1 kJ in 4 ns

E_{las}~4.9 kJ in 10 ns

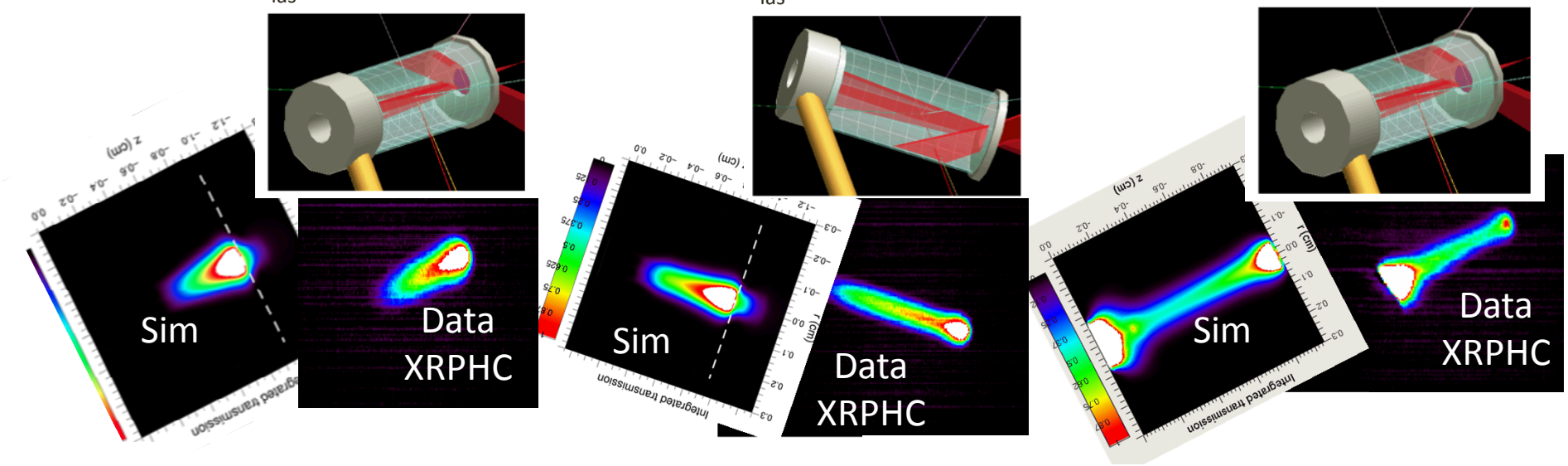

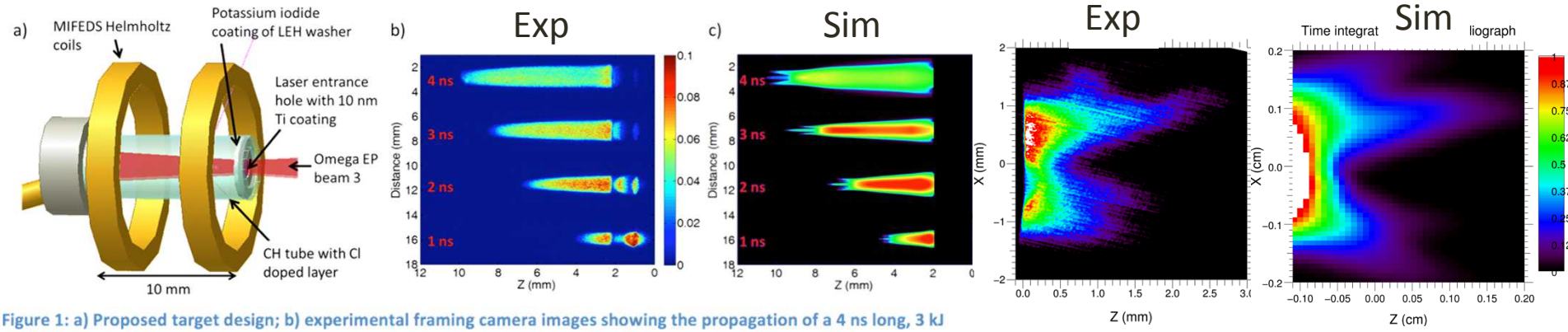

Figure 1: a) Proposed target design; b) experimental framing camera images showing the propagation of a 4 ns long, 3 kJ OMEGA EP beam through a pure Ar gas at several times; c) Simulated images of the experiment from HYDRA.

Outline

1. Magnetized Liner Inertial Fusion (MagLIF)
2. Comparisons of MagLIF-related experiments to simulations
3. OMEGA-EP laser-heating experiments
4. Magnetized hohlraum experiments at OMEGA
5. Mini-MagLIF at OMEGA

Adequate coupling of the laser is required for indirect drive ignition

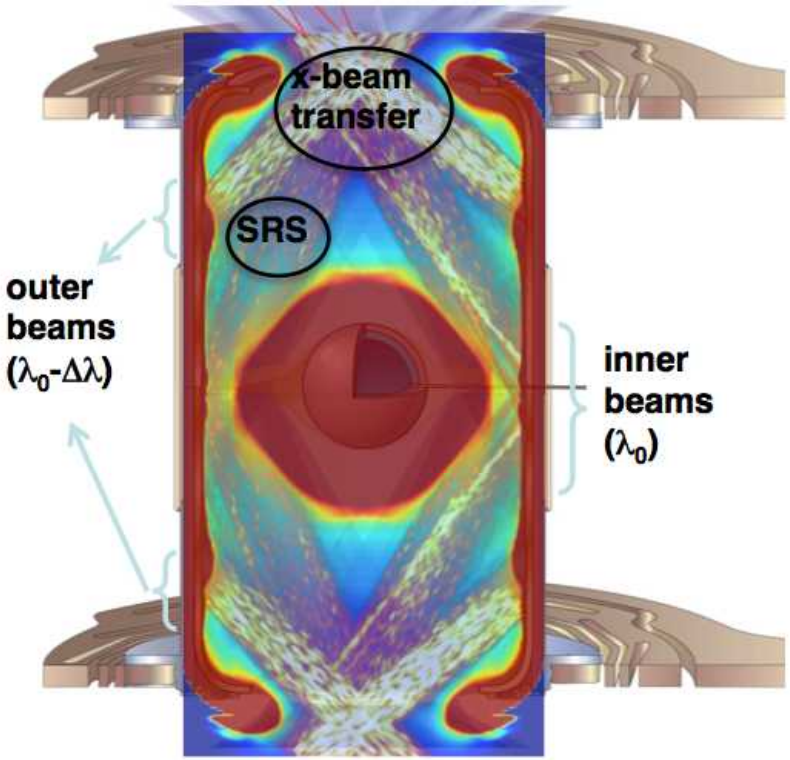

- laser-hohlraum coupling affects:
  - radiation drive (implosion velocity)
  - radiation symmetry
  - preheat

- lower than expected T_e is inferred [1] in the underdense plasma for NIF ignition hohlraums:
  - significant collisional absorption in cooler, low-Z plasma (symmetry)
  - substantial SRS on inner beams (drive, symmetry, preheat, …)

Higher coronal plasma temperatures can improve laser-plasma coupling in hohlraum targets

1. M.D. Rosen *et al.*, *HEDP* **7**, 180 (2011)

Slide courtesy D. S. Montgomery

Use of External Magnetic Fields in Hohlraum Plasmas to Improve Laser-Coupling

- **Increased underdense plasma temperatures are desirable for NIF ignition hohlraums**
  - improve laser propagation through long-scale-length low-Z plasma (less inverse bremsstrahlung absorption)
  - possibly mitigate LPI with higher T_e (higher $k\lambda_D$, more Landau damping)
- **Magnetic insulation can increase the plasma temperature with $B_z \geq 10$-T in gas-filled hohlraums**
- **Omega experiments using gas-filled hohlraums demonstrate an increased plasma temperature with $B_z = 7.5$-T**
  - plasma conditions measured with 4ω Thomson scattering
- **2-D HYDRA simulations are in good agreement with experimental results**

Los Alamos NATIONAL LABORATORY EST.1943

Slide courtesy D. S. Montgomery

Experiments are performed at Omega using gas-filled hohlraums and an external B-field

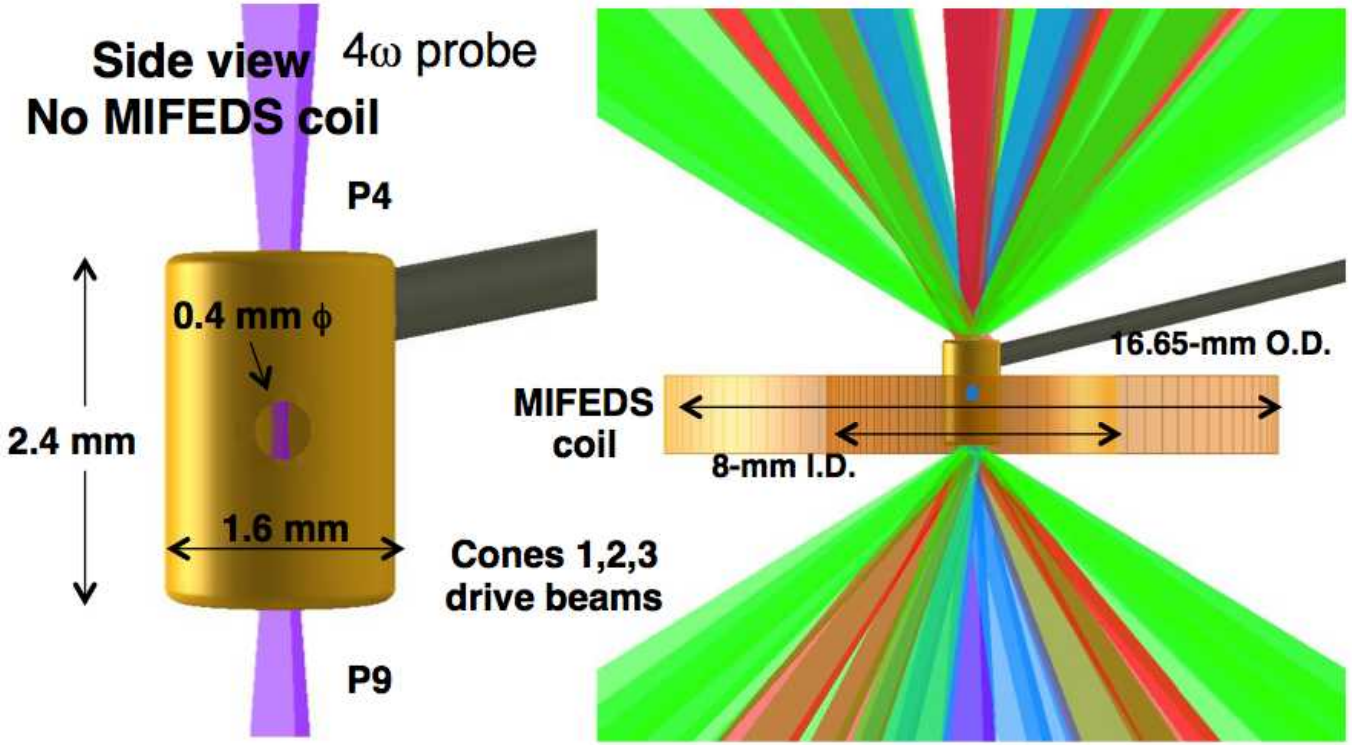

Actual B(r,z) imposed

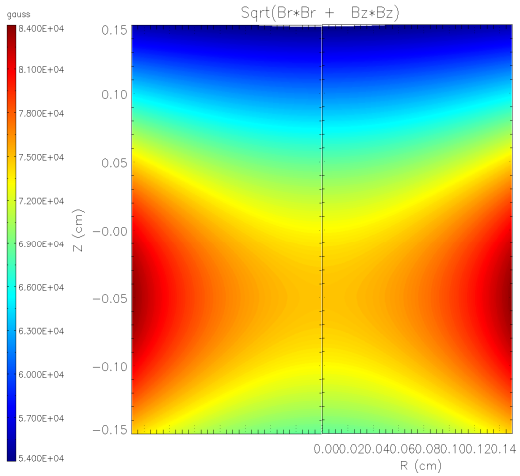

- 19-kJ of 3ω in 1-ns pulse (39 beams, 3 cones), gas-fill 0.95-atm 25% C_5H_{12} + 75% CH_4
- plasma conditions measured using 4ω Thomson scattering, delayed 0.3-ns
- external B_z applied using MIFEDS coil in a 400-ns pulse†

† Gotchev *et al.*, *Rev. Sci. Instrum.* **80**, 043504 (2009).

Slide courtesy D. S. Montgomery

Simulations show window and wall motion

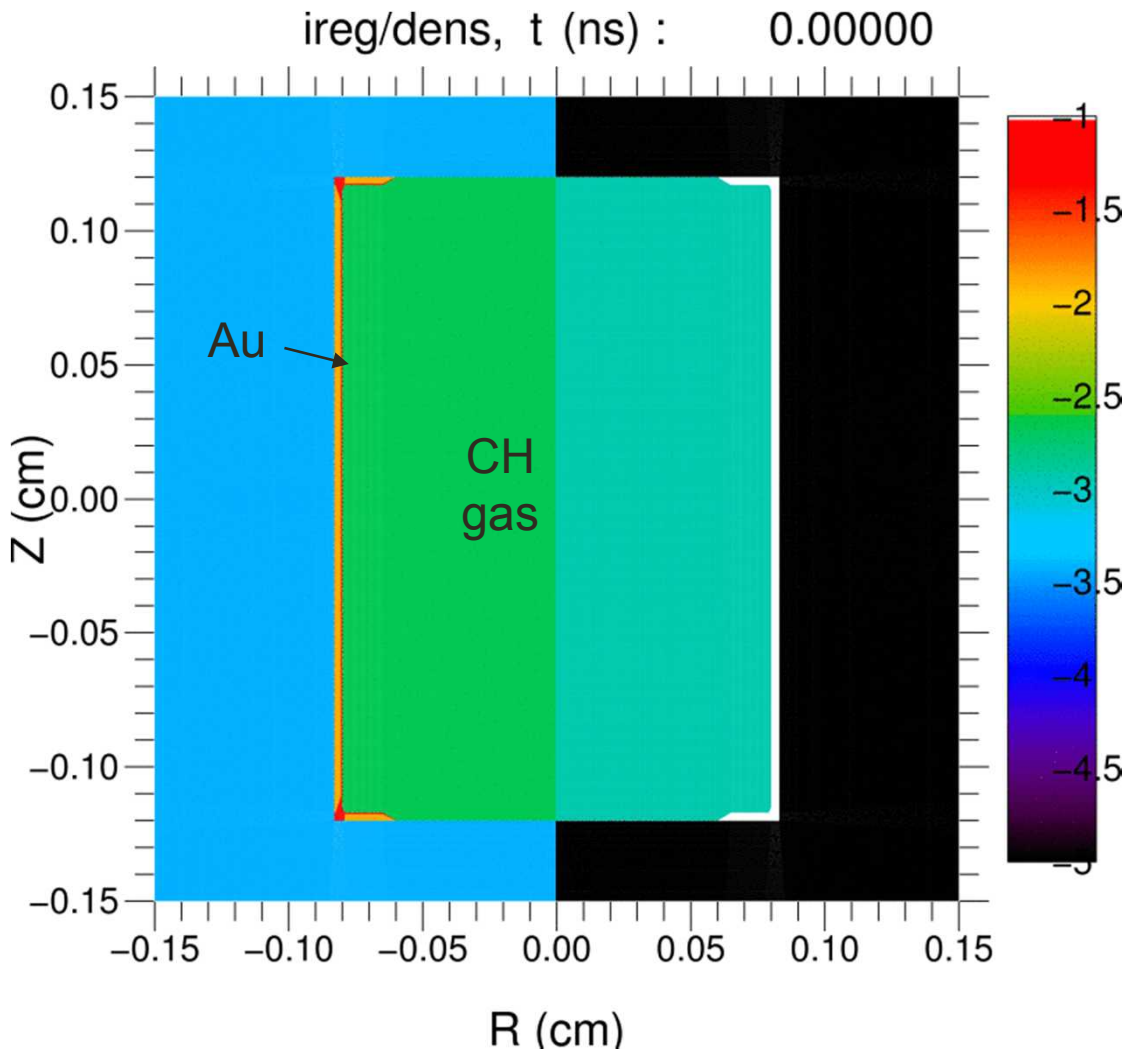

- Material regions
  Au (red)
  CH gas (green)
- Log(density)
- Plots very similar with and without B_z

  (i.e. $\beta >> 1$, B-field affects thermal conduction but not hydro)

Simulations show an increase in plasma T_e with B_z=7.5 T

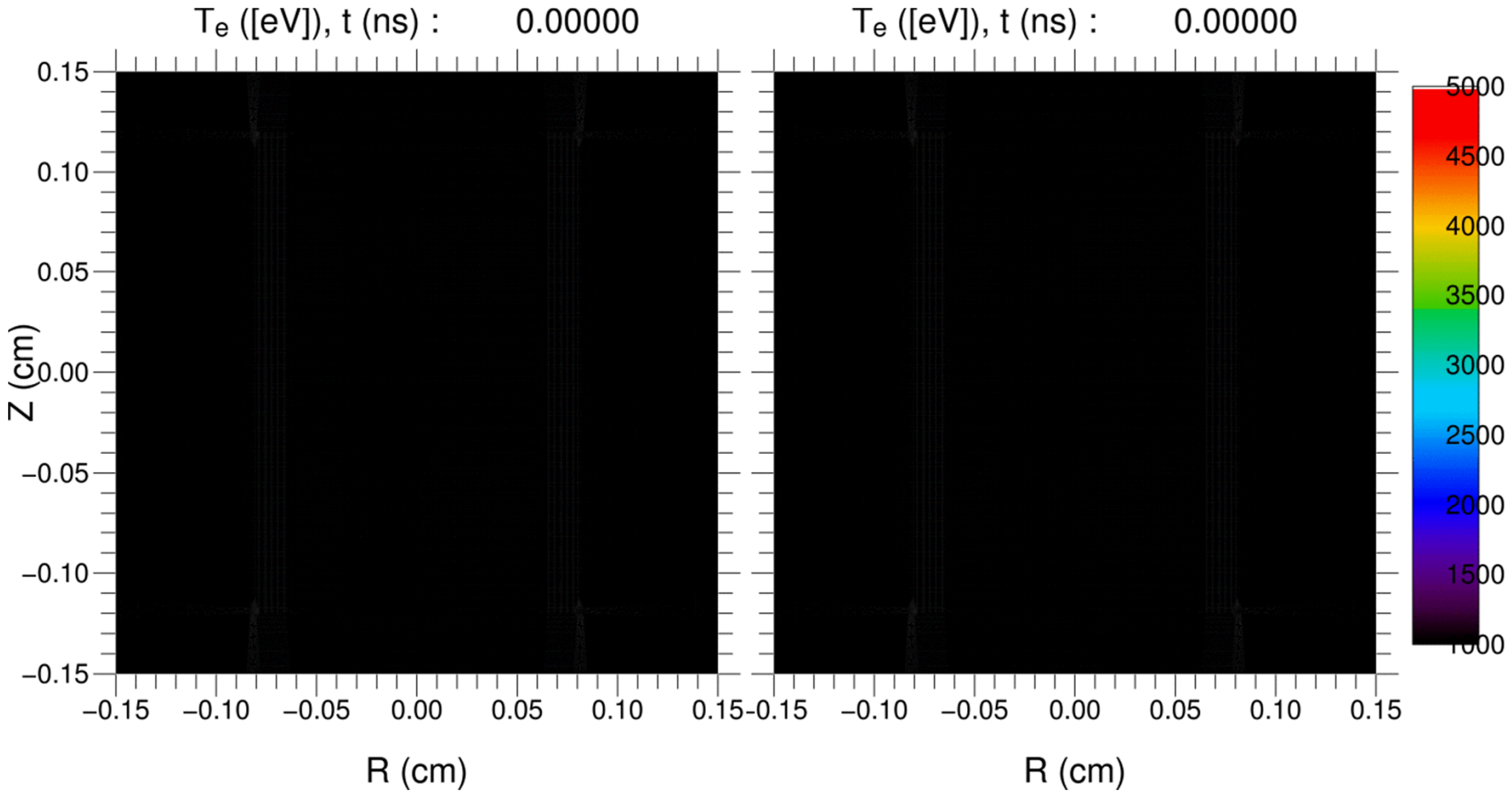

MHD modeling and experiments are in general agreement regarding T_e trend

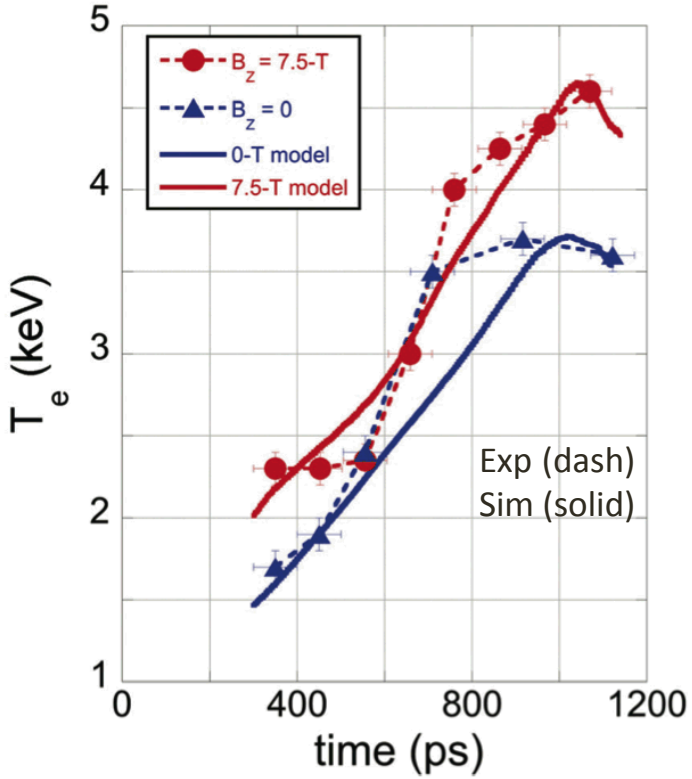

FIG. 3. Measured electron temperature versus time for B = 0 (blue triangles) and B = 7.5-T (red circles). Over-plotted as solid lines are the 2-D HYDRA model for B = 0 (blue) and B = 7.5-T (red).

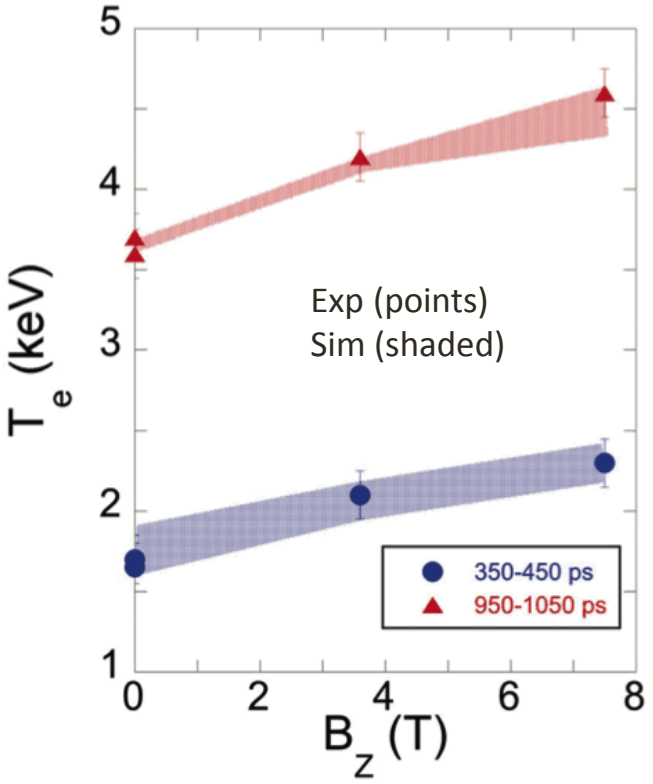

FIG. 4. Measured electron temperature versus B-field for early time 350–450 ps (blue circles) and late time 950–1050 ps (red triangles). Results from the 2-D HYDRA simulations shown as blue and red shaded regions.

Adapted from D. S. Montgomery, et. al., Phys. Plasmas 22, 010703 (2015).

Outline

1. Magnetized Liner Inertial Fusion (MagLIF)
2. Comparisons of MagLIF-related experiments to simulations
3. OMEGA-EP laser-heating experiments
4. Magnetized hohlraum experiments at OMEGA
5. Mini-MagLIF at OMEGA

LLE is pursuing "mini-MagLIF" as a direct-drive approach using OMEGA to implode and preheat

Sandia National Laboratories

A seed field of 15 T and laser energy of 10 kJ over 1mm can be provided on OMEGA

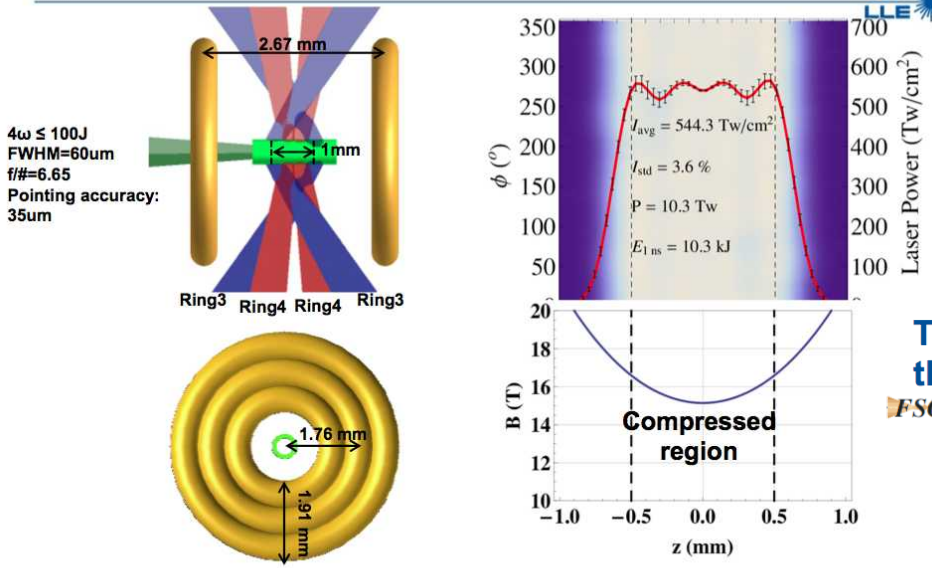

Scaled experiment to study relevant magneto-inertial physics

The target size is scaled according to the kinetic energy that can be coupled to the implosion

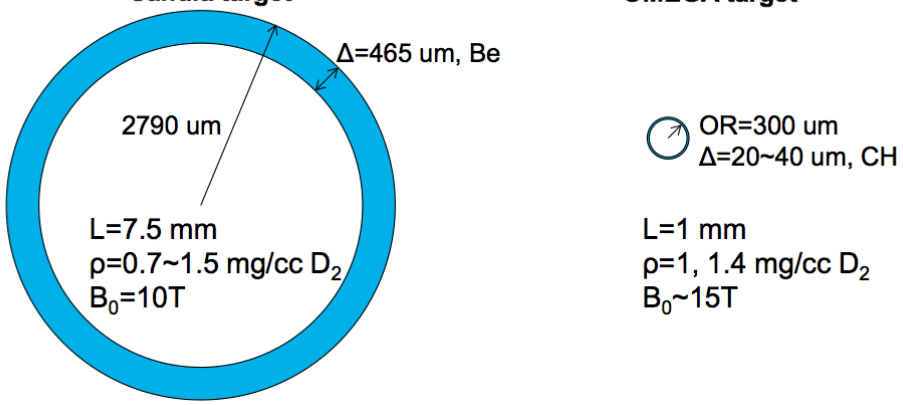

- **The Sandia design couples approximately 1 MJ cm^{-1} to the liner****
- **Omega can couple approximately 0.01 MJ cm^{-1} to a cylindrical shell**

Ion temperature increase and yield enhancement predicted by multiple codes

*M. R. Gomez et al., Phys. Rev. Lett. **113**, 155003 (2014)
** S. A. Slutz et al., Phys. Plasmas **17**, 056303 (2010

Slides courtesy J. R. C. Davies, P.-Y. Chang, et. al.

Initial integrated HYDRA setup of the mini-MagLIF on OMEGA target

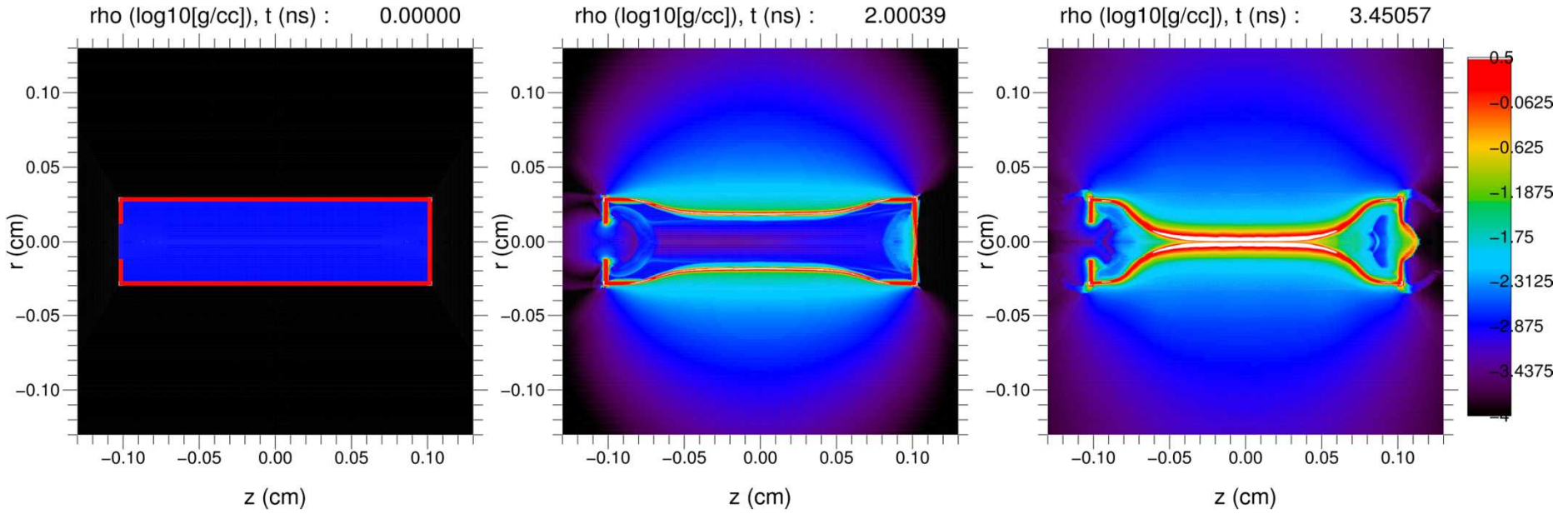

- L=2 mm, OD=600 μm, Δ_{shell}=30 μm (CH), δz_{win}=1.5 μm, ρ_{gas}=1.5 mg/cc (DD), B_z^0=15 T
- Compression: ~10 kJ of 3ω in 2.5 ns at f/6.65
- Coupling: ~8 kJ total, ~1 kJ final K.E.$_{shell}$
- Heater beam: ~80 J of 4ω also in 2.5 ns with FWHM~60 μm, delayed Δt = 1.2 ns

Integrated preheat+implosion simulations are used to evaluate various physics issues

Sandia National Laboratories

Preheating timing and effectiveness

Lin(T_e)

Lin(T_i)

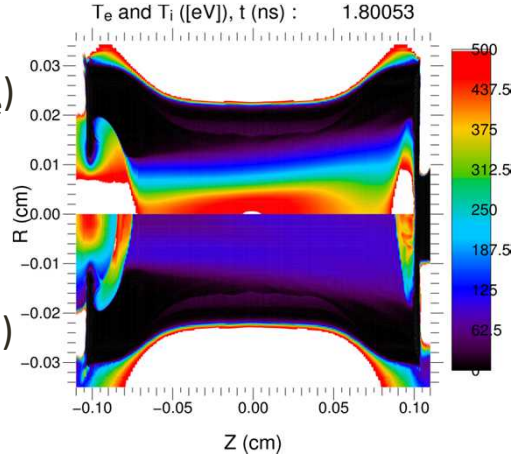

Window and far wall ablation and mix

Log(E_{dep})

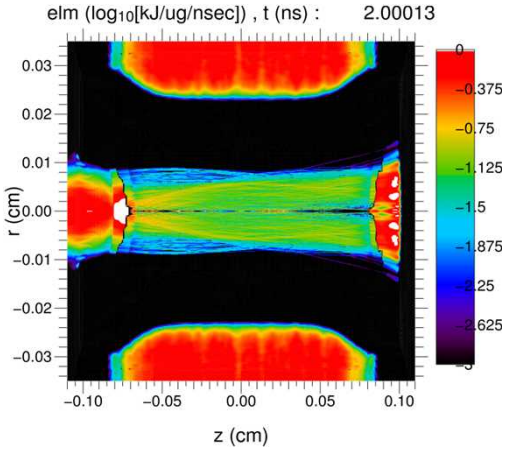

Heater beam refraction off compression shock

Log(ρ) from 10^{-4} to 3 g/cc

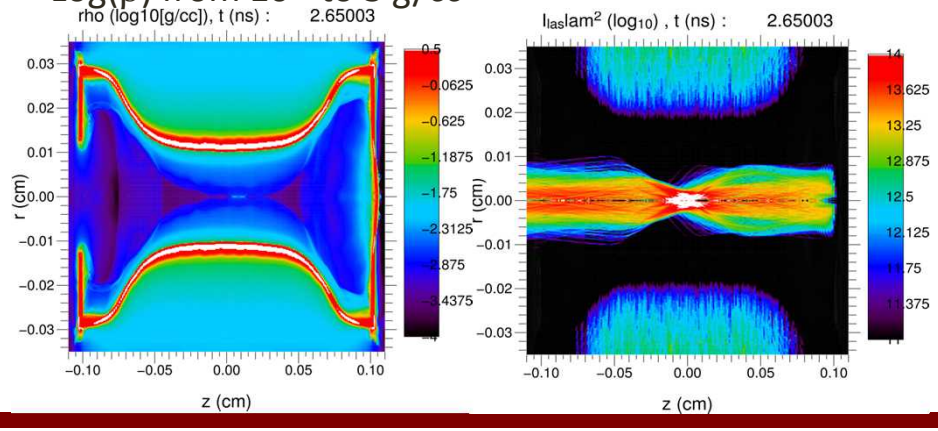

Temperature at center of gas vs time

Lin(T_e)

Lin(T_i)

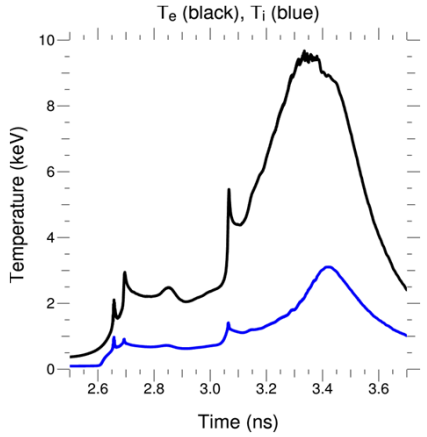

Probe at {r=0, z=0}

Compression, shocks, and heater beam raise temperatures to 1 keV ($T_e \neq T_i$) and above

Sandia National Laboratories

Log(T_e and T_i), from 0.2 keV to 5 keV

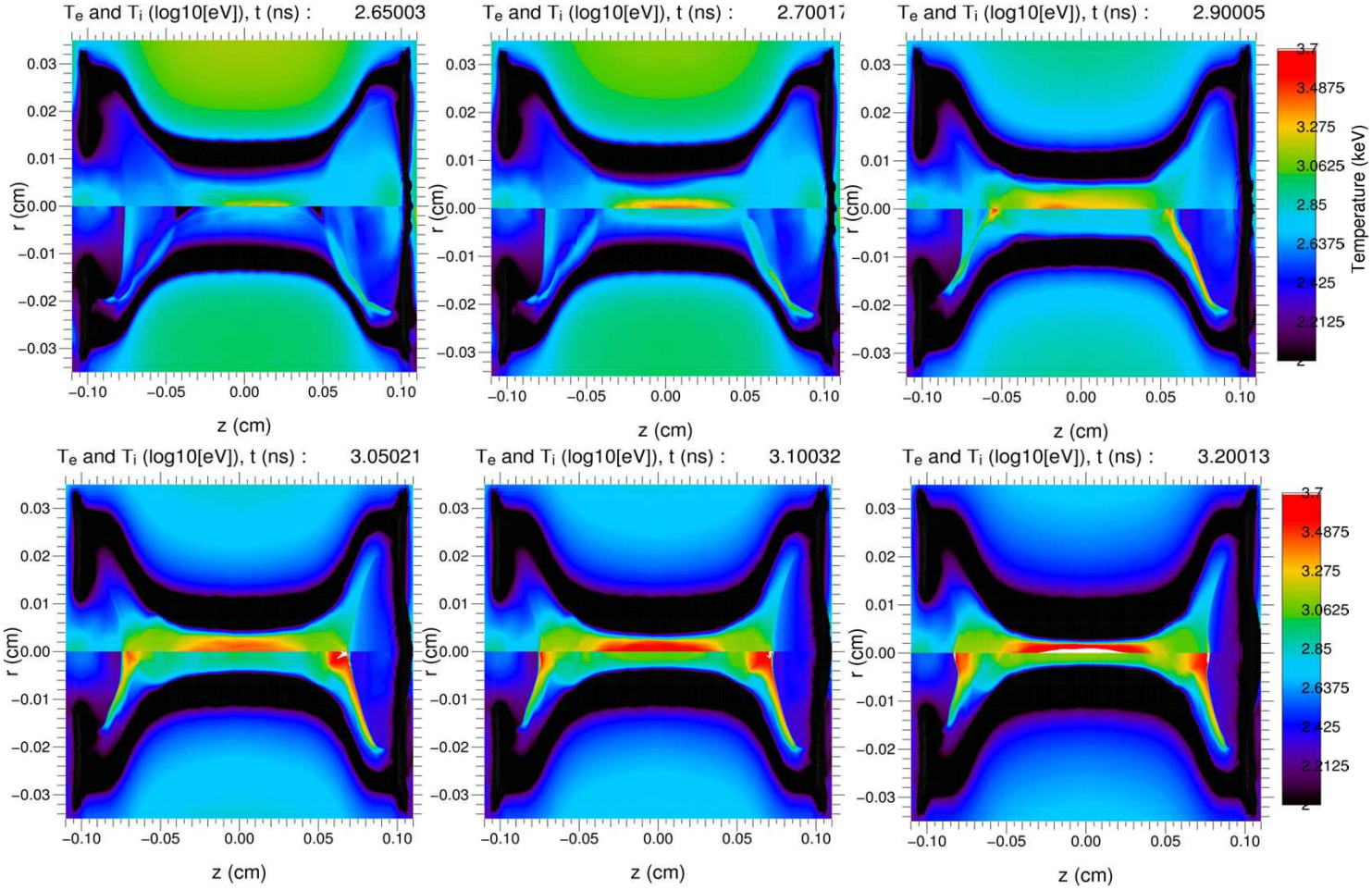

Probe at {r=0, z=0}

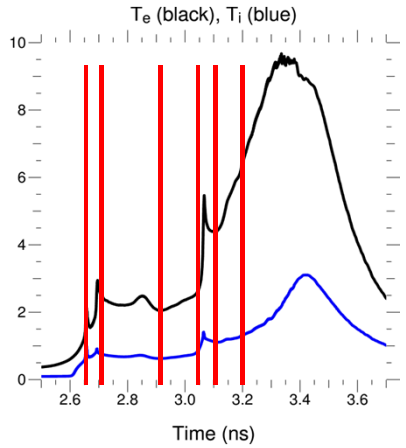

Progression of late time density: channel self-focusing, LPI, and reflection

Sandia National Laboratories

Log(ρ) from 10^{-4} to 3 g/cc

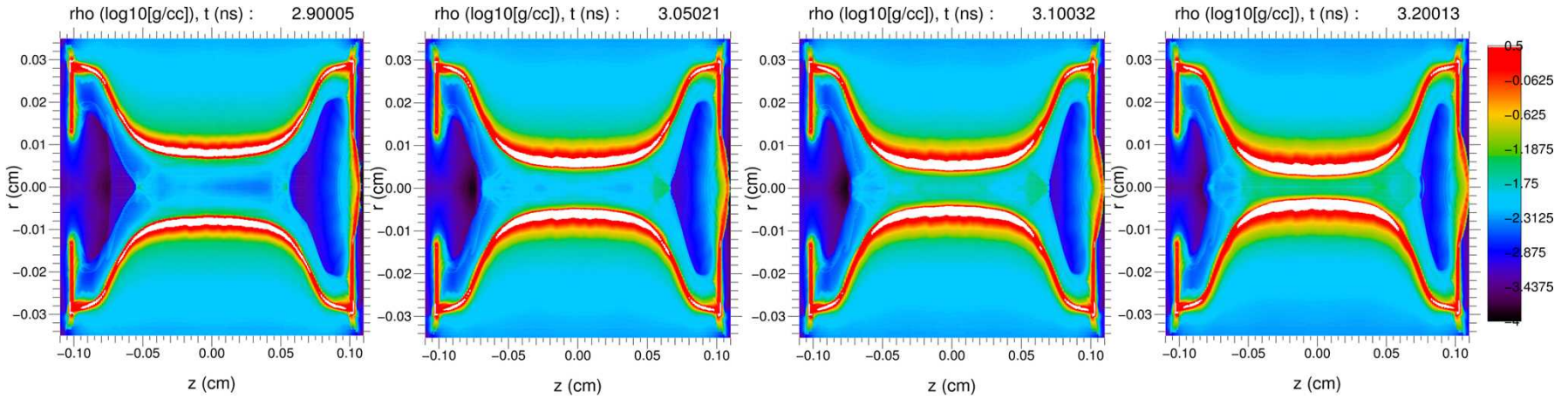

Log(e^- density), from 0.1* to 1.0*$n_{crit}^{4\omega}$

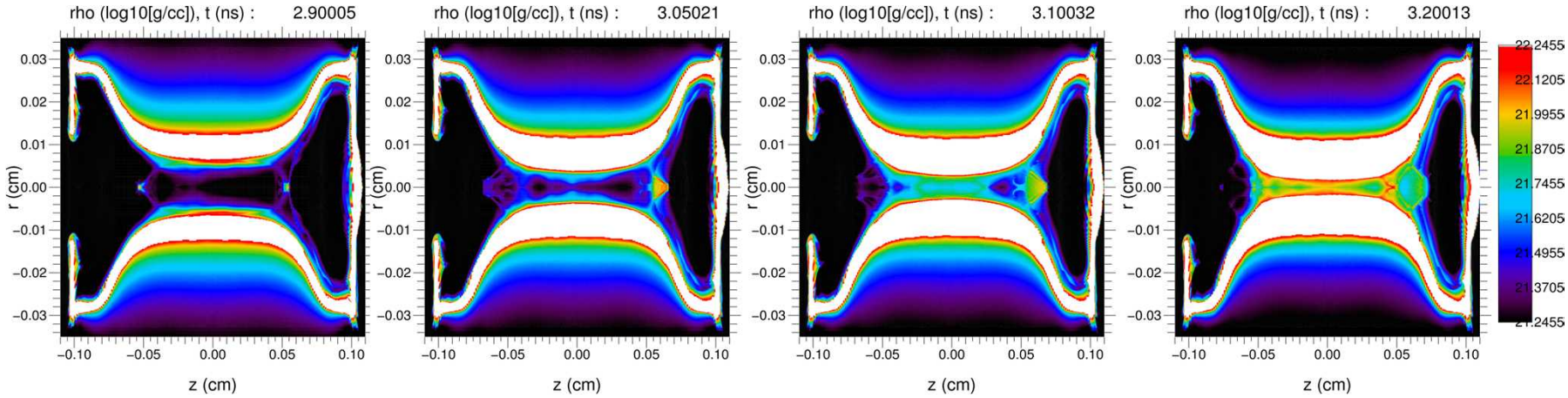

Plasma pressure may prevent window and wall mix, and CR_{2D}~45 (r_{stag}~6μm) from CR_{1D}~35 (r_{stag}~7-8μm)

Sandia National Laboratories

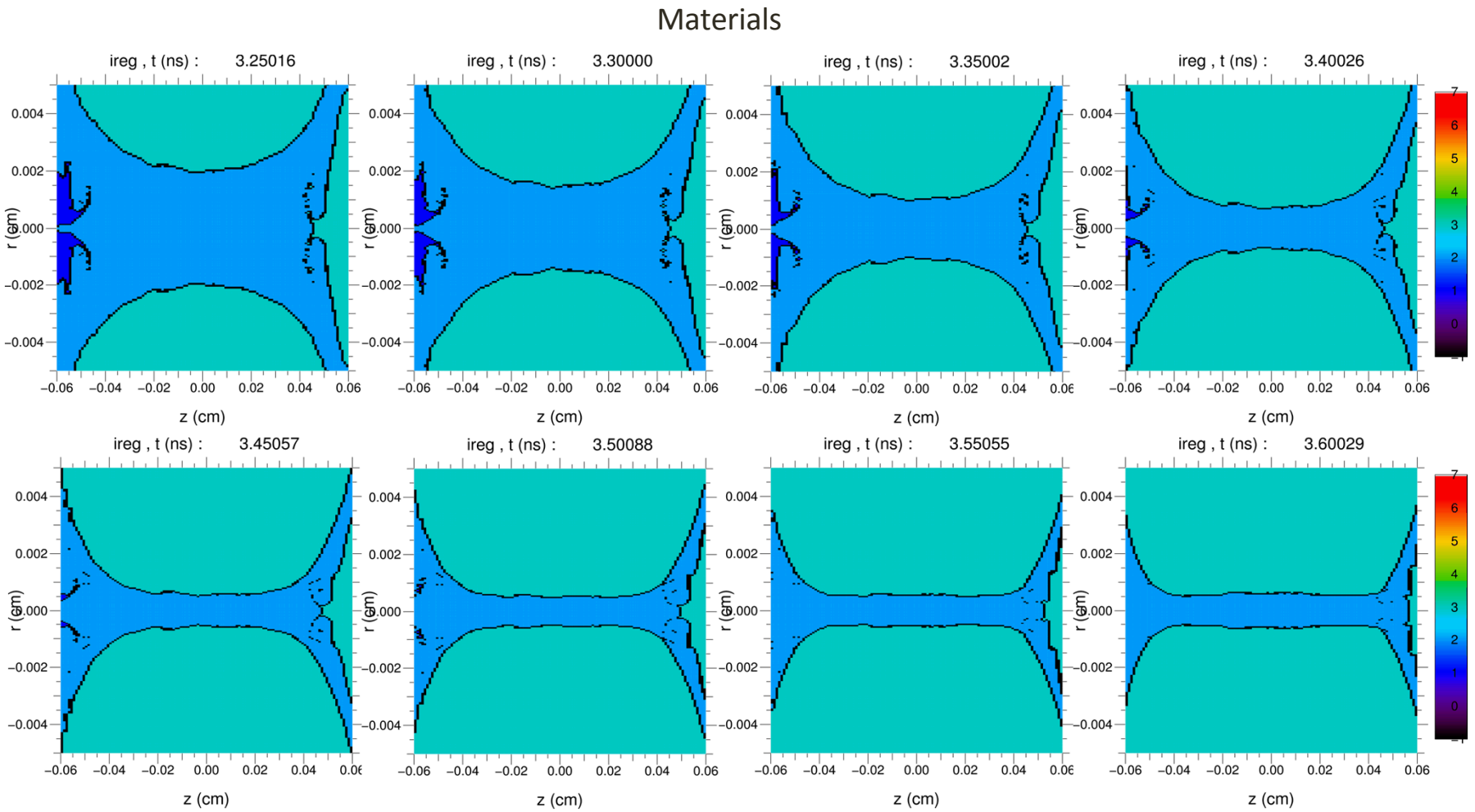

At late time, compression leads to T_i~3 keV although plasma remains out of equilibrium

Sandia National Laboratories

Log(T_e and T_i), from 0.2 keV to 9.3 keV

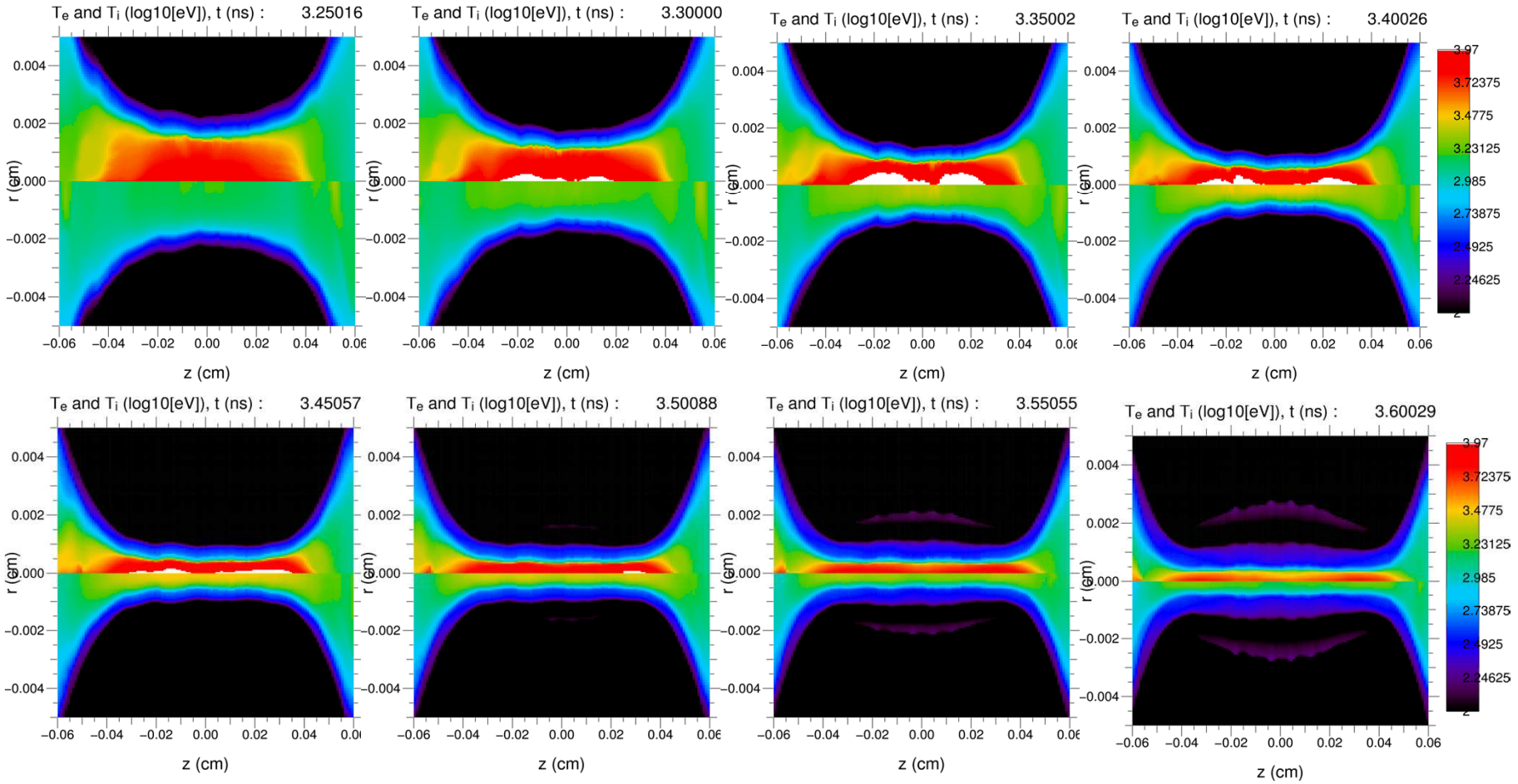

Fusion performance

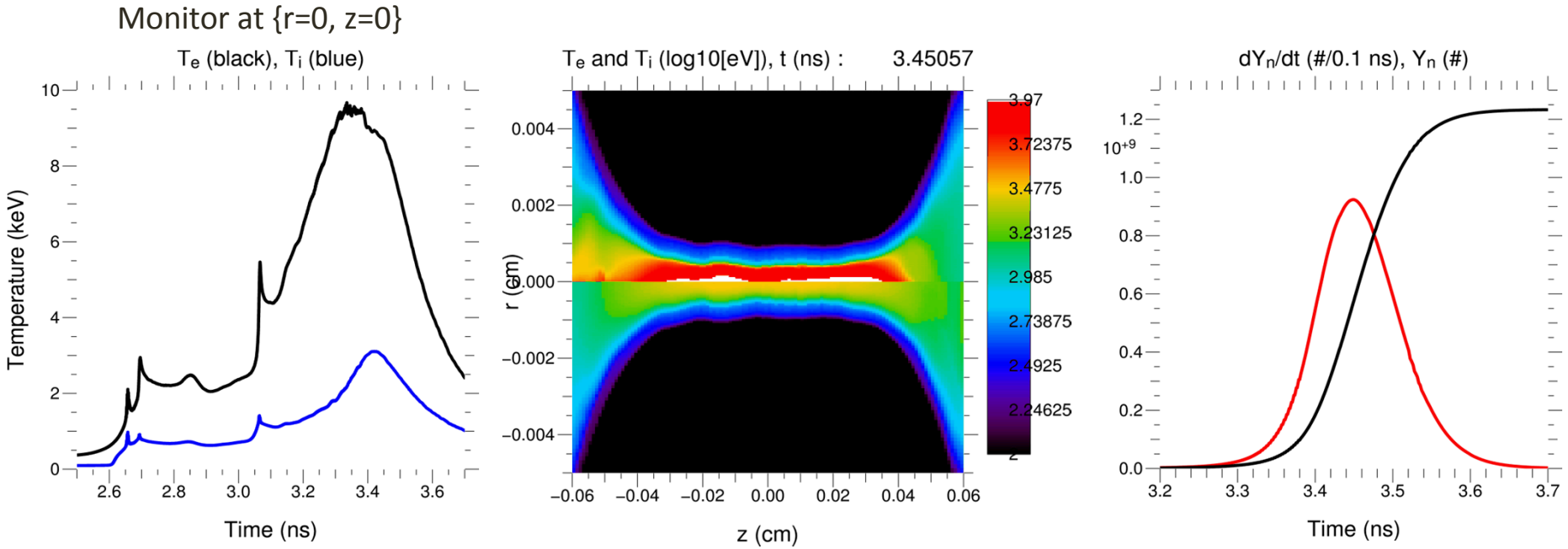

- Burn time ~200 ps
- T_i~3 keV for T_i^0~0.1 keV and B_z^0=15 T
- $\langle B_z^f \rangle$~130±30 MG in hot spot, or
  $r_{stag}/r_{L,\alpha}$~0.14±0.03, or
  $r_{stag}/r_{L,D}^{30keV}$ ~2.2±0.5 (no Knudsen)
- Y_n^{DD}~1.6e9 from dz~1mm (~15-30% of 1D)

- Mass loss (not that bad):

from ± 400 μm : 26%

from ± 300 μm : 46%

from ± 200 μm : 54%

- Flux loss (no Nernst yet): 58%
- E_{gas}^{stag} ~ 85 J

LLE has already conducted separate implosion- and preheat-focused experiments

Sandia National Laboratories

Two different experiments were conducted on 4/21

UR LLE

Implosion experiments

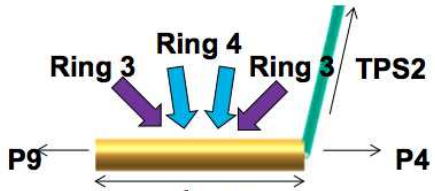

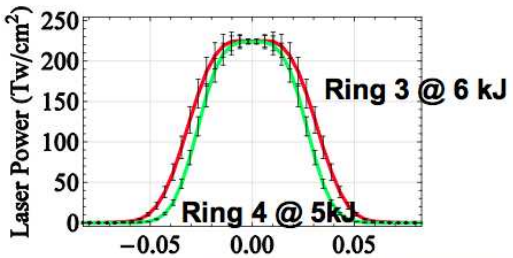

Preheat experiments

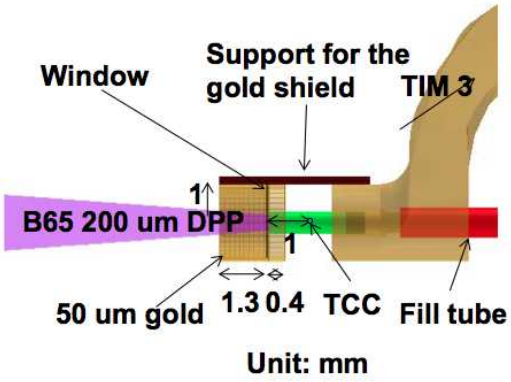

ROCHESTER

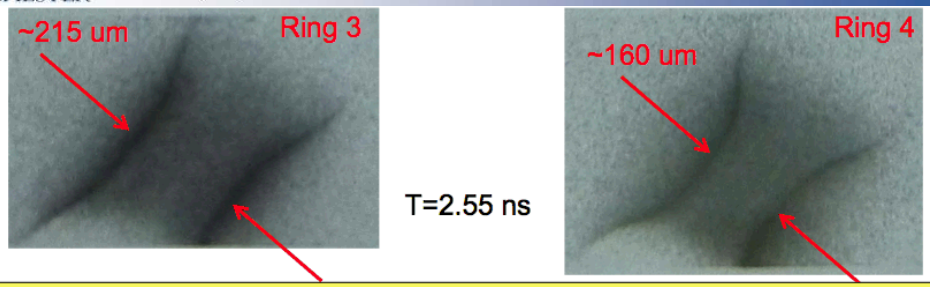

The results will be used to bench mark the coupling efficiency in simulations. It will be used to determine the power of different rings for shot in September.

Preliminary analysis is very encouraging

Slides courtesy J. R. C. Davies, P.-Y. Chang, et. al.

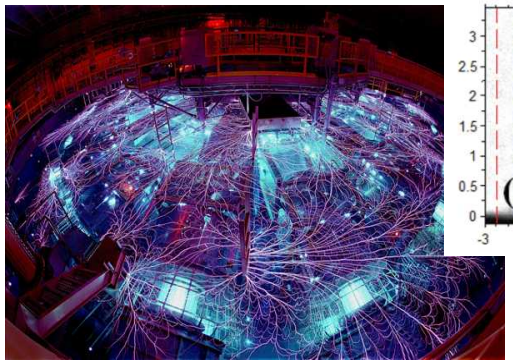

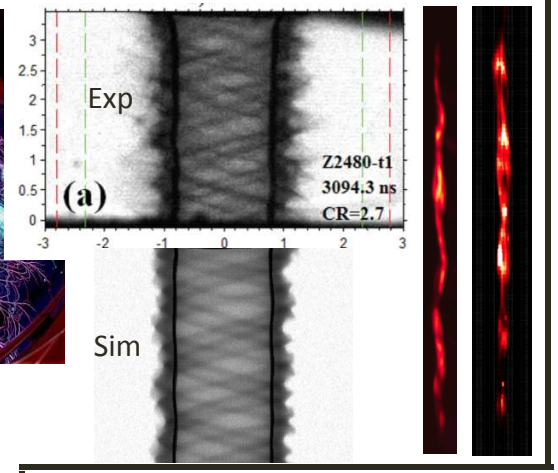

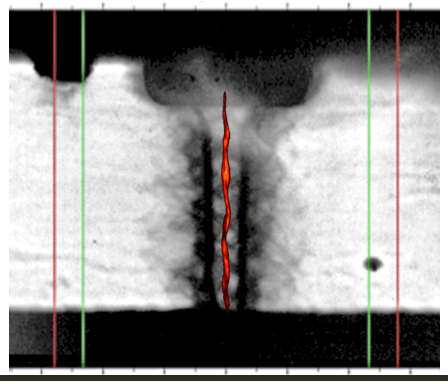

B field enables high convergence MagLIF and fusion yields

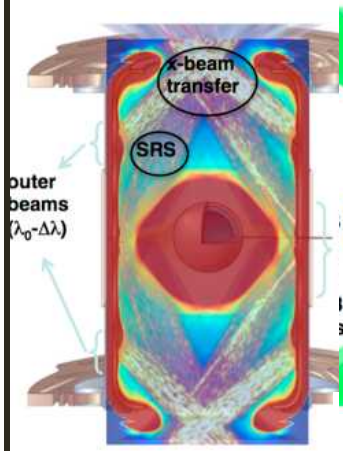

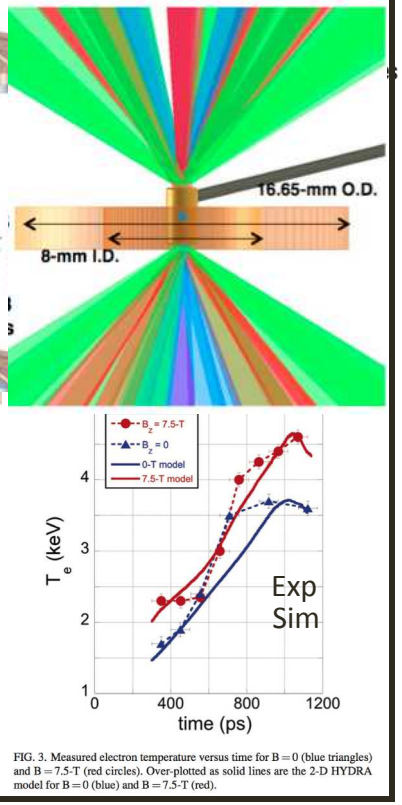

FIG. 3. Measured electron temperature versus time for B = 0 (blue triangles) and B = 7.5-T (red circles). Over-plotted as solid lines are the 2-D HYDRA model for B = 0 (blue) and B = 7.5-T (red).

B field increases hohlraum T_e at OMEGA

Summary

Magnetized gas laser preheat at ZBL, OMEGA EP, and NIF

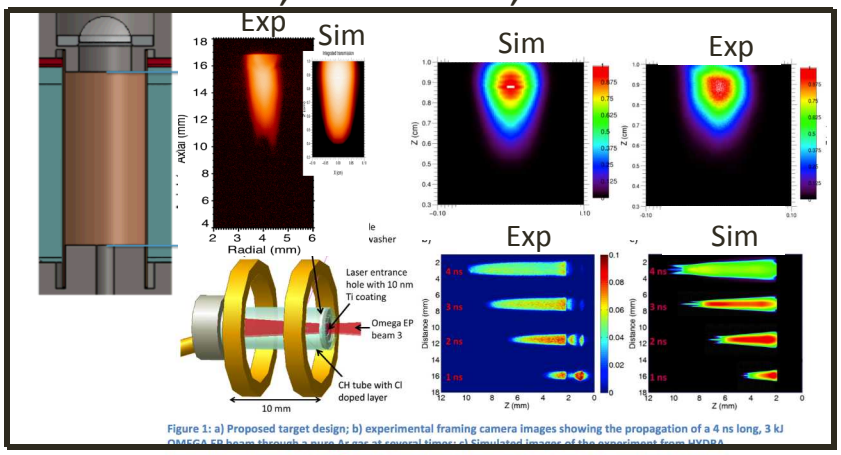

Figure 1: a) Proposed target design; b) experimental framing camera images showing the propagation of a 4 ns long, 3 kJ OMEGA EP beam through a pure Ar gas at several times; c) Simulated images of the experiment from HYDRA

Direct-drive “mini-MagLIF”